Functional Analysis of the *Saccharomyces cerevisiae* Npr1 Protein Kinase

Inauguraldissertation

zur
Erlangung der Würde eines Doktors der Philosophie
vorgelegt der
Philosophisch-Naturwissenschaftlichen Fakultät
der Universität Basel

von

Stefan Gander
aus Zürich, ZH

Basel, 2007

Genehmigt von der Philosophisch-Naturwissenschaftlichen Fakultät

auf Antrag von

Prof. Dr. Mike Hall

Dr. Paul Jenö

PD Dr. Jan Hofsteenge

Basel, den 11.12.2007

Prof. Dr. Hans-Peter Hauri

Dekan

Summary

The uptake and processing of nutrients is highly regulated. Cells adapt to changes of the availability of nutrients to provide a complete set of transporters and metabolizing enzymes for optimal use of the available nutrients. The *Saccharomyces cerevisiae* nitrogen permease reactivator protein (NPR1) plays an important role in nitrogen regulation by controlling the sorting and stability of several amino acid permeases. Npr1 is a hyperphosphorylated protein that belongs to a fungus-specific family of Ser/Thr protein kinases. Its activity is regulated by the TOR (target of rapamycin) signaling pathway. Inhibition of TOR by the immunosuppressant drug rapamycin or growth on a poor nitrogen source causes dephosphorylation of Npr1 by the Sit4 phosphatase. Previously, the rapamycin sensitive phosphorylation sites had been determined. They are clustered in two regions of an N-terminal serine-rich domain of Npr1. Besides *in vivo* phosphorylation, Npr1 underwent intense autophosphorylation when assayed *in vitro*. Investigation of Npr1 autophosphorylation revealed three autophosphorylation sites previously mapped in untreated GST-Npr1. Autophosphorylation had no regulatory effect on Npr1 kinase activity. To learn more about Npr1 substrate requirements, a set of classical protein kinase substrates were tested. From a set of basic proteins, myelin basic protein (MBP) was found to be an optimal substrate for Npr1. To find physiologically relevant Npr1 substrates, a KESTREL-based approach disclosed ribosomal protein Rpl24a as an excellent substrate for Npr1. The Npr1 consensus sequence was investigated with a set of peptides designed around the phosphorylation site of Rpl24a. Basic residues at position P-3 and P+1 are crucial determinants of the consensus sequence. Since Rpl24a is unlikely to be a *bona fide* substrate, an interactor-based substrate screen with GST-Npr1 as bait was carried out. Physiologically relevant interactors were the ubiquitin ligase Rsp5 and the AMP-activated Ser/Thr protein kinase Snf1 and its two subunits Snf4 and Gal83. The Npr1-Rsp5 interaction was immunologically confirmed and shown by point mutations to be specific. However, Rsp5 turned out not to be a direct protein substrate for Npr1. On the other hand, Npr1 was not ubiquitinated when tested with anti-ubiquitin antibodies. Functional analysis of the N-terminal serine-rich domain of Npr1 indicated a substrate binding domain between residues 252-413 that anchors the substrate for phosphorylation by the catalytic domain. However, the significance of this finding needs to be clarified with respect to the function of Npr1 *in vivo* where the N-terminal domain proved to be dispensable for growth and permease sorting.

Abbreviations

CID	collision-induced dissociation
CNBr	cyanogen bromide
ESCRT	endosomal sorting complex required for transport
ESI	electrospray ionization
GST	glutathione-S-transferase
HPLC	high performance liquid chromatography
IMAC	immobilized metal affinity chromatography
KESTREL	kinase substrate tracking and elucidation
LC/MS	liquid chromatography coupled to mass spectrometry
NCR	nitrogen catabolite repression
MALDI-TOF	matrix-assisted laser desorption ionization time-of-flight
MBP	myelin basic protein
MS	mass spectrometry
MS/MS	tandem mass spectrometry
m/z	mass-to-charge ratio
MVB	multivesicular body
NPR1	nitrogen permease reactivator protein
PVC	prevacuolar compartment
TFA	trifluoro acetic acid
TOR	target of rapamycin

Table of Contents

1 Introduction

1.1 The Role of Nutrients in *Saccharomyces cerevisiae*

Growth and proliferation in microorganisms depend on two nutritional inputs: a carbon and a nitrogen source. Yeast cells can assimilate a variety of carbon and nitrogen compounds but if the cells grow in media containing alternative sources they discriminate between preferred and non-preferred ones. Therefore, to optimally use the available nutrients, yeast cells respond to the quality of the carbon and nitrogen source present in the environment. Depending on the availability of nutrients, the cells adapt their metabolic and transcriptional program to provide the proper set of proteins responsible for uptake, transport, and metabolism of nutrients. In addition, cells execute the appropriate developmental program like vegetative or filamentous growth, or cell cycle arrest and mating (Fig. 1). Except for the pheromone-dependent mating, the choice of developmental program depends on the quantity and quality of the nutrients.

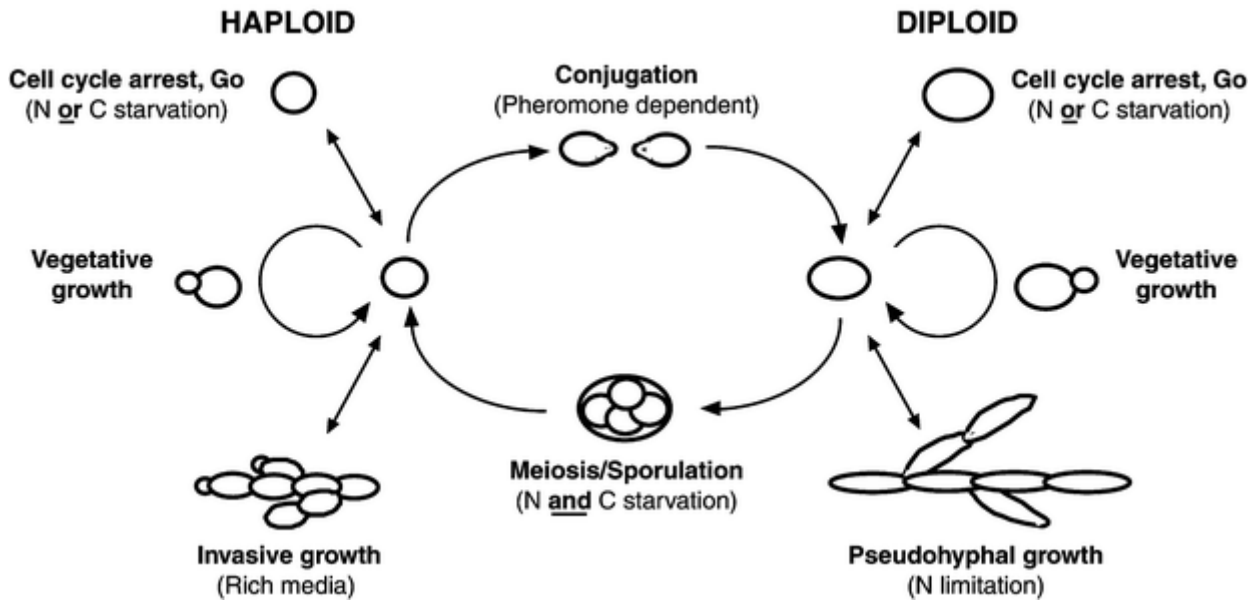

Figure 1: Yeast growth and development

Once every cell cycle haploid and diploid yeast cells have to choose a developmental program. The decision is influenced by the availability of nutrients (Forsberg and Ljungdahl, 2001).

Numerous signal transduction pathways allow for adaptation of yeast cells to a given nutrient input. In the following part the sensing, uptake, and processing of nutrients and their regulatory mechanisms are briefly discussed.

1.2 Carbon Regulation

For *Saccharomyces cerevisiae* glucose (or fructose) is the preferred carbon source, but a variety of fermentable and non-fermentable carbon sources can be utilized. Glucose and hexoses are taken up by the hexose transporters HXT1-HXT17, and GAL2 (Kruckeberg, 1996). Addition of glucose to cells grown in a non-fermentable carbon source leads to profound metabolic and transcriptional reprogramming termed glucose repression (Santangelo, 2006). Within 20 min after addition of glucose expression of about 40% of the 6200 genes in *S. cerevisiae* increases at least two-fold (Wang *et al*., 2004). Glycolysis is activated and gluconeogenesis is inhibited. Genes encoding enzymes involved in the uptake and metabolism of alternative carbon sources (ethanol, lactate, glycerol) and gene products involved in stress resistance are repressed (Rolland *et al*., 2002). Also, genes involved in respiration, gluconeogenesis, and glyoxylate cycle are down-regulated during growth in the preferred (glucose, fructose) carbon source. Three signaling pathways play redundant and overlapping roles in this process, mediated respectively, by protein kinase A (PKA), Snf1 and the glucose sensors Reg2 and Snf3 (Schneper *et al*., 2004).

PKA becomes activated by the addition of glucose to the growth medium. This activation is mediated either by the monomeric Ras GTPases or the Gα homolog Gpa2 and the putative G-protein coupled receptor Gpr1 (Schneper *et al*., 2004). This pathway leads to the production of cyclic AMP (cAMP) that activates the cAMP-dependent protein kinase A by binding to its negative regulatory subunit Bcy1 which dissociates from the catalytic subunits encoded by *TPK1/2/3*. PKA apparently regulates processes such as glycogen accumulation and stress response as well as growth by suppression of *MSN2* and *MSN4* gene expression (Smith *et al*., 1998).

The Snf1 kinase is activated when glucose is limiting (Wilson *et al*., 1996; Woods *et al*., 1994). The kinase functions as a heterotrimeric protein complex in association with the catalytic α subunit Snf1, the activating γ subunit Snf4 and three alternative β subunits Sip1, Sip2 or Gal83 (Jiang and Carlson, 1997) which regulate substrate specificity. Snf1 becomes activated by phosphorylation of the activation loop by the three upstream kinases Sak1, Elm1, and Tos3 (Hong *et al*., 2003; Nath *et al*., 2003; Sutherland *et al*., 2003). Protein phosphatase 1 (Glc7) in complex with Reg1 acts antagonistically to Snf1 in glucose repression by dephosphorylating Snf1 (Hedbacker and Carlson, 2008). Snf1 controls the subcellular localization of the transcription factor Mig1, the major repressor of glucose-repressed genes (Rolland *et al*., 2002). In the absence of glucose, Snf1 probably phosphorylates Mig1 and causes its translocation to the cytoplasm (De Vit *et al*., 1997).

Rgt2 and Snf3 are unique members of the hexose transport family which act as glucose sensors (Santangelo, 2006) that, via their long cytoplasmic C-terminal tail, are responsible for low glucose induction of hexose transporter genes *HXT2* and *HXT4* (Ozcan *et al*., 1996; Ozcan and Johnston, 1995).

1.3 Nitrogen Regulation

1.3.1 General Overview

Yeast cells require nitrogen to produce amino acids for protein synthesis and building blocks for RNA and DNA synthesis. The amino nitrogen of glutamate serves as the source of 85% of the total cellular nitrogen whereas the amide group of glutamine is the source of the remaining 15% (Cooper, 1982). For the assimilation of nitrogen, transport proteins, called permeases, are required and metabolic enzymes for the production of ammonia from nitrogen containing compounds. Ammonia reacts with α-ketoglutarate, provided by the carbon metabolism (intermediate of the TCA cycle), to produce glutamate (Fig. 2). This reaction is catalyzed by the $NADP^+$-linked glutamate dehydogenase (*GDH1*) (Grenson *et al*., 1974). In an ATP dependent process, glutamine synthetase (*GLN1*) catalyzes the production of glutamine from glutamate and ammonia (Mitchell, 1985; Mitchell and Magasanik, 1983). In the reverse direction, glutamate is produced from glutamine and α-ketoglutarate by the glutamate synthetase (*GLT1*) (Miller and Magasanik, 1990). The NAD^+-linked glutamate dehydrogenase (*GDH2*) catalyzes the conversion from glutamate back to α-ketoglutarate (Miller and Magasanik, 1990).

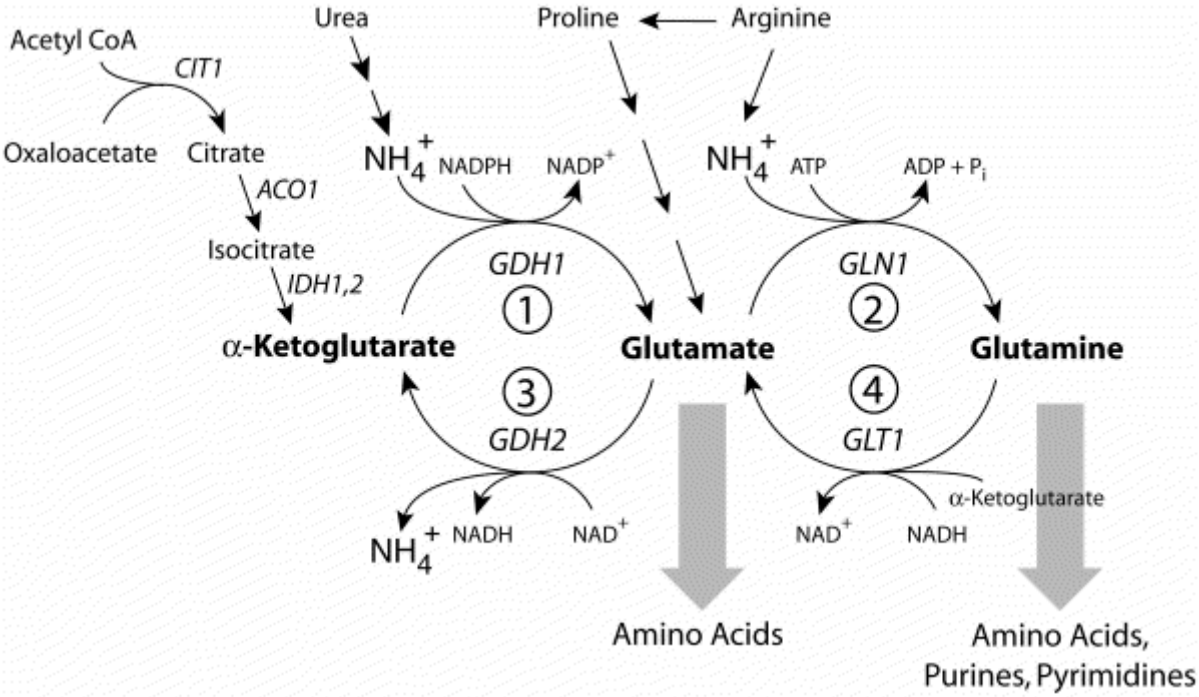

Figure 2: Nitrogen metabolism

Glutamate and Glutamine serve as building blocks for the cellular synthesis of amino acids, DNA and RNA. Glutamate is synthesized from α-ketoglutarate and ammonia. In turn, glutamine is produced from glutamate and ammonia. Nitrogen containing compounds like urea, proline, and arginine are fed into the pathway at intermediate points (Magasanik and Kaiser, 2002).

Yeast cells can grow in different nitrogen media, and, in analogy to carbon sources, they discriminate between good (preferred) and poor (non-preferred) nitrogen media. *S. cerevisiae*, like most microorganisms, transports, accumulates, and processes good nitrogen sources in preference to poor ones. The general response to the quality of nitrogen source in the growth medium is termed nitrogen regulation. Nitrogen catabolite repression (NCR) is the repression of enzymes and permeases for the utilization of non-preferred compounds when preferred nitrogen sources are available (Magasanik, 1992). This is achieved mainly by repressing the transcription of genes involved in the utilization of non-preferred nitrogen sources, but also by post-translational regulation like the intracellular sorting of permeases. Nitrogen sources that do not derepress pathways for the utilization of alternative nitrogen sources are preferred nitrogen sources. According to this, glutamine, asparagine and mixtures of amino acids and peptides in commercial Bactopeptone are preferred nitrogen sources, even though strain differences exist. In the Σ1278b strain for example, ammonia is a preferred nitrogen source whereas in the S288C strain ammonia is neither preferred nor non-preferred (Magasanik and Kaiser, 2002). Similarly, glutamate cannot be classified as either good or poor nitrogen source. Nitrogen sources that derepress pathways for the utilization of alternative nitrogen sources are considered to be non-preferred (for example, proline,

urea, ornithine, γ-aminobutyrate (GABA), and allantoin). These compounds have to be metabolized to glutamine and glutamate by various enzymes to serve as building blocks for amino acid, RNA, and DNA synthesis.

A prerequisite for a proper physiological response is the ability to sense and transduce information regarding the quality of nitrogen sources present in the extra- and intracellular environment. Nitrogen sensing and signal transduction pathways in yeast consist of the extracellular amino acid sensor SPS, the extracellular ammonia sensor Mep2 and the intracellular nitrogen sensing systems involving Gcn2 and the TOR pathway (Fig. 3). The different pathways have distinct as well as overlapping functions.

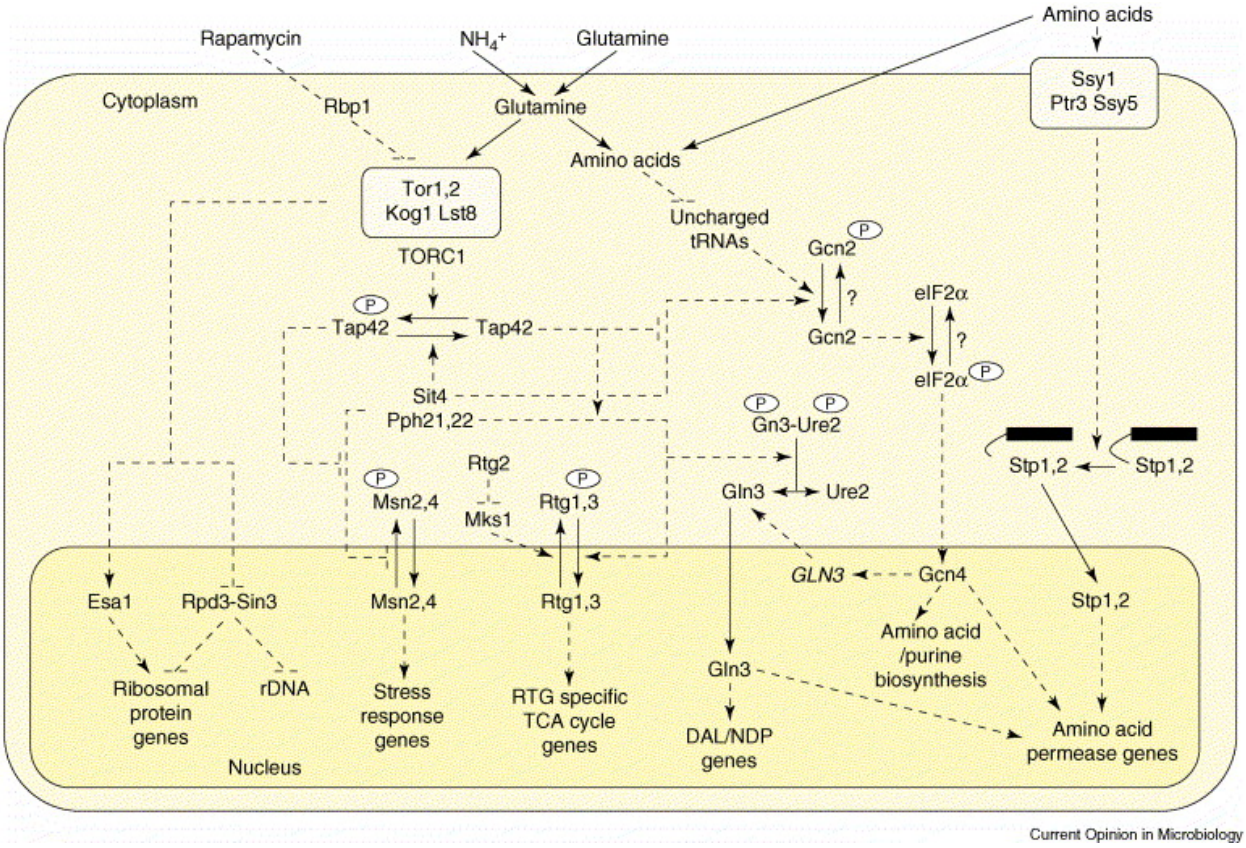

Figure 3: Nitrogen regulated signaling

Overview of yeast signaling pathways that sense and transduce the availability of nitrogen in the environment (Schneper *et al*., 2004). See text for details.

1.3.2 The SPS Sensor Complex

Extracellular amino acids are sensed by the integral plasma membrane protein Ssy1 (Klasson *et al*., 1999) in conjunction with two peripheral membrane proteins, Ptr3 and Ssy5. These proteins constitute the SPS (Ssy1-Ptr3-Ssy5) sensor complex (Forsberg and Ljungdahl, 2001). *SSY1* encodes

a unique member of the amino acid permease gene family. It possesses a 200-amino-acid N-terminal extension essential for its signaling function that is not present in permeases solely dedicated for the uptake of amino acids (Klasson *et al*., 1999). The two homologous zinc-finger transcription factors Stp1 and Stp2 are downstream effector components of the SPS signaling pathway (Andreasson and Ljungdahl, 2002; de Boer *et al*., 2000). Stp1 and Stp2 contain N-terminal regulatory domains that function as cytoplasmic retention motifs. In response to extracellular amino acids, the SPS sensor induces rapid proteolytic removal of N-terminal inhibitory domains of Stp1 and Stp2 (Andreasson and Ljungdahl, 2002). The proteolyzed forms of Stp1 and Stp2 are efficiently targeted to the nucleus where they bind to specific upstream activator sequences present within SPS sensor-regulated promoters (de Boer *et al*., 2000). The transcription of several genes encoding amino acid permeases (*AGP1*, *BAP2*, *BAP3*, *DIP5*, *GNP1*, *TAT1,* and *TAT2*) (Didion *et al*., 1998; Forsberg and Ljungdahl, 2001; Iraqui *et al*., 1999; Klasson *et al*., 1999) as well as non-permease genes (*PTR2*, *CAR1*) (Barnes *et al*., 1998; Klasson *et al*., 1999) depend on SPS sensor signaling.

1.3.3 The Ammonium Sensor Mep2

Another extracellular nitrogen sensor is the ammonium sensor Mep2. Mep2 belongs to the MEP gene family consisting of *MEP1*, *MEP2*, and *MEP3* (Dubois and Grenson, 1979). The Mep proteins are ammonium transporters with 11 predicted transmembrane domains (Marini *et al*., 1994). *MEP2* is the most divergent member of the Mep family and encodes a high-affinity ammonium permease that is N-terminally glycosylated in a region where other members are not (Marini and Andre, 2000). In addition to its role in ammonia uptake, Mep2 has been proposed to act as an ammonium sensor required for pseudohyphal growth of diploid yeast cells induced by ammonium limitation (Lorenz and Heitman, 1998). Filamentation of diploid yeast cells enables them to explore the environment for more favorable nitrogen sources (Gimeno *et al*., 1992). Mep2 regulates formation of filaments by acting upstream of GPA2 and RAS2 (Lorenz and Heitman, 1998). The Npr1 kinase (discussed in detail below) is a likely regulator of the Mep proteins since it is required for optimal ammonium uptake in cells grown on a non-preferred nitrogen source (Grenson *et al*., 1974). *Npr1* mutant cells and cells lacking all three MEP genes show a similar growth defect on low-ammonia medium (Feller *et al*., 2006). However, Npr1 was shown to be only indirectly involved in the regulation of pseudohyphal growth by affecting the stability of Mep2 at the plasma membrane (Boeckstaens *et al*., 2007).

1.3.4 Sensing the Intracellular Amino Acid Levels: the General Amino Acid Control

Intracellular amino acid concentrations are sensed by the general amino acid control (GAAC) mechanism (Hinnebusch, 1986). The signal for amino acid starvation in yeast is uncharged tRNA. If cells are starved for any single amino acid its tRNA binds C-terminally to the kinase domain of the Gcn2 protein kinase. This binding activates the kinase (Wek *et al*., 1995) which in turn phosphorylates the α subunit of translation initiation factor eIF2. Phosphorylation of the α subunit of eIF2 leads to only a slight inhibition of general protein synthesis but does activate the translation of the transcription factor Gcn4, the primary regulator of GAAC (Hinnebusch and Natarajan, 2002). Gcn4 induces the transcription of over 70 genes that encode enzymes for the biosynthesis of all 20 amino acids. Recent experiments using microarrays showed that Gcn4 affects the transcription of a large number of genes (about 1000) in response to amino acid starvation (Kleinschmidt *et al*., 2005; Natarajan *et al*., 2001). In addition to amino acid starvation, the Gcn4 pathway is induced by purine starvation (Rolfes and Hinnebusch, 1993), glucose limitation (Yang *et al*., 2000), and exposure to DNA-damaging agents (Natarajan *et al*., 2001) and rapamycin (Valenzuela *et al*., 2001).

1.3.5 TOR, an Intracellular Nutrient Sensor?

The Tor (target of rapamycin) kinases were found to be central controllers of the nitrogen catabolite repression. TOR was originally identified genetically by mutations in yeast that acquired resistance to the growth-inhibitory properties of the immunophilin-immunosuppressant complex FKBP-rapamycin (Heitman *et al*., 1991). TOR is a phosphatidylinositolkinase-related protein kinase (PIKK) (Cafferkey *et al*., 1993) that is conserved in all eukaryotes examined. Unlike all the other eukaryotes, yeast harbors two different TOR genes, termed *TOR1* and *TOR2* with 67% sequence identity (Helliwell *et al*., 1994). Early genetic observations suggested that TOR1 and TOR2 have a shared function that is required for transit through G_1 phase which is sensitive to rapamycin and TOR2 has an additional, unique function that TOR1 is unable to perform. This essential function of TOR2 is insensitive to rapamycin (Cafferkey *et al*., 1993; Helliwell *et al*., 1998; Helliwell *et al*., 1994; Kunz *et al*., 1993; Zheng *et al*., 1995).

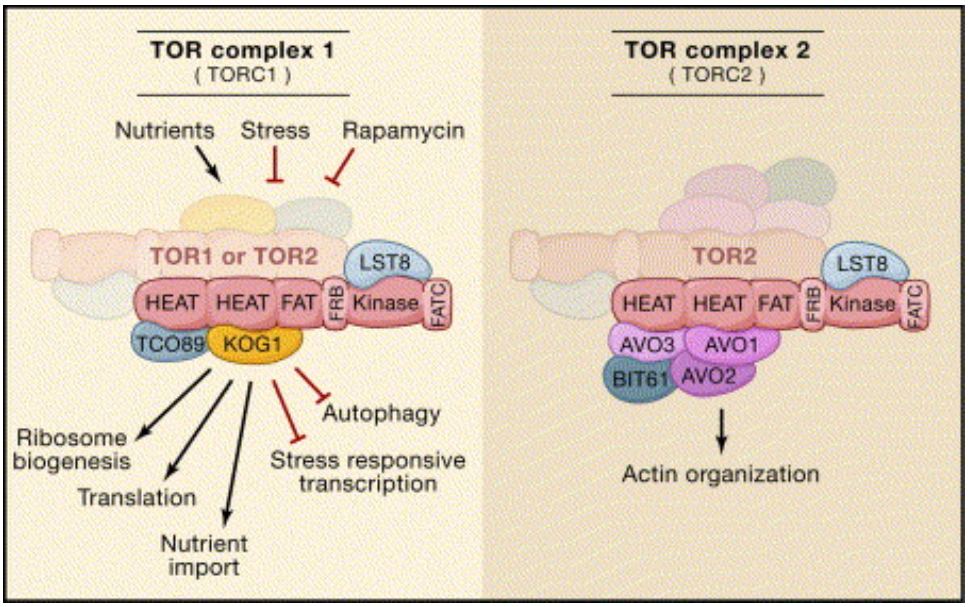

Figure 4: The two TOR complexes in *Saccharomyces cerevisiae*

The TOR complexes are shown as dimers with its associated proteins. TORC1 consists of TOR1 or TOR2, LST8, KOG1, and TCO89 and is positively regulated by nutrients and negatively by stress and rapamycin-treatment. TORC1 outputs that promote the accumulation of mass are depicted with black arrows, stress- and starvation-induced processes that TORC1 regulates negatively with red bars. TORC2 consists of TOR2, LST8, AVO1-3, and BIT61 and regulates actin organization. Upstream regulators of TORC2 are not known. The different domains of TOR (HEAT, FAT, FRB, Kinase, and FATC) are indicated (Wullschleger *et al*., 2006).

The TOR-shared and TOR2-unique functions define two separate signaling pathways that are mediated by the two distinct multiprotein complexes TOR complex 1 (TORC1) and TOR complex 2 (TORC2) (Fig. 4) (Loewith *et al*., 2002). TORC1 contains either Tor1 or Tor2 and the three associated proteins Lst8, Kog1, and Tco89 (Loewith *et al*., 2002; Reinke *et al*., 2004). TORC1 is inhibited by the FKBP-rapamycin complex. Disruption of TORC1 in yeast mimics the phenotype seen after rapamycin treatment, suggesting that TORC1 is the physiological target of rapamycin (Loewith *et al*., 2002). TORC1 positively controls protein synthesis at multiple levels like translation initiation, expression and assembly of the translation machinery, mRNA turnover, and the activity of high affinity amino acid permeases that pump amino acids for immediate use by the translation machinery (De Virgilio and Loewith, 2006). In contrast TORC1 negatively regulates a number of stress-related functions like autophagy and the activities of different stress-responsive transcription factors (De Virgilio and Loewith, 2006). TORC2 contains Tor2 together with the proteins Lst8, Avo1, Avo2, Avo3, Bit2, and Bit6 (Fadri *et al*., 2005; Loewith *et al*., 2002; Reinke *et al*., 2004). TORC2 fails to bind the FKBP-rapamycin complex which makes it insensitive to rapamycin (Loewith *et al*., 2002). TORC2 is important for the cell-cycle dependent polarization of

the actin cytoskeleton to facilitate trafficking of macromolecules from the mother cell to the bud, the main place of growth (Loewith *et al*., 2002). Activation of mammalian TORC1 involves the tuberous sclerosis proteins TSC1 and TSC2 and the small GTPase Rheb which integrates signals from growth factors, nutrients, energy, and stress (Wullschleger *et al*., 2006). However, TORC1 in *S. cerevisiae* responds to nutrients despite the absence of functional Rheb and TSC orthologs. Upstream regulators of TORC1 in yeast remain elusive.

1.3.6 The GATA Transcription Factors

TORC1 plays an important role in nitrogen regulation by preventing nuclear localization of the transcription factor Gln3 in cells growing in a good nitrogen source (Beck and Hall, 1999; Cardenas *et al*., 1999). Rapamycin treatment induces dephosphorylation and subsequent nuclear localization of Gln3 where it activates transcription of genes encoding permeases and enzymes needed to transport and adaptation to poor nitrogen sources (Beck and Hall, 1999; Bertram *et al*., 2000; Cardenas *et al*., 1999). Gln3 belongs to the zinc-finger GATA family of transcription factors. The target of the GATA family proteins is a sequence containing the nucleotides GATA at its core (Omichinski *et al*., 1993). Four GATA factors, Gln3, Gat1/Nil1 and the transcriptional repressors Dal80, and Deh1/Gzf3 are involved in the transcription of nitrogen-responsive genes (Magasanik and Kaiser, 2002). Dal80 and Deh1 repress gene expression by competing with Gln3 and Gat1 activators for binding to their target GATA sequence (Coffman *et al*., 1997). Expressions of all GATA factor encoding genes, except *GLN3*, are regulated by GATA factors themselves which also includes autoregulation (Cooper, 2002). NCR and Dal80 mediated repression of nitrogen regulated genes are different mechanisms. NCR is the absence of transcriptional activation in cells growing in a good nitrogen source whereas Dal80 mediated repression is a competitive modulation of GATA factor-mediated transcriptional activation during growth on a poor nitrogen source. *DAL80* expression is highly NCR-sensitive which means that very little Dal80 exists during times of strong NCR, i.e. during growth on a good nitrogen source (Cooper, 2002). The presence of a preferred nitrogen source in the growth medium is responsible for the inability of Gln3 and Gat1 to activate gene expression. The protein responsible for retaining Gln3 in the cytoplasm is Ure2 which was found to bind to Gln3 for preventing its nuclear localization (Beck and Hall, 1999; Bertram *et al*., 2000; Blinder *et al*., 1996; Courchesne and Magasanik, 1988). A similar Gat1-Ure2 complex has not yet been reported. The regulation of the binding of Gln3 to Ure2 is not fully understood. One model is that the binding of Gln3 to Ure2 requires TOR-dependent phosphorylation of Gln3 and/or Ure2 (Beck and Hall, 1999; Cardenas *et al*., 1999; Hardwick *et al*., 1999). When cells grow on a

good nitrogen source TOR is active and promotes phosphorylation of Gln3 that is necessary for Ure2 binding (Beck and Hall, 1999). The shift to a nitrogen poor medium or rapamycin treatment results in the release of Gln3 from Ure2, its dephosphorylation and translocation to the nucleus (Beck and Hall, 1999; Bertram *et al*., 2000; Blinder *et al*., 1996). Whether the phosphorylation of Gln3 is the reason for its binding to Ure2 or whether Ure2 stabilizes the phosphorylated form of Gln3 is not yet clear. Dephosphorylation of Gln3 is mediated by the type 2A-related phosphatase Sit4. Under nutrient-rich conditions Tap42 becomes phosphorylated by TOR (Jiang and Broach, 1999) and binds and thereby inactivates Sit4. Upon nitrogen starvation or rapamycin treatment, Tap42 gets dephosphorylated and Sit4 is released and becomes activated (Beck and Hall, 1999; Di Como and Arndt, 1996). Activated Sit4 in turn dephosphorylates Gln3 (Cutler *et al*., 2001). Alternatively, it is conceivable that TOR indirectly controls the binding of Tap42 to Sit4 by regulating the Tap42-interacting protein Tip41, an inhibitor of Tap42 and Sit4 interaction (Jacinto *et al*., 2001). In either way TOR inhibits the function of the Sit4 phosphatase via promoting the binding between Tap42 and Sit4 which leads to the cytoplasmic retention of Gln3. Recent observations have led to the suggestion that TOR regulation of Gln3 may be even more complicated as in the model described above. It was found that association with Tap42 is required for Sit4 phosphatase activity making Tap42 a positive rather than a negative regulator of Sit4 (Duvel *et al*., 2003; Wang *et al*., 2003a). Further, Gln3 phosphorylation is not dependent on the nitrogen source and under certain conditions also phosphorylated Gln3 was found in the nucleus (Cox *et al*., 2004; Tate *et al*., 2005).

1.3.7 Nitrogen-Regulated Intracellular Permease Sorting

Yeast encodes over 250 membrane transporters which are responsible for the selective transport of nutrients (Van Belle and Andre, 2001). Among them are 19 amino acid transporters with distinct substrate specificity, affinity, and transport capacity. The amino acid permeases are integral membrane proteins with 12 predicted transmembrane domains and are delivered to the plasma membrane via the secretory pathway. They are responsible for the uptake of amino acids, polyamines, and choline from the environment for protein synthesis and for use as a source of nitrogen (Andre, 1995; Regenberg *et al*., 1999). The permeases can be divided into two classes according to their regulation and function. One group of permeases are repressed during growth on a preferred nitrogen source and coordinately derepressed if the cells are shifted to a poor nitrogen source. Representatives of this group are the general amino acid permease Gap1, which transports all naturally occurring amino acids (Jauniaux and Grenson, 1990), and Put4, which transports only

proline (Lasko and Brandriss, 1981; Vandenbol *et al*., 1989). These permeases are important to provide the cells with nitrogen containing compounds that are fed into the production of glutamate and glutamine (Courchesne and Magasanik, 1983; Wiame *et al*., 1985). The other class includes permeases that are present at the plasma membrane when cells grow on a good nitrogen source. Some of them are down-regulated when the cells are shifted to a poor nitrogen source. Members of this class are mostly specific for particular amino acids, or chemically related compounds, such as the histidine permease Hip1 (Tanaka and Fink, 1985), the basic amino acid permease Can1 (Hoffmann, 1985), and Tat2, a tryptophan permease (Schmidt *et al*., 1994). The amino acids taken up by these permeases are destined directly for protein synthesis (Magasanik and Kaiser, 2002).

The effect of nitrogen regulation on permease sorting was extensively investigated with Gap1. Gap1 activity can be measured by the uptake of radio-labeled citrulline which is exclusively taken up by the Gap1 permease (Grenson *et al*., 1970). Σ1278b cells grown on proline showed a high activity of Gap1 and when shifted to an ammonia containing medium, Gap1 activity declined rapidly (Grenson, 1983a). The decreased Gap1 activity was explained by down-regulation of Gln3 mediated Gap1 transcription. However, in an *ure2* mutant, which expresses Gap1 constitutively, the same inactivation of Gap1 was observed (Grenson, 1983a). Therefore, nitrogen regulation of Gap1 activity occurs also post-transcriptionally. The same results were obtained in the S288C strain using glutamate as a nitrogen source. In this strain glutamate acts as a bad nitrogen source concerning transcription (high level of Gap1 transcription). However, in spite of the high level of Gap1 transcription low Gap1 activity was observed at the plasma which means, that Gap1 activity has to be regulated post-transcriptionally (Roberg *et al*., 1997b; Stanbrough and Magasanik, 1995). It was shown by another line of evidence that post-transcriptional regulation of Gap1 occurs during protein sorting in the late secretory pathway. In cells growing on glutamate, Gap1 is located in the ER and Golgi compartments and was directly delivered to the vacuole without ever reaching the plasma membrane. Shifting cells to urea containing media caused a drastic increase in Gap1 activity accompanied by the redistribution of Gap1 to the plasma membrane (Roberg *et al*., 1997b). The decline in Gap1 activity upon shifting Σ1278b cells from proline to ammonia is accompanied by degradation of the Gap1 protein. This suggests that endocytosis of Gap1 is largely responsible for ammonia inactivation (Hein and Andre, 1997). On one hand, the quality of the nitrogen source probably controls an intracellular sorting event that governs the rate of delivery of Gap1 to the plasma membrane. On the other hand, the nitrogen input influences endocytosis which determines the rate at which Gap1 is removed from the plasma membrane (Magasanik and Kaiser, 2002). In S288C cells Gap1 has unusual intracellular distribution. Even under poor nitrogen conditions, the

steady state distribution of Gap1 reveals that less than half of the protein is in the plasma membrane and the majority is located in intracellular compartments that probably correspond to the Golgi and the pre-vacuolar compartment (PVC) (Helliwell *et al*., 2001; Roberg *et al*., 1997b). One possible explanation is that Gap1 engages in a recycling loop between the *trans*-Golgi and the PVC which would serve as an internal storage of Gap1 to rapidly adjust Gap1 activity at the plasma membrane in response to changes in the environment.

1.3.8 Proteins Influencing Gap1 Sorting

There are two groups of mutations found to effect intracellular sorting of Gap1. Mutations that cause constitutive sorting of high levels of Gap1 to the plasma membrane regardless of the nitrogen source were found in the genes *NPI1/RSP5*, *BUL1*, *BUL2* and *NPI2/DOA4* (Helliwell *et al*., 2001; Soetens *et al*., 2001; Springael *et al*., 1999). The other group contains mutations located in the *SEC13*, *LST4*, *LST7*, *LST8*, and *NPR1* genes. Mutations in these genes cause constitutive sorting of Gap1 to the vacuole, regardless of the nitrogen source (Grenson, 1983b; Roberg *et al*., 1997a; Vandenbol *et al*., 1990; Vandenbol *et al*., 1987). The first group of mutations consists of proteins responsible for ubiquitination and deubiquitination of Gap1. *RSP5* is a gene encoding a HECT E3 ubiquitin ligase which catalyzes the addition of an ubiquitin moiety to specific lysine residues in target proteins (Hein *et al*., 1995; Huibregtse *et al*., 1995). *DOA4* encodes an ubiquitin isopeptidase which is responsible for deubiquitination of proteins to maintain levels of free ubiquitin in the cell (Papa and Hochstrasser, 1993; Springael *et al*., 1999). Ubiquitination seems to be important for the down-regulation of Gap1 activity at the plasma membrane. Gap1 itself is subject to ubiquitination because increased Gap1ubiquitination occurred when cells where shifted from a poor to a good nitrogen medium (Springael and Andre, 1998). Gap1 is ubiquitinated at lysines 9 and 16 of the amino-terminal cytosolic domain of Gap1 (Soetens *et al*., 2001). Although ubiquitination generally serves as a recognition signal for degradation by the proteasome (Hochstrasser, 1996), studies in yeast have shown that ubiquitination of plasma membrane proteins results in their endocytosis followed by vacuolar degradation (Hicke, 1997). Lys48-linked poly-ubiquitination (C-terminal Gly of ubiquitin is linked to Lys48 of the previous ubiquitin) is the signal for degradation by the proteasome, whereas mono-ubiquitination and Lys63-linked poly-ubiquitination seems to be the signal for vacuolar degradation (Hicke, 1997). Besides its role in the early steps of endocytosis, ubiquitin is also important for multivesicular body (MVB) sorting (Katzmann *et al*., 2001). The ESCRT complexes are responsible for recognition and sorting of ubiquitinated proteins targeted to the MVB pathway as well as for recruitment of the ubiquitin hydrolase Doa4 for deubiquitination

(Babst *et al*., 2002; Katzmann *et al*., 2001). Ubiquitination of Gap1 is essential for its down-regulation because in an *npi1* mutant, which produces abnormally low levels of Rsp5, or an *npi2* mutant lacking the Doa4 enzyme, Gap1 is not ubiquitinated and stays at the plasma membrane after shifting cells to a good nitrogen medium (Springael and Andre, 1998; Springael *et al*., 1999). Further, it was shown that Gap1 is poly-ubiquitinated in a Lys63-linked manner (Springael *et al*., 1999). Poly-ubiquitination depends on the two redundant gene products, Bul1 and Bul2, which are essential for the down-regulation of Gap1. Overexpression of Bul1 and Bul2 is causing Gap1 to be sorted to the vacuole regardless of the nitrogen source whereas the double mutant, *bul1 bul2*, causes Gap1 to be delivered to the plasma membrane more efficiently than in wild type cells (Helliwell *et al*., 2001). Bul1 and Bul2 act on Gap1 sorting through their interaction with Rsp5 via one of three WW domains present in Rsp5. WW domains are protein-protein interaction modules that bind to short proline-rich motifs like the Pro-Pro-X-Tyr (PPXY) motif (Sudol and Hunter, 2000) that is present in Bul1 and Bul2. With a point mutation in the PPXY motif of Bul1 that specifically abolishes interaction with Rsp5, the mutant Bul1 is no longer able to affect Gap1 sorting (Helliwell *et al*., 2001; Yashiroda *et al*., 1998). The *bul1 bul2* double mutant blocks the formation of poly-ubiquitinated Gap1, but at the same time, increases the amount of mono-ubiquitinated forms of Gap1, whereas the temperature sensitive *rsp5-1* mutation prevents all Gap1 ubiquitination. Since the *bul1 bul2* double mutant has the same effect on Gap1 sorting as *rsp5-1*, it seems that poly-ubiquitination is the key determinant for Gap1 trafficking from the Golgi to the vacuole (Magasanik and Kaiser, 2002).

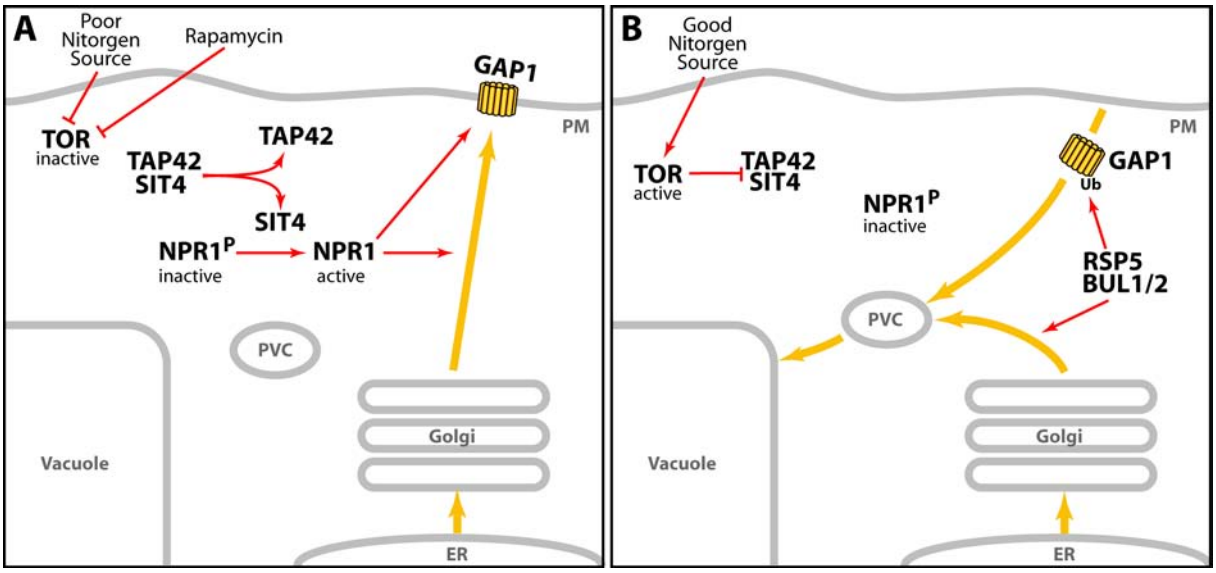

Figure 5: Sorting of the general amino acid permease GAP1.

A: Upon nitrogen starvation, or inactivation of TOR by rapamycin, the SIT4 phosphatase is activated by dissociation from its regulatory subunit TAP42. SIT4 dephosphorylates Npr1 which in turn positively influences the sorting of GAP1 from the Golgi to the plasma membrane where it is stabilized.
B: Under good nitrogen conditions, TOR keeps SIT4 inactive by promoting the formation of a complex between SIT4 and TAP42. Npr1 in its hyperphosphorylated form ($NPR1^P$) is inactive and can no longer stabilize Gap1 at the plasma membrane. Gap1 becomes ubiquitinated by the Rsp5/Bul1/2 ubiquitin ligase, leading to its sorting via the prevacuolar compartment (PVC) to the vacuole where it is degraded. Newly synthesized Gap1 is directly sorted to the vacuole without ever reaching the plasma membrane.

Sec13, which is a subunit of the COPII coat required for vesicular transport from the ER to the Golgi, is necessary for Gap1 sorting to the plasma membrane (Roberg *et al*., 1997b). Although the exact mechanism of how Sec13 is involved in Gap1 sorting remains unclear, the function of Sec13 in Gap1 sorting can be separated from its role in ER to Golgi transport (Roberg *et al*., 1997a). Mutations in *LST8*, *LST4*, and *LST7* were found in a synthetic lethal screen with *sec13-1* (Roberg *et al*., 1997a). *LST8* encodes a positively acting component of the TOR pathway that affects Gap1 sorting by negatively regulating the transcription factors Rtg1/3 and Gln3, thereby limiting the synthesis of α-ketogluterate, glutamate and glutamine (Chen and Kaiser, 2003). The role of LST4 and LST7 has not been elucidated. Actually the first mutation affecting Gap1 sorting was *npr1* (Grenson, 1983b; Vandenbol *et al*., 1990; Vandenbol *et al*., 1987). *NPR1* encodes a Ser/Thr protein kinase which is necessary for stabilization of Gap1 at the plasma membrane, as well as for the transport of newly synthesized Gap1 to the plasma membrane (De Craene *et al*., 2001). In *npr1* mutants growing on proline or urea, the amount of *GAP1* transcripts is unaltered (Vandenbol *et al*., 1990), but Gap1 is inactive (Dubois and Grenson, 1979; Grenson, 1983b). Using a temperature sensitive *npr1* mutant ($npr1^{ts}$) it was shown that upon loss of NPR1 function in proline-grown cells, Gap1 was endocytosed and targeted to the vacuole, where it was degraded (De Craene *et al*., 2001).

As mentioned before, ubiquitination of Gap1 is essential for its down-regulation. Inactivation of Npr1 triggers an increase of Gap1 ubiquitination and in an *npr1*^{ts}/*npi1* double mutant Gap1 remains active and stable at the plasma membrane when cells are shifted to the restrictive temperature (De Craene *et al*., 2001). Therefore, Npr1 prevents ubiquitination dependent endocytosis of Gap1 when cells grow in nitrogen poor media. Since Npr1 is a protein kinase and Gap1 was shown to be phosphorylated (Stanbrough and Magasanik, 1995), it is tempting to say that Npr1 directly phosphorylates Gap1 and thereby preventing its down-regulation. However, an *npr1* mutation does not prevent the phosphorylation of Gap1, indicating that the target of the Npr1 kinase may not be Gap1 itself (De Craene *et al*., 2001). Further, the Npr1 kinase also affects the fate of newly synthesized Gap1 by promoting its delivery to the plasma membrane if cells are starved for nitrogen. By combining *npr1Δ* with an *act-1*, *sec4-8*, *pep12Δ*, or *pep4Δ* mutation, newly synthesized Gap1 is directly sorted via the prevacuolar compartment to the vacuole without passing via the plasma membrane (De Craene *et al*., 2001). It thus seems that Npr1 and Rsp5 control sorting of newly synthesized Gap1 and its stability at the plasma membrane in an antagonistic fashion. Other combinations of mutations that have been tested include *npr1 rsp5* double mutants (Grenson, 1983b), *npr1 bul1 bul2* triple mutants (Soetens *et al*., 2001), and *lst4 bul1 bul2* triple mutants (Helliwell *et al*., 2001). In all three cases, the combined mutants caused Gap1 to be always delivered to the plasma membrane. One explanation is that Npr1 and Lst4 are negative regulators of the E3 ubiquitin ligase complex containing Rsp5, Bul1 and Bul2. Alternatively, sorting of newly synthesized Gap1 is controlled at two stages. First at the *trans*-Golgi, where Gap1 delivery to the PVC and from there to the vacuole is regulated by ubiquitination, and second at the PVC, where Npr1 and Lst4 promote recycling of Gap1 back to the Golgi (Magasanik and Kaiser, 2002).

1.4 The Npr1 Protein Kinase

Beside its role in regulating Gap1 sorting, the Npr1 kinase is also required for the optimal activity of several transport systems for nitrogenous compounds like the proline permease Put4, the inducible γ-aminobutyrate (GABA)-specific permease Uga4, the ureidosuccinate and allantoate permease Dal5 (Andre *et al*., 1993; Grenson, 1983b), and several ammonium transport systems (Dubois and Grenson, 1979). Other permeases like the tryptophan permease Tat2 are down-regulated upon nitrogen starvation in an Npr1 dependent way (Schmidt *et al*., 1998). Further, Npr1 was proposed to be involved in the control of Gln3 mediated transcription (Crespo *et al*., 2004) and pseudohyphal growth, a response of diploid *S. cerevisiae* to nitrogen starvation (Lorenz and Heitman, 1998). Recent data suggested that the Npr1 kinase is not directly involved in the

regulation of Gln3 mediated transcription and pseudohyphal growth (Boeckstaens *et al*., 2007; Feller *et al*., 2006; Tate *et al*., 2006). The induction of Gln3 mediated transcription in ammonium-grown *npr1* cells results from the inability of the cells to take up ammonia because the ammonium transporters Mep1, Mep2, and Mep3 are inactivated (Feller *et al*., 2006; Tate *et al*., 2006). Growth of cells in low ammonia is similarly affected in *npr1* mutant cells and cells lacking the three MEP genes (Feller *et al*., 2006). Growth of cells lacking Npr1 is also affected on nitrogen sources like citrulline, ornithine and tryptophan (Boeckstaens *et al*., 2007) which can be explained by the Npr1 dependent down-regulation of Gap1 activity. But not all observed growth defects can be interpreted in terms of impaired nitrogen source uptake since the growth of *npr1* cells is also affected on nitrogen sources like arginine, even though the specific arginine uptake activity is not impaired (Dubois and Grenson, 1979). Cells that lack Npr1 also show a severe growth defect on GABA, isoleucine, and tyrosine (Boeckstaens *et al*., 2007). The growth defect in *npr1* cells that is independent on the transport activity of the specific nitrogen compound could be explained by the inefficient retrieval of catabolic ammonium escaping from the cells due to an impaired Mep activity (Boeckstaens *et al*., 2007). How exactly Npr1 regulates these processes at the molecular level is unknown.

Sequence analysis of the *NPR1* gene showed that it encodes an 86 kDa Ser/Thr protein kinase of 790 amino acid residues (Fig. 6) (Vandenbol *et al*., 1990; Vandenbol *et al*., 1987). The amino-terminal part of Npr1 (residues 17-413) comprises a serine-rich domain with 26% serine content whereas the carboxy-terminal part of Npr1 (residues 438-742) contains sequence motifs characteristic of the catalytic domain of protein kinases (Vandenbol *et al*., 1990). For example, the sequence GAGAGGSV (residues 445-452) defines the glycine-rich loop in subdomain I involved in ATP binding and the catalytic loop HRDLKLDN (residues 559-566) in subdomain VI is implicated in catalysis and ATP binding (Hanks *et al*., 1988). Two more kinase-specific motifs, the Asp-Phe-Gly (residues 579-581) and Ala-Pro-Glu (residues 608-610) sequence stretches are required for activity. The lysine involved in transferring the γ-phosphate from ATP to the substrate is located at residue 467. Interestingly, a WW domain-interacting PPXY motif can be found (Ingham *et al*., 2004) at the C-terminal end of Npr1. Npr1 sequence analysis on EMBnet AUSTRIA (https://emb1.bcc.univie.ac.at/toolbox/pestfind) revealed three putative PEST motifs in Npr1. Two of them are located in the N-terminal domain (residues 33-51 and 73-105) and one is located around the PPXY motif (residues 680-691). PEST sequences are signals for protein instability. Phosphorylation within PEST sequences often specify their recognition and processing by the ubiquitination pathway (Lanker *et al*., 1996).

Npr1 belongs to the fungus-specific Npr/Hal5 subfamily of protein kinases (Hunter and Plowman, 1997). The members of this subfamily (Stk1/Stk2 and Hal4/Hal5) are highly conserved in the kinase domain, suggesting that these kinases are functionally related and that they are regulated in an analogous manner (Kaouass *et al*., 1997). The kinases Stk1 and Stk2 are involved in polyamine transport (Kaouass *et al*., 1997), while Hal4 and Hal5 regulate the Trk1/2 potassium transporter activity in response to potassium starvation (Mulet *et al*., 1999). Recent results indicate that Hal4/Hal5 stabilize the Trk1 transporter at the plasma membrane under low potassium conditions by preventing their endocytosis and vacuolar degradation (Perez-Valle *et al*., 2007) similar to the Npr1 mediated stabilization of Gap1 at the plasma membrane.

NPR1 transcription is independent of the quality of the nitrogen source (Vandenbol *et al*., 1987). Its activity is regulated through the TOR signaling pathway by means of phosphorylation (Schmidt *et al*., 1998). Npr1 isolated from cells grown on ammonia is highly phosphorylated whereas rapamycin treatment leads to substantial dephosphorylation of Npr1 (Jacinto *et al*., 2001). In nitrogen-poor media or upon rapamycin treatment, Sit4 phosphatase is activated (see 1.3.6) and dephosphorylates Npr1 (Schmidt *et al*., 1998). As a consequence Gap1 is sorted to the plasma membrane where it is stabilized whereas Tat2 is rapidly endocytosed and targeted to the vacuole (Beck *et al*., 1999; Roberg *et al*., 1997b; Schmidt *et al*., 1998).

Figure 6: Phosphorylation sites and domains of Npr1

The blue part of the schematic representation of Npr1 indicates the serine-rich domain of Npr1 with the phosphorylation sites indicated as black dots. In the upper part, the positions of the phosphorylated serines of the two phosphorylation clusters are indicated. The red part represents the catalytic domain of Npr1. At the bottom, the typical sequence motifs of a kinase domain as well as the protein interaction domain (PPSY) are indicated. See text for details.

Mass spectrometric analysis of the phosphorylation sites of Npr1 revealed 24 phosphorylation sites on ten tryptic peptides (Bonenfant, 2003). The sites are clustered in two regions of the N-terminal serine-rich domain between residues 45-435 of Npr1. For the ten phosphopeptides, 22 specific sites of phosphorylation were determined. All of the ten phosphopeptides, except two, showed a reduced extent of phosphorylation when isolated from rapamycin-treated cells. Interestingly, no phosphorylation was found in the C-terminal catalytic part of Npr1 (Bonenfant, 2003). Such complex phosphorylation is intriguing and naturally, the upstream kinases acting on Npr1 remain to be determined.

To test the physiological role of Npr1 phosphorylation, deletion mutants of Npr1 were constructed to remove the phosphorylation clusters of Npr1 individually (Δ1-143, Δ252-413) or in combination (Δ1-413) and the growth behavior and Gap1 activity of the mutants were tested. Kinase-dead Npr1 showed a severe growth defect and drastically reduced Gap1 activity in nitrogen-poor media

showing that the kinase activity is required for proper growth and Gap1 sorting on non-preferred nitrogen sources. Surprisingly, none of the three deletion mutants caused a phenotypic effect neither on Gap1 sorting nor for growth indicating that the N-terminal domain of Npr1 is dispensable (Altermatt, 2005). Therefore, the function of the N-terminal part of Npr1 is at present enigmatic and needs further investigations.

1.5 Protein Phosphorylation

1.5.1 The Regulatory Role of Protein Phosphorylation

Phosphorylation is one of the most frequently occurring post-translational modifications in proteins. In eukaryotic cells, protein phosphorylation on serine, threonine and tyrosine residues plays a crucial role in modulating protein function. It is critically involved in the regulation of nearly all cellular processes and signaling pathways. It has been estimated that 30% of all cellular proteins are phosphorylated on at least one residue at any given time (Zolnierowicz and Bollen, 2000). Protein kinases, the enzymes that catalyze the transfer of the γ-phosphate from ATP to specific amino acids in proteins, constitute one of the largest protein families, accounting for approximately 2% of the genes in any given eukaryotic genome (Manning *et al*., 2002). Out of the 6,144 yeast genes 117 encode protein kinases in the superfamily of eukaryotic protein kinases and 10 encode atypical kinases (Hunter and Plowman, 1997; Rubenstein and Schmidt, 2007). Few of these kinases are constitutively active. Unregulated kinase activity causes severe defects and can even be lethal. Cells have thus developed a variety of finely tuned mechanisms to precisely control the activities of these enzymes. The mechanisms regulating the activities of protein kinases in *Saccharomyces cerevisiae* can be divided into seven major categories: phosphorylation within the activation loop, phosphorylation outside the activation loop, dephosphorylation, protein binding, binding of nonprotein ligands, protein accumulation, and subcellular localization (Rubenstein and Schmidt, 2007). Other kinases are regulated in a more complex manner.

1.5.2 Substrate Specificity

For proper function a kinase has to be specific for certain substrates. Kinases vary greatly in the number of substrates and phosphorylation sites that they phosphorylate. For example, the mammalian protein kinase MEK1 phosphorylates only four sites whereas cyclin-dependent kinases probably phosphorylate hundreds of sites (Ptacek *et al*., 2005; Ubersax *et al*., 2003). The catalytic domain of classical protein kinases are structurally similar (Hanks and Hunter, 1995; Hanks *et al*., 1988). They contain a small N-terminal lobe of β-sheets and a large C-terminal lobe of α-helices (Ubersax and Ferrell, 2007). ATP and the protein substrate bind in the cleft between the two lobes where a set of conserved residues catalyze the transfer of the γ-phosphate from the ATP to the hydroxyl oxygen of the Ser, Thr or Tyr residue of the substrate. Although all classical kinases share this features, they differ in terms of the charge and hydrophobicity of surface residues at the catalytic site which is an important determinant in substrate specificity. It regulates the recognition

of short sequences around the site of phosphorylation in substrates called the consensus sequence. In most cases the active site of the kinase interacts with four amino acids on either side of the phosphorylation site on the basis of charge, hydrogen bonding or hydrophobic interactions (Ubersax and Ferrell, 2007). Consensus sequences that are recognized by specific kinases were found by mutational analysis of known substrates and from peptide library screens (Hutti *et al*., 2004; Kemp *et al*., 1975; Pearson and Kemp, 1991; Songyang *et al*., 1994). As an example, the crystal structure of PKA reveals that two Glu residues in the catalytic cleft of the kinase create anionic binding sites for the P-3 (three amino acids N-terminal of the phosphorylation site) and P-2 position of the substrate and that there is a hydrophobic pocket in the kinase that favors a hydrophobic residue at position P+1 (Taylor *et al*., 2005; Zheng *et al*., 1993). The consensus sequence that was found for PKA (RRX(S/T)Φ, where Φ represents a hydrophobic residue) (Songyang *et al*., 1994) fits perfectly in the local environment of the active site. Therefore, if the consensus sequence of a kinase is known, possible substrates can be suggested and phosphorylation sites can be predicted. However, the presence of a consensus sequence in a protein does not guarantee that the protein is an *in vivo* substrate of the kinase, and authentic phosphorylation sites do not always conform to the consensus (Ubersax *et al*., 2003).

A second level of substrate specificity is mediated by docking motifs on substrates with interaction domains on the kinase that are often spatially separated from the catalytic site (Biondi and Nebreda, 2003; Holland and Cooper, 1999). Docking motifs could function to increase the local concentration of the substrate around the kinase or serve to align the kinase precisely with the phosphorylation site (Deshaies and Ferrell, 2001; Ubersax and Ferrell, 2007). An example for a docking site is the D domain on MAPK substrates consisting of a basic and two hydrophobic residues, typically 50-100 residues away from the site of phosphorylation, which bind to a negatively charged area and a hydrophobic groove on the kinase (Kallunki *et al*., 1994; Lee *et al*., 2004; Tanoue *et al*., 2000). Several docking interactions have allosteric effects that either positively or negatively regulate kinase activity. Other issues that have an effect on substrate specificity are modular binding partners of kinases that contain docking domains for substrates, scaffold proteins, and the localization of the kinase (Ubersax and Ferrell, 2007).

1.5.3 Identification of Phosphorylation Sites

A prerequisite for the analysis of protein phosphorylation is the identification of phosphorylation sites and their quantification. There are several reasons that make it rather difficult to analyze phosphoproteins. The stoichiometry of phosphorylation is generally low, which means, that only a

small fraction of the available intracellular pool of a protein is phosphorylated at any given time. One protein can exist in several differently phosphorylated forms which complicates the analysis of all phospho variants. Further, especially signaling molecules are present at low abundance in cells. Another challenge is that analytical techniques used for studying protein phosphorylation have a limited dynamic range which means, that although major phosphorylation sites might be located easily, minor sites pose major challenges to the analytical system. Finally, it may be difficult to momentarily 'freeze' the phosphorylation state when subcellular structures are disrupted during cell lysis (Mann *et al*., 2002).

Different techniques have been applied for phosphoprotein labeling. A classical strategy is *in vivo* labeling with [^{32}P]-orthophosphate or *in vitro* phosphorylation using purified kinases and [γ-^{32}P]-ATP. Traditionally phosphorylation sites have been mapped by several approaches including Edman degradation, thin-layer chromatography of peptide fragments and mutational analysis. Recent developments in mass spectrometry made it an important tool for the analysis of phosphoproteins. Nowadays, the identification of phosphorylation sites in a complex milieu is carried out almost exclusively by mass spectrometry. The low stoichiometry of phosphorylation, the reversible nature of the modification, and comparably weak ionization of phosphopeptides requires enrichment of phosphopeptides prior to mass spectrometric analysis. Several phosphate-specific techniques have been proposed including chemical derivatisation of phosphorylated residues (McLachlin and Chait, 2003; Qian *et al*., 2003; Tao *et al*., 2005; Thaler *et al*., 2003; Thompson *et al*., 2003), antibody-based capture, immobilized metal affinity chromatography (IMAC) with various immobilized metal ions (Ficarro *et al*., 2002; Kokubu *et al*., 2005; Larsen *et al*., 2005; Nuhse *et al*., 2003; Pinkse *et al*., 2004; Posewitz and Tempst, 1999), and strong cation exchange chromatography (Tashiro *et al*., 2006). With the IMAC technique the negatively charged phosphopeptides are purified by their affinity towards metal ions such as Fe3+ and Ga3+. Also titanium dioxide has been shown to have a high affinity and specificity to phosphopeptides. A major limitation is the specificity of these techniques because of the pronounced affinity for interfering acidic groups (Asp and Glu) and electron donors (His, Cys) (Mann *et al*., 2002).

The next step is to determine the site(s) of phosphorylation. In many studies, prior separation by reverse-phase chromatography is coupled to electro spray ionization (ESI). Phosphopeptides can be specifically detected by the pronounced loss of phosphoric acid via β-elimination from phosphoserines and phosphothreonines (Aebersold and Goodlett, 2001). The neutral loss of 98 Da however, often suppresses the formation of sequence-specific fragment ions which makes identification and localization of phosphorylation sites by data bank searching difficult. To

circumvent this problem, peptide ions that had lost phosphoric acid are isolated and subjected to another round of collision induced fragmentation in an MS^3 scan.

Finally, as the function of a given protein is often modulated by phosphorylation, changes in the extent of phosphorylation of a given site have to be determined. Comparison of the signals from the same peptide under different conditions can give an estimate of relative abundances of phosphorylation. Alternatively, and more accurately, relative quantification is typically performed by stable-isotope labeling followed by analysis of the mixture and comparison of intensities. The most common labeling strategies for phosphoproteomics are stable isotope labeling with amino acids in cell culture (SILAC) (Ong *et al*., 2002), enzymatic labeling with [^{18}O]-water (Schnolzer *et al*., 1996), addition of istopically labeled peptide standards in the AQUA (absolute quantification) method (Gerber *et al*., 2003), esterification with isotopically enriched alcohols (e.g. methanol or ethanol) (Goodlett *et al*., 2001), and use of the isobaric reagent iTRAQ (isobaric tags for relative and absolute quantification) (Ross *et al*., 2004).

1.6 Aim of the Present Study

The *Saccharomyces cerevisiae* Npr1 protein kinase was shown to act downstream of TOR as a regulator of the stability and sorting of different amino acid permeases. However, direct upstream regulators and downstream substrates are not known so far. The aim was to undertake a KESTREL (kinase substrate tracking and elucidation) screen in yeast cell extracts to identify proteins that become phosphorylated by activated GST-Npr1. These ^{32}P-labelled proteins are then purified and identified by mass spectrometric means and the identified proteins are tested for *in vivo* phosphorylation to see if they are *bona fide* substrates for Npr1. In addition, the sites of phosphorylation of the potential Npr1 substrates are identified to design suitable peptide substrates for Npr1. These peptides are used to define a minimal consensus sequence for Npr1 which, in turn, is used for the prediction of physiologically relevant substrates. To screen for upstream Npr1 interactors, GST-tagged Npr1 is used as a bait for nutrient-dependent association of partner proteins followed by their mass spectrometric identification. The biological relevance of the interactors is characterized by biochemical means.

2 Material and Methods

2.1 Chemicals

Yeast extract, bacto peptone, yeast nitrogen base without amino acids and without ammonium sulfate, and bacto agar were from Becton Dickinson (Sparks, MD), yeast nitrogen base without amino acids and with ammonium sulphate from US Biological (Swampscott, MA), proline, adeninesulfate, L-arginine-HCL, L-histidine-HCL, L-isoleucine, L-leucine, L-lysine-HCL, L-methionine, L-phenylalanine, L-tryptophan, L-tyrosine, L-valine, L-glutamine, benzamidine, and reduced glutathione were obtained from Sigma-Aldrich (Buchs, Switzerland). L-threonine, PMSF, and IPTG were purchased from AppliChem (Darmstadt, Germany). HindIII, EcoR1, pepstatin, leupeptin, aprotinin, and alkaline phosphatase were from Roche Diagnostics (Rotkreuz, Switzerland), and rapamycin, calyculin A, and okadaic acid from LC Laboratries (Woburn, MA). Glutathione-Sepharose 4B and [γ-^{32}P]-ATP was used from Amersham Biosciences (Otelfingen, Switzerland). Endoproteinase LysC (Achromobacter protease 1) was from Wako Chemicals (Osaka, Japan) and trypsin (Sequencing Grade Modified Trypsin) was from Promega (Madison, WI). TFA was obtained from Applied Biosystems (Warrington, UK) and cyanogen bromide was from Fluka (Buchs, Switzerland). PreScission protease was obtained from GE Healthcare (Zurich, Switzerland). All other chemicals and reagents were of highest grade available.

2.2 Strains and Media

Strain	Genotype
TB50a	MATa leu2 ura3 trp1 his3 rme1 HMLa
JC19-1a	TB50a npr1::HIS3MX
Σ1278b	MATa ura3
YPA1	Σ1278b npr1::kanMX6

Table 1: Yeast strains used in this study.

Saccharomyces cerevisiae strains used in this work are listed in Table 1. Cells were grown either in YPD medium (1% yeast extract, 2% bacto peptone and 2% glucose) or in synthetic medium. Synthetic, nitrogen-poor medium was made of yeast nitrogen base without amino acids and without

ammonium sulphate containing 0.1% (w/v) proline and 2% glucose. Synthetic, nitrogen-rich medium was prepared with yeast nitrogen base without amino acids and with ammonium sulphate (0.5% final concentration), supplemented with amino acids and 2% glucose. The concentration of the amino acids used for nitrogen-rich medium was as follows: 20 mg/l L-arginine-HCL, 20 mg/l L-histidine-HCl, 30 mg/l L-isoleucine, 100 mg/l L-leucine, 30 mg/l L-lysine-HCl, 20 mg/l L-methionine, 50 mg/l L-phenylalanine, 200 mg/l L-threonine, 40 mg/l L-tryptophan, 30 mg/l L-tyrosine, 150 mg/l L-valine. The amino acids were supplemented with 20 mg/l adeninesulfate. Media for plates contained 2% bacto agar and were prepared as described above.

2.3 Molecular Biology Techniques

DNA ligation was done with the Rapid DNA Ligation Kit (Roche Diagnostics, Rotkreuz, Switzerland) according to the manufacturer's recommendation. Inserts were separated from the backbone after cleavage at 37°C for 1 h with the appropriate restriction endonuclease on 1-2% agarose gels and DNA was purified with the QIAquick Gel Extraction Kit (QIAGEN, Hilden, Germany) as described in the manufacturer's protocol. The ligation mixture was transformed into $CaCl_2$ competent UT580 *E. coli* cells according to standard procedures. Transformants were selected on LB plates containing ampicillin and plasmids were isolated with the GenElute Miniprep Kit (Sigma-Aldrich) according to the manufacturer's instructions. The plasmids were stored in 50 µl water at -20^{o}C.

2.4 Construction of Plasmids

Name	Genotype	Description
pBS1	pGST	YEplac195 (2µ, *URA3*) containing GST (Bonenfant *et al*., 2003)
pBS2	pGST-NPR1	YEplac195 containing GST-NPR1 under its own promoter (Bonenfant *et al*., 2003)
pBS22	pGST-NPR1Δ1-143	pGST-NPR1 lacking amino acids 1-143 of *NPR1*
pBS23	pGST-NPR1Δ252-413	pGST-NPR1 lacking amino acids 252-413 of *NPR1*
pBS24	pGST-NPR1Δ1-431	pGST-NPR1 lacking amino acids 1-431 of *NPR1*
pBS25	pGST-NPR1Δ432-513	pGST-NPR1 lacking amino acids 432-513 of *NPR1* (leads to a kinase-dead Npr1)
pBS26	pGST-NPR1ΔY676G	pGST-Npr1 containing a Y676G pointmutation in the PPXY motive of *NPR1*
	pGST-RSP5	pGEX vector containing *RSP5* for bacterial expression (provided by S. Helliwell)

Table 2: Plasmids used in this study.

To construct the plasmids pBS22, pBS23, and pBS24, the centromeric plasmids pPA1 (NPR1Δ1-143), pPA2 (NPR1Δ252-413), pPA2 (NPR1Δ1-431) (Altermatt, 2005) were cleaved with HindIII. The resulting fragments, containing the *NPR1* genes, were re-ligated into the HindIII-cleaved pBS2 backbone. A kinase-dead version of Npr1 was generated by cleaving pBS2 with EcoRI followed by religation of the backbone. This removes residues 432-513 of *NPR1* which contain the ATP binding site (residue 444-452) of the kinase domain.

2.5 Yeast Transformation

Transformation of yeast was performed with the LiAc/SS-DNA/PEG method (Gietz *et al*., 1995).

2.6 Purification of GST-Npr1

2.6.1 Buffers

For GST-Npr1 purification, the following buffer were used: lysis buffer (100 mM Tris-HCl, pH 8.0, 150 mM NaCl, 1% NP40, 1 mM EDTA, 1 mM benzamidine, 1 μg/ml pepstatin, 1 μg/ml leupeptin, 1 μg/ml aprotinin, 1 mM PMSF, 20 nM calyculin A, and 200 nM okadaic acid), washing buffer 1 (100 mM Tris-HCl pH 8.0, 150 mM NaCl, 1% NP40), washing buffer 2 (100 mM Tris-HCl pH 8.0, 150 mM NaCl, 0.1% NP40), washing buffer 3 (100 mM Tris-HCl pH 8.0, 150 mM NaCl), and elution buffer (100 mM Tris-HCl pH 8.0, 150 mM NaCl, 20 mM reduced glutathione).

2.6.2 Yeast Cell Cultures

GST-Npr1 was purified from cultures of JC19-1a or YPA1 cells (Table 1) carrying the 2μ plasmid pBS2 plasmid (Table 2). Cells were grown to OD_{600} 0.8-1.0. Rapamycin treatment was with 0.2 mg/l rapamycin for 15 min, and glutamine treatment was with 4 mM L-glutamine for 15 min. The deletion mutants of Npr1 (Table 2) were treated in the same way.

2.6.3 Large-Scale Purification

All manipulations were carried out at 4°C. Cells from a 10 l culture were harvested in a Sorvall H6000A rotor at 4,500 rpm for 10 min. The cell pellet was washed with cold water and resuspended in 50 ml lysis buffer and approximately 25 ml glass beads (Biospec Products, Bartelsville, OK) were added. The cells were disrupted with six 30 s bursts. Between individual bursts, the cells were cooled for 2 min on ice. The lysate was collected and the beads were washed with 25 ml lysis buffer containing twice concentrated protease inhibitors. Cell debris was pelleted for 10 min at 4,300 rpm (Megafuge 1.0R, Heraeus Instruments, Berlin, Germany). The cleared lysate was divided in two halves and loaded separately onto two columns packed with 1 ml Glutathione-Sepharose 4B which had been equilibrated with washing buffer 1. The columns were washed with 20 ml washing buffer 1, followed by 10 ml washing buffer 2, and 5 ml washing buffer 3. Bound GST-Npr1 was desorbed with elution buffer and 0.5 ml fractions were collected. GST-Npr1 containing fractions from the two columns were pooled and glycerol was added to 50% for storage at -20°C. The purity of the protein was checked by SDS polyacrylamide gel electrophoresis.

2.6.4 Small-Scale Purification

All manipulations were carried out at 4°C. Cells from a 100-200 ml liter culture were harvested in a Sorvall GS-3 rotor at 4,500 rpm for 10 min and washed with 10 ml cold water. Cells were resuspended in 1 ml lysis buffer and transferred to a 2 ml screw cap tube (Sarstedt, Nümbrecht, Germany). Glass beads were added till the liquid reached the top of the tube and the cells were lysed in a bead beater (Fast Prep FP120, Thermo Savant, Waltham, MA) with six 30 s bursts. In between the bursts, the cells were cooled on ice for 2 min. The tip of the tube was punctured with a hot syringe needle and the tube was placed onto a 2 ml collection tube. The lysate was collected by centrifugation at 1,500 rpm for 1 min. 200 µl of lysis buffer containing five times concentrated protease inhibitors were added and cell debris was pelleted for 5 min at 12,000 rpm. The protein concentration of the supernatant was determined by the Bradford assay. GST-Npr1 was purified by adding 100 µl of a 50% suspension of Glutathione-Sepharose 4B that had been equilibrated with washing buffer 1. The lysate was incubated for 30 min with the beads on an end-over-end rotator. The Sepharose beads were washed four times with 1 ml washing buffer 1 (2,500 rpm, 1 min), two times with washing buffer 2, and once with washing buffer 3.

2.7 Measuring GST-Npr1 Kinase Activity

Kinase assays were performed in 80 µl of 100 mM Tris-HCl, pH 8.0, 1 mM DTT, 10 mM $MgCl_2$, 10% glycerol and 20 µM [γ-^{32}P]-ATP. The reaction mixture was incubated at 37°C for 30 min in a thermo shaker set to 1,200 rpm. The assay was stopped by adding 6 times concentrated SDS sample buffer. Proteins were separated by SDS polyacrylamide gel electrophoresis and phosphorylated proteins were visualized by autoradiography.

Alternatively, kinase assays with GST-Npr1 bound to the Sepharose beads was performed with 5 µg peptide instead of myelin basic protein. GST-Npr1 was removed by centrifugation at 2,500 rpm for 1 min. The reaction mixture was spotted onto phosphocellulose squares (2 x 2 cm, P81, Whatman, Maidstone, UK). The paper squares were washed three times with 400 ml 0.5% phosphoric acid for 15 min and once with 100 ml acetone for 5 min. After drying, bound radioactivity on the squares was counted by liquid scintillation counting. The kinetic parameters K_m and V_{max} were calculated from Lineweaver–Burk double-reciprocal plots (Ferrari *et al*., 2005). For HPLC separation, the reaction mixture was stopped by adding TFA to a 1% final concentration and the mixture was analyzed by reverse-phase chromatography (see 2.16).

2.8 *In vitro* Dephosphorylation of GST-Npr1

Glutathione-Sepharose bound-GST-Npr1 from nitrogen-rich medium was incubated with 1 unit alkaline phosphatase (Roche Diagnostics) in 50 µl 50 mM Tris-HCl, pH 8.0, 100 mM NaCl, 10 mM $MgCl_2$, and 1 mM DTT for 1 h at 37°C. The beads were washed four times with 1 ml washing buffer 1, twice with 1 ml washing buffer 2 and once with 1 ml washing buffer 3. GST-Npr1 kinase activity was measured with MBP as described above.

2.9 Npr1 Autophosphorylation

For the determination of the autophosphorylation sites, GST-Npr1 was isolated with 500 µl Glutathione-Sepharose beads from a 6 l rapamycin-treated JC19a cell culture that was grown in nitrogen-rich media. Autophosphorylation was done on-beads in 700µl at 20 µM [γ^{32}P]-ATP in the absence of a substrate. Unincorporated ATP was washed from the beads with washing buffer 1. GST-Npr1 was digested from the beads in 200 µl washing buffer 3 with 2 µg endoproteinase LysC for 2 h at 37°C in a thermo shaker set to 1,200 rpm. The beads were removed by centrifugation and the LysC digest was incubated with 2 µg trypsin over night at 37°C. The reaction was stopped with TFA to 1% final concentration. Phosphopeptides were enriched and analyzed by reverse-phase chromatography. Radioactive peptides were located by liquid scintillation counting.

2.10 KESTREL Substrate Search

400 ml of TB50a cells were grown in YPD to an OD_{600} of 1.0. The cells were lysed in 2 ml lysis buffer (100 mM Tris-HCl, pH 8.0, 1% NP40, 1 mM EDTA, 1 mM benzamidine, 1 µg/ml pepstatin, 1 µg/ml leupeptin, 1 µg/ml aprotinin, 1 mM PMSF). The cleared lysate was loaded on an anion exchange column (MonoQ HR 5/5, Amersham Pharmacia Biotech, Uppsala, Sweden) connected to an Äkta FPLC system (Amersham Pharmacia Biotec). The column was equilibrated with buffer A (100 mM Tris-HCl, pH 8.0) and bound proteins were eluted at 1 ml/min with a linear 40 min gradient from buffer A to buffer B (100 mM Tris-HCl, pH 8.0, 500 mM NaCl) and 1 ml fractions were collected. For the kinase assay 40 µl of two adjacent fractions were pooled and used as protein substrates.

2.11 CNBr-Cleaved Protein Library

400 ml of TB50a cells grown in YPD to an OD_{600} of 1.0 were lysed in 4 ml lysis buffer (100 mM Tris-HCl, pH 8.0, 150 mM NaCl, 0,1% SDS, 1 mM EDTA, 1 mM benzamidine, 1 µg/ml pepstatin,

1 µg/ml leupeptin, 1 µg/ml aprotinin, 1 mM PMSF) in four 2 ml screw cap tubes as described above. After clearing the lysate at 12,000 rpm for 5 min, 2.2 µl Na-deoxycholate (10mg/ml) per 100 µl homogenate was added and the extract was incubated on ice for 30 min. Proteins were precipitated by adding 42 µl 20% TCA per 100 µl extract and incubation on ice for 30 min. Proteins were collected by centrifugation at 12,000 rpm for 5 min and SDS was extracted from the protein pellet by three washes with 1 ml acetone:acetic acid:triethylamine (90:5:5) (Henderson *et al*., 1979). The pellets were dried in a speed vac and redissolved in 2 ml 70% formic acid containing 100 mg cyanogen bromide. Cleavage of proteins was done over night on a thermo shaker set to 1,200 rpm at ambient temperature in the dark. The digest was centrifuged for 10 min at 12,000 rpm. The supernatant was injected at 0.75 ml/min onto a Vydac214TP54 C4 reverse-phase HPLC column (4.6 x 250 mm, Grace Vydac) that had been equilibrated in 0.1% TFA. After thorough washing of the column to remove traces of formic acid, bound proteins were eluted at 750 µl/min with a linear 60 min gradient from solvent A (0.1% TFA) to solvent B (80% Acetonitril, 0.1% TFA) and fractions were collected every minute. The pH of the fractions was neutralized with 20 µl 2 M Tris-HCl (pH 8.0) and dried to about 300 µl in a speed vac. For the kinase assay 40 µl of two adjacent fractions were used as protein substrates.

2.12 Analysis of *in vivo* Phosphorylation of Rpl24a

To search for *in vivo* phosphorylation of Rpl24a the lysis buffer (see 2.10) was supplemented with phosphatase inhibitors (10 mM NaF, 10 mM NaN_3, 10 mM pNpp, 10 mM $NaPP_i$, 10 mM β-glycerophosphate). Rpl24a was isolated from TB50a cells as described above. 100 µl of the Rpl24a-containing fraction was digested with 2 µg LysC for 2 h at 37°C. The digestion was stopped by acidifying with TFA (1% final concentration). Phosphopeptides were enriched with TiO_2 tips (see 2.1.5) and analyzed by reverse-phase chromatography. Fractions containing the peptide carrying the Ser26 phosphorylation were analyzed by LC-MS/MS (see 2.17).

2.13 Western Blotting

GST-Npr1 was isolated from lysates of 100 ml cultures of YPA1 cells transformed with pBS2 and electrophoresed on a 10% SDS gel. GST-Npr1 was blotted onto nitrocellulose membranes (Portran 0.45 µm, Schleicher&Schuell, Dassel, Germany) in 50 mM Tris-HCl, pH 7.5, 100 mM glycine, 0.01% SDS and 10% methanol at 450 mA for 30 min. The blot was blocked with TBST (20 mM Tris-HCl, pH 7.5, 150 mM NaCl, 0.1% Tween 20) containing 5% milk powder for 1 h at room temperature. Goat anti-GST and rabbit anti-Rsp5 antibodies were diluted 1:5,000, rabbit anti-

ubiquitin antibody was diluted 1:100 in TBST containing 2.5% milk powder and 10 mM sodium azide. The blot was incubated with the primary antibody over night at 4°C. The next day the membrane was washed once for 15 min and three times for 5 min in TBST at room temperature. HRP conjugated anti goat antibody (Pierce, Rockford, IL) or anti-rabbit antibody (Pierce, Rockford, IL) was diluted 1:10,000 in TBST containing 2.5% milk powder and was added to the blot for 1 h at room temperature. The blot was washed as before and secondary antibodies were detected with the ECL reagent (Amersham Biosciences, Otelfingen, Switzerland) according to the manufacturer's instructions.

2.14 Purification of GST-Rsp5

A 10 ml bacterial culture (BL21 *E. coli*) transformed with a plasmid encoding GST-RSP5 was induced for GST-Rsp5 expression with 0.4 mM IPTG for 3 h at 37°C. All subsequent steps were done at 4°C. Bacteria were harvested for 10 min at 4,300 rpm (Megafuge 1.0R) and lyzed by sonication in 1 ml lysis buffer (PBS, pH 7.4, 1% Triton X-100, Complete protease inhibitors from Roche Diagnostics, and 1mM PMSF). Cell debris was pelleted at 12,000 rpm for 5 min and GST-Rsp5 was adsorbed to Glutathione-Sepharose with a 40 µl bead suspension for 2 h on an end-over-end rotator. The beads were washed three times with washing buffer (PBS, pH 7.4, 1% Triton X-100) and twice with cleavage buffer (50 mM Tris-HCl, pH 7.0, 150 mM NaCl, 1 mM EDTA, 1 mM DTT, 0.01% Triton X-100). Rsp5 was cleaved from the beads with 2 µl PreScission protease in 50 µl cleavage buffer for 5 h on ice. The Glutathione-Sepharose beads were removed by centrifugation and Rsp5 was stored at -80°C.

2.15 Peptide Synthesis

Peptides were assembled on 4-Hydroxymethylphenoxyacetyl polyethylene glycol-dimethylacrylamide co-polymer resin (HMPA-PEGA, Novabiochem, 0.40 mmol/g loading) by the Fmoc strategy (26) using a model 433 peptide synthesizer (Applied Biosystems, San José, CA). Amino acid side chain protection was *t*-butyl for Asp, Ser, and Thr, trityl for Asn and Gln, while Lys and Arg were protected by *t*-butyloxycarbonyl and 2,2,4,6,7-pentamethyldihydrobenzofuran-5-sulfonyl, respectively. Peptide chain assembly was in DMF containing 0.45 M HBTU (2-(1-benzotriazol-1-yl)-1,1,3,3–tetramethyluronium hexafluorophosphate), N-Hydroxybenzotriazole (HOBt), and N-ethyldiisopropylamine (DIEA) according to the manufacturer's recommendations. The peptides were cleaved from the resin with TFA/H_20/thioanisole/ethanedithiol (40:2:2:1) containing phenol (67 mg/ml). After precipitating the peptides with cold ether, they were washed

several times with ether, and lyophilized. The crude peptides were purified by preparative reverse-phase HPLC on a PrepNova-Pak HR C18, (250 x 10 mm, 6 μm bead size, Waters, Milford, MA) at 12 ml/min using a linear gradient from 5% to 50% acetonitrile in 0.08% TFA. The molecular mass of the peptide was confirmed by mass spectroscopy and analytical reverse-phase HPLC indicated a purity of at least 98%.

2.16 Phosphopeptide Enrichment

Phosphopeptides were enriched with TiO_2 tips (Glygen, Columbia, MD). The columns were primed with 200 µl water, 200 µl methanol, and equilibrated with 200 µl 80% AcCN/0.1% TFA/300 mg/ml lactic acid (Sugiyama *et al*., 2007). The sample was acidified with TFA to 1% final concentration and loaded onto the column. The column was washed twice with 200 µl 80% AcCN/0.1% TFA/300 mg/ml lactic acid, twice with 200 µl 80% AcCN/0.1% TFA, and twice with 200 µl 0.1% TFA. Bound peptides were eluted with 100 µl 50 mM phosphate buffer, pH 8.0. The TiO_2 eluate was acidified with TFA to 1% final concentration.

2.17 Reverse-Phase Chromatography

Reverse-phase chromatography was done with a Vydac218TP52 C18 reverse-phase HPLC column (2.1 x 250 mm, Grace Vydac, Hesperia, CA) on a HP-1090 Liquid Chromatograph (Hewlett Packard) at a flow rate of 150 µl/min. The column was equilibrated with solvent A (0.1% TFA) and the acidified samples (0.1-1% TFA final concentration) were loaded manually via a 100 µl sample loop. The peptides were eluted with a linear 60 min gradient from 2% to 75% solvent B (80% acetonitrile, 0.1% TFA) except for the kinase assay (see 2.6.1) where a 90 min gradient was used. The effluent was monitored at 214 nm and fractions were collected every minute.

2.18 Mass Spectrometric Analysis

2.18.1 LC/MS

The digested proteins were separated by capillary liquid chromatography using a 300SB C-18 column (0.3x50 mm) (Agilent Technologies, Basel, Switzerland). An 85 min linear gradient from 2 to 60% solvent B (80% acetonitrile/0.1% formic acid) in solvent A (0.1% formic acid/2% acetonitrile) was delivered with a Rheos 2200 pump (Flux Instruments, Basel, Switzerland) at a flow of 50 µl/min. A pre-column split was used to reduce the flow to approximately 500 nl/min. 10 µl sample were injected with an autosampler thermostatted to 4°C onto a trap column (300SB C-

18 column, 0.3x50 mm, Agilent Technologies, Basel, Switzerland) for efficient desalting. The eluting peptides were ionized at 1.6 kV.

2.18.2 Mass Spectrometry

Peptides were analyzed on an Orbitrap FT hybrid instrument (Thermo Finnigan, San Jose, CA, USA). Data were acquired in data-dependent mode using Xcalibur software (Thermo Finnigan). The precursor ion scan MS spectra (*m/z* 300-2,000) were acquired in the Orbitrap at a resolution of 60,000. The three most intensive ions were isolated and fragmented in the linear ion trap by collision induced dissociation. Fragment ions were scanned in the Orbitrap with a resolution of 7,500. If required an MS^3 scan was performed if the most intense ion in the MS/MS spectra originated from a neutral loss of *m/z* 49 or 32.67 Da for a doubly or a triply charged peptide. The ion that underwent neutral loss of phosphoric acid was further fragmented and scanned in the Orbitrap at 7,500 resolution. In data-dependent LC-MS/MS experiments, dynamic exclusion was used with 30 s exclusion duration.

2.18.3 Databank Searching

MS/MS and MS^3 spectra recorded by the instrument were searched by the SEQUEST software (Eng *et al*., 1994) against the NCBI non-redundant databank. The search parameters were as follows: differential modification of 80 Da on Ser, and Thr (phosphorylation) and 16 Da on Met (oxidation), window for the precursor ion mass of 1.01 Da and the fragment ion mass tolerance of 0.5 Da, minimum cross correlation coefficient of 1.5, 2.0, and 2.5 for singly, doubly, and triply charged precursor ions, ΔC_n of 0.1.

3 Results

3.1 The Npr1 Kinase Responds to the Nitrogen Input

Npr1 belongs to a subfamily of fungus-specific protein kinases of the NPR/HAL5 family (Hunter and Plowman, 1997) and is involved in the post-Golgi sorting and the degradation of amino acid permeases (Magasanik and Kaiser, 2002). Up to now, the activity of Npr1 has been correlated with the optimal activity of several transport systems for nitrogenous compounds like the general amino acid permease Gap1 (Grenson, 1983b) but no substrates have so far been used for direct measurement of Npr1 activity.

To learn more about the substrate requirements of Npr1, a set of classical protein kinase substrates were phosphorylated *in vitro* with purified GST-Npr1 kinase from rapamycin-treated cells. The substrates containing acidic consensus sequences like calmodulin and eIF2 were not phosphorylated by GST-Npr1 at all (results not shown). Next, a set of substrates with basic consensus sequences like myelin basic protein (MBP), histone H4, histones from calf thymus type II-AS, and histone from calf thymus, were tested (Fig. 7).

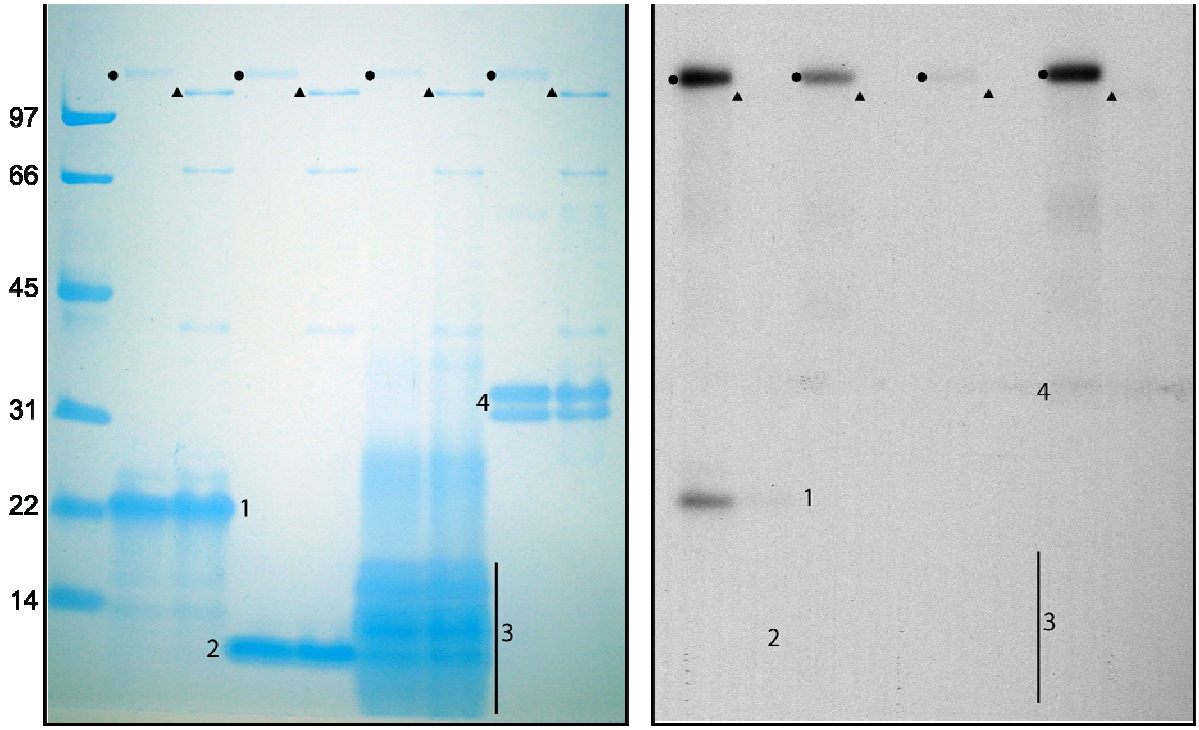

Figure 7: Substrates phosphorylated *in vitro* by GST-Npr1.

Myelin basic protein (MBP, 1), histone H4 (H4, 2), histone from calf thymus type II-AS (HII, 3), and histone from calf thymus (H, 4) were phosphorylated with GST-Npr1 (wt, marked with a circle) and kinase-dead GST-Npr1 (KD, marked with a triangle). The proteins were resolved on a 10% tris-tricine gel. **A:** Coomassie-blue stained gel. **B:** Autoradiograph of the phosphorylated substrates. For all assays 5 µg protein was used. For calf thymus histone, 50 µg was used in the assay.

Myelin basic protein was phosphorylated in a robust manner, while none of the histones were phosphorylated to any appreciable extent. A kinase-dead version of GST-Npr1, in which residues 432-512 had been deleted, was unable to phosphorylate MBP which rules out the possibility that a contaminating protein kinase other than Npr1 was responsible for MBP phosphorylation. Therefore, MBP was used as an *in vitro* substrate for all subsequent experiments.

Rapamycin mimics nitrogen starvation by inhibiting the core of the multiprotein complex TORC1 (Loewith *et al*., 2002). Isolation of GST-Npr1 from yeast cells that had been grown in a nitrogen-rich medium results in a protein that migrates as a diffuse band on SDS gel electrophoresis. In addition, GST-Npr1 obtained from a good nitrogen source migrates slower than the well focused band of phosphatase-treated GST-Npr1 (Fig. 8A). The mobility shift of GST-Npr1 following phosphatase treatment indicates substantial phosphorylation of GST-Npr1. Rapamycin treatment of

cells grown in nitrogen-rich medium results in a GST-Npr1 band whose migration resembles the phosphatase-treated protein, although with considerable smearing (Fig. 8A). Similar GST-Npr1 preparations were obtained from cells that had been grown in proline medium following treatment with glutamine (Fig. 8A). The shift was caused by treating the cells with 4 mM glutamine for 15 min before the cells were harvested and lysed. *In vitro* kinase assay with MBP showed a substantial increase of substrate phosphorylation following rapamycin treatment. A decrease of substrate phosphorylation was observed by treating the proline-grown cells with glutamine. Autophosphorylation of GST-Npr1 remained unaffected by the treatment (Fig. 8B).

A

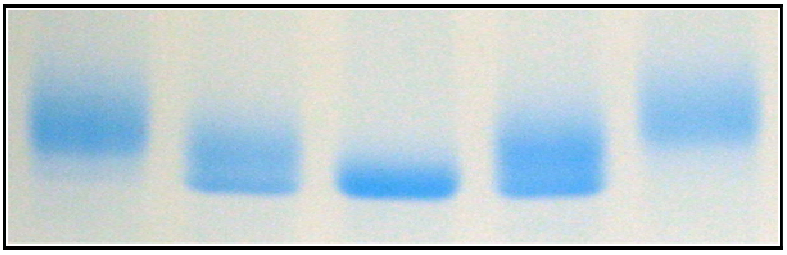

Figure 8: Activation and inactivation of Npr1.

A: Colloidal-blue stained GST-Npr1 isolated from yeast cells grown in nitrogen-rich medium (NH_4^+) or nitrogen-poor medium (Pro). rapa, AP, gln indicates treatment with rapamycin, alkaline phosphatase, or glutamine, respectively.
B: Colloidal-blue stained gel and autoradiograph of a kinase assay with GST-Npr1. MBP is marked with a triangle.

GST-Npr1 becomes activated by dephosphorylation when cells are grown in nitrogen-poor media. Therefore, to see if GST-Npr1 was activatable *in vitro*, the protein isolated from cells grown in rich nitrogen medium was treated with alkaline phosphatase. Although the shift to a faster migrating band indicated complete dephosphorylation of GST-Npr1 by alkaline phosphatase, phosphorylation of myelin basic protein was drastically decreased (Fig. 9). It appears therefore, that Npr1 requires a delicate balance between phosphorylation and dephosphorylation for optimal activity.

Figure 9: Phosphatase-treatment of GST-Npr1.

Colloidal-blue stained gel and autoradiograph of GST-Npr1 kinase (marked with a circle) isolated from cells grown in a nitrogen-rich medium (NH_4^+). rapa, AP indicates rapamycin or alkaline phosphatase treatment. The kinase activity of GST-Npr1 was measured with 5 µg MBP.

3.2 Autophosphorylation of Npr1 Does not Effect Kinase Activity

The previous experiments demonstrate that, in addition to substrate phosphorylation, extensive autophosphorylation of GST-Npr1 occurred, even though the extent of autophosphorylation varied with the substrate and assay conditions. Since Npr1 is subject to extensive regulation by phosphorylation, it is tempting to say that autophosphorylation is a self-regulatory mechanism to prevent 'over activation': as soon as sufficient activation is reached, Npr1 switches itself off by way of autophosphorylation. If this were the case, one would expect autophosphorylation whose extent equals *in vivo* phosphorylation at least at certain sites. To investigate this further, GST-Npr1 that had been isolated from proline-grown cells was incubated with ATP in the absence of a substrate.

Incubation with ATP alone induced no observable shift when compared to the treatment with glutamine (Fig. 10). Also, when GST-Npr1 was autophosphorylated prior to the addition of a substrate, no drop in substrate phosphorylation occurred (results not shown). Therefore, the extent to which Npr1 phosphorylates itself is minimal when compared to phosphorylation caused by nitrogen inactivation. Hence, the shift in electrophoretic mobility caused by Npr1 phosphorylation arises from upstream protein kinases and not by Npr1 autophosphorylation.

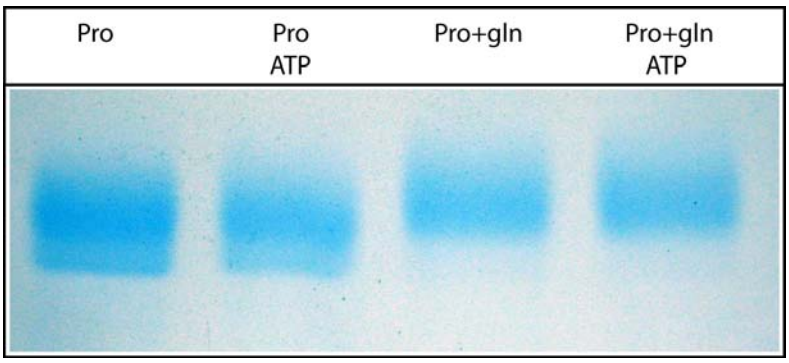

Figure 10: Mobility-shift of GST-Npr1 upon autophosphorylation

Colloidal blue stained gel of GST-Npr1 isolated from cells grown in proline media (Pro) and from proline-grown cells treated with glutamine (Pro+gln). Isolated GST-Npr1 was incubated with or without ATP in the absence of a substrate to allow autophosphorylation of GST-Npr1.

Despite the lack of an obvious autophosphorylation effect on Npr1, it was hoped that elucidation of the sites of autophosphorylation would reveal some insights into the consensus sequence of Npr1. Following autophosphorylation with [γ-^{32}P]-ATP, GST-Npr1 was digested with trypsin and one half of the digest was separated on a C18 reverse-phase column (Fig. 11A) and the other half was passed over a titanium dioxide column to enrich for phosphopeptides and subsequently chromatographed on a C18 reverse-phase column (Fig. 11B). The radioactivity recovered from the TiO_2 column eluted in four separate peaks from the reverse-phase column even though additional, unlabelled peptide peaks were obtained (Fig. 11C). The radioactivity from the crude digest eluted in the same four peaks (results not shown) indicating that no radiolabeled phosphopeptides were lost during phosphopeptide enrichment.

Figure 11: Autophosphorylation sites of Npr1

A/B: GST-Npr1 from rapamycin-treated cells was autophosphorylated with [γ-^{32}P]-ATP and digested with trypsin. The peptides were separated on a C18 reverse-phase column without (A) and with (B) prior enrichment of phosphopeptides.
C: Elution of radioactively labeled phosphopeptides from the C18 reverse-phase column.

The four radioactive peaks were further analyzed by LC/MS/MS to reveal the sites of autophosphorylation. The mass spectrum of peak 1 yielded a prominent triply and doubly charged ion of *m/z* 558.56 Da and 837.34 Da, respectively (Fig. 12A). The mass of the peptide matched exactly the calculated mass of the tryptic peptide SSSHIGSVSNSSSSDR (residues 45-60 of Npr1) with an additional phosphate. To confirm the assignment and to identify the site of autophosphorylation, the doubly and triply charged precursor ions were subjected to fragmentation. The fragmentation of the doubly charged peptide resulted in a prominent loss of phosphoric acid, observable as an intense *m/z* 788.35 Da ion (Fig. 12A). The presence of unphosphorylated y_{11} and y_{12} ions suggested that the site of phosphorylation resides in one of the three N-terminal serines of the peptide. Since the y_{14} ions were found to be phosphorylated the site of phosphorylation was assigned to the third serine from the N-terminus. This residue corresponds to Ser47 of Npr1 and had already been identified as an *in vivo* phosphorylation site in a previous study (Bonenfant, 2003). Interestingly, this site is rapamycin insensitive (Bonenfant, 2003) and is therefore most likely an autophosphorylation site.

The mass spectrum of peak 2 was dominated by a doubly charged ion of *m/z* 576.26 Da. This ion fits perfectly to the mass of the SQHSSIGDLK peptide carrying one phosphate (calculated mass 576.26 Da, observed mass 576.26 Da, residues 353-362 of Npr1) (Fig. 12B). As before, the fragmentation spectrum is dominated by the ion that underwent neutral loss of phosphoric acid (*m/z* 5527.27 Da). The y_6 ion was found to be phosphorylated and additional loss of phosphoric acid was observed, placing the site of phosphorylation to serine 5 of the phosphopeptide (corresponding to Ser357 of Npr1). Again, this site had been identified previously and was found to be rapamycin sensitive (Bonenfant, 2003). It should be noted that when the same peptide was obtained from cells grown in a good nitrogen source, additional phosphorylation on Ser353 and Ser356 was found (Bonenfant, 2003). Therefore, it is conceivable that phosphorylation encountered in this region of Npr1 results from phosphorylation by upstream protein kinases and autophosphorylation on Ser357 and that the rapamycin-sensitivity results from Ser353 and Ser356.

The peptide in peak 5 was observed as an intense doubly charged ion with an *m/z* of 860.38 Da. The calculated mass of the singly phosphorylated tryptic peptide SGSFSSQLGNFFFSK (residues 255-269 of Npr1) fits perfectly to the observed mass spectrum (Fig. 12C). The most intense ion in the fragmentation spectrum of *m/z* 811.88 Da results again from neutral loss of phosphoric acid. The sequence of the peptide was confirmed by the fragmentation spectrum and the serine at position 3 (corresponding to Ser257) was assigned to carry the phosphorylation due to the presence of unphosphorylated y_{11} and phosphorylated y_{13} ions. This site had also been previously found to be

rapamycin-sensitive (Bonenfant, 2003) but additional phosphorylation sites were found on Ser259 and Ser260. Therefore, the rapamycin sensitivity observed previously results from dephosphorylation of Ser259 and Ser260 and Ser257 phosphorylation is caused by autophosphorylation.

Unfortunately, any attempt to identify peptide 6 failed, most probably due to its large size. The unlabeled peptides in peaks 3 and 4 could be identified as HNMLGGCPK (peptide from the GST tag) and GEDHHHTQVDQSEAHIAGLEK (residues 763-782 of Npr1). They bound to the TiO_2 column most probably because of the histidines which are notoriously known to interact with immobilized metal ions (Mann *et al*., 2002).

Although not all autophosphorylation sites could be positively identified, the present study clearly shows that the extent to which Npr1 becomes autophosphorylated is negligible compared to *in vivo* phosphorylation. Furthermore, autophosphorylation has no influence on Npr1 kinase activity. Two out of the three autophosphorylation sites found in this study, namely serine at position 47 and 257 of Npr1, fulfill at least part of the Npr1 consensus sequence with a basic residue at position P-3 (see 3.4).

Figure 12: Identification of GST-Npr1 autophosphorylation sites

The radioactive peaks from the HPLC (Figure 5B) were analyzed by LC/MS/MS. **A:** Peak 1. **B:** Peak 2. **C:** Peak 5. The left panels represent the base peak chromatogram of the peptide eluted during LC/MS, the middle panels show the MS precursor spectra at the peak maximum, and the right panels represent the MS/MS fragmentation spectra of the ions that had been selected for fragmentation (boxed in the precursor spectrum). The identified phosphorylation sites are indicated with an asterisk. Phosphorylated fragment ions are indicated with a "P".

3.3 A Proteomics Screen for Npr1 Substrates

Although it was shown that Npr1 is involved in the sorting of amino acid permeases like Gap1 (De Craene *et al*., 2001; Grenson, 1983b), Mep2 (Dubois and Grenson, 1979; Feller *et al*., 2006), Put4 (Andre *et al*., 1993; Grenson, 1983b), and Tat2 (Schmidt *et al*., 1998) and even influences the sorting of the transcription factor Gln3 (Crespo *et al*., 2004), no direct targets of the Npr1 kinase have so far been found. In a first attempt, the KESTREL (kinase substrate tracking and elucidation) method was used to screen for *in vivo* substrates of Npr1 (Knebel *et al*., 2001).

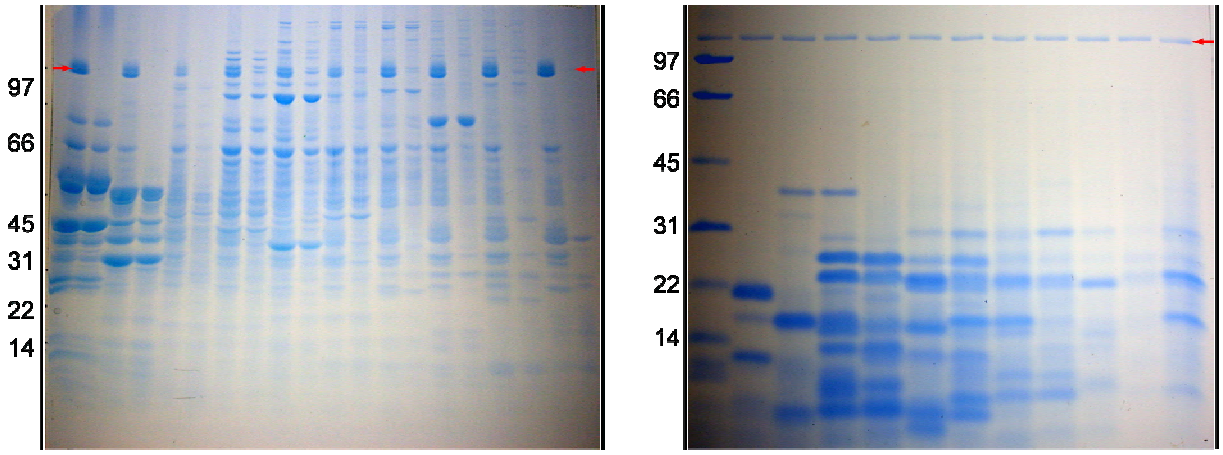

Figure 13: Npr1 substrate search

A: Fractionation of a yeast cell lysate on a MonoQ anion-exchange column. The proteins were eluted with a linear NaCl-gradient from 0-0.5 M. **B/C**: Coomassie-blue stained gel (B) and autoradiograph (C) of kinase assays with (+) or without (-) GST-Npr1. For each assay two neighboring fractions were pooled. GST-Npr1 is marked with red arrows. **D:** Reverse-phase HPLC of a CNBr-digest of a yeast cell lysate. **E/F**: Coomassie-blue stained gel (E) and autoradiograph (F) of kinase assays with active GST-Npr1. For each assay two neighboring fractions were pooled. The protein band at the top (marked with red arrows) represents GST-Npr1. The radioactive bands labeled 1-7 were digested and subjected to MS/MS identification.

A yeast lysate from TB50a cells grown in YPD medium was separated on an anion-exchange column. The protein containing fractions (flow through and fractions 16-43) were used as substrates for *in vitro* kinase assays with purified GST-Npr1 from rapamycin-treated cells (Fig. 13B/C). To check for endogenous kinase activity each fraction was incubated with [γ^{32}P]-ATP without exogenously added GST-Npr1. The individual kinase assays were checked for substrate phosphorylation by SDS gel electrophoresis. In all assays, GST-Npr1 underwent intensive autophosphorylation (Fig. 13C). The radioactively labeled proteins phosphorylated by GST-Npr1 were in-gel digested and subjected to protein identification via LC/MS/MS. Surprisingly, all radioactive bands (5-7, Fig. 13C) analyzed by mass spectrometry were identified as GST-Npr1 degradation products with serine at position 47 being phosphorylated (results not shown). It appears that the main phosphorylation products derive from C-terminal degradation products of GST-Npr1 that mask potential Npr1 substrates.

In parallel, the KESTREL method was modified (Fig. 13D-F). A yeast (TB50a) lysate was digested with cyanogen bromide (CNBr) and the resulting fragments were separated on a C4 reverse-phase column (Fig. 13D). Cyanogen bromide cleaves proteins at the C-terminal end of methionine. Since the occurrence of methionine in proteins is low, relatively large fragments are generated upon CNBr cleavage and it was assumed that the structural determinants (consensus sequence) for a potential Npr1 substrate were left intact. Also, it is likely that endogenous protein kinases will be either inactivated by CNBr cleavage or at least by the harsh cleavage conditions employed. After evaporating the organic solvent and pH adjustment, individual fractions were phosphorylated with rapamycin-treated GST-Npr1 and the kinase reactions were subjected to SDS gel electrophoresis on Tris-Tricine gels (Fig. 13E-F). Robust phosphorylation of a number of candidate substrates was evident by this method (Fig. 13F). To reveal the identity of the radioactive bands, they were excised, in-gel digested with trypsin and analyzed by LC/MS/MS (Fig. 14 and 15).

Figure 14: Identification of Rpl24a

The phosphopeptide in band 1 (Fig. 13) was identified as a peptide of the ribosomal protein Rpl24a. **A:** The LC/MS run (top panel) was searched for doubly charged peptides that underwent neutral loss (49 Da, H_3PO_4). An intense neutral loss was recorded at the scan at 31.5 min (middle panel) originating from the precursor mass of 451.72 Da (bottom panel). **B:** Fragmentation pattern of the 451.72 Da precursor ion corresponding to the Rpl24a peptide spanning residues 24 to 30. NL: neutral loss of H_3PO_4 from the doubly charged precursor ion (49 Da). **C:** MS^3 fragment spectrum of the GDS*KIFR peptide that underwent neutral loss. Fragment ions containing a dehydroalanine (phosposerine that had lost phosphoric acid) are indicated with a "Δ".

Eight different peptides of the most intensely phosphorylated protein in fraction 36/37 allowed to identify it as Rpl24a (*RPL24A*). To locate the site of phosphorylation, the LC-MS chromatogram was searched for the occurrence of peptides that had undergone neutral loss of phosphoric acid. A doubly charged peptide of *m/z* of 451.72 Da eluting early in the gradient showed neutral loss of 49 Da (Fig. 14). The MS/MS spectrum was dominated by the phosphate-specific fragmentation, but yielded very few diagnostic daughter ions which precluded identification of the peptide by data bank searching. Therefore, the peptide was re-fragmented by an MS^3 scan. This time, a richer fragmentation spectrum was obtained that allowed unambiguous identification of the GDSKIFR peptide encompassing residues 24-30 of Rpl24a. It was phosphorylated at the serine at position 26 of the whole protein.

Likewise, the radioactive bands 2-4 (Fig. 14F) were subjected to in-gel digestion with trypsin in the same manner, analyzed by LC/MS/MS and the peptides undergoing neutral loss of phosphoric acid were used to determine the site(s) of phosphorylation (Fig. 15). In contrast to Rpl24a peptide, both phosphorylated and unphosphorylated forms of the peptides were found and were used for identification. The phosphopeptide from band 2 showed a prominent neutral loss in the MS/MS spectrum (*m/z* 459.67 Da, Fig. 15A). The peptide sequence was identified as RFNS*SIGR of the ribosomal protein Rpl17a (*RPL17A*). The phosphopeptide of band 3 yielded neutral loss of *m/z* 49 Da (Fig. 15B) was identified as KVIS*NPLLAR deriving from the ribosomal protein Rps24a (*RPS24A*). The phosphopeptide isolated from band 4 (*m/z* 490.77 Da, Fig. 15C) produced enough ions to identify the peptide as LAAS*VVGVGK from ribosomal protein Rpl19a (*RPL19A*).

Figure 15: Identification of Rpl17a, Rps24, and Rpl19a

The phosphoproteins of bands 2-4 (Fig. 13) were identified as Rpl17a (A), Rps24a (B), and Rpl19a (C). The left panels show the base peak chromatogram (black) and the ion tracings for the unphosphorylated (red) and the phosphorylated (green) peptide. The corresponding MS/MS fragmentation spectra for the unphosphorylated (upper) and the phosphorylated (lower) peptide are shown on the right panels.

Similar to the results obtained in the above studies with protein substrates (see 3.1), the newly identified protein substrates are also basic (Table 3). The site of phosphorylation of the most readily phosphorylated Rpl24a is embedded in a sequence stretch that has a basic Arg and Lys at the P-3 and P+1 position, respectively. Two of the less readily phosphorylated ribosomal proteins contain a basic residue at the P-3 position. The protein phosphorylated most weakly lacks such a basic residue at P-3.

Protein	Peptide Sequence
Rpl24a	R.GDS*KIFR.F
Rpl17a	R.RFNS*SIGR.T
Rps24a	R.KVIS*NPLLAR.K
Rpl19a	R.LAAS*VVGVGK.R

Table 3: Peptide sequences of the identified proteins

The serine that was found to be phosphorylated is marked with an asterisk. Trypsin cleaved at the period.

3.4 Npr1 Recognizes a Basic Consensus Sequence Motif

Kinase specificity typically depends on the primary amino acid sequence surrounding the target phosphorylation site (Manning *et al*., 2002). Based on the *in vitro* phosphorylation sites in the ribosomal protein Rpl24a one can deduce the minimal consensus sequence (K/R)XXS(K/R) for a potential substrate. To further characterize the requirements for substrate phosphorylation by the Npr1 kinase, synthetic peptides containing the Rpl24a phosphoacceptor site were tested.

In a first attempt no phosphorylation was obtained with the decamer FVRGDSKIFR surrounding the phosphorylation site of Rpl24a. Next, a 35-mer encompassing residues 16-50 of Rpl24a (Rpl24a[16-50]) was synthesized and tested for phosphorylation in a kinase assay. At 20 μM ATP concentration, the peptide was rapidly and efficiently phosphorylated with very favorable kinetic

parameters (Fig. 16 and Table 4) while at 200 μM ATP and 5 μg peptide near quantitative phosphorylation was obtained after 30 min (results not shown).

Figure 16: Phosphorylation of the Rpl24a[16-50] peptide by Npr1

A: Time course of ^{32}P incorporation into the Rpl24a[16-50] peptide by GST-Npr1. **B:** Chromatogram of the Rpl24a[16-50] peptide on a C18 reverse-phase column. **D/E:** Chromatogram of the Rpl24a[16-50] peptide after phosphorylation with wild-type GST-Npr1 (D) and kinase-dead GST-Npr1 (E). The phosphorylated peptide is marked with an asterisk.

Analysis of the kinase assay by reverse-phase chromatography with a shallow gradient of acetonitrile showed that the Rpl24a[16-50] peptide was separated into two distinct peaks (Fig. 16C). Mass spectrometric analysis revealed that the first peak corresponds to the unphosphorylated and the second peak to the phosphorylated form of the peptide. Incubation of the Rpl24a[16-50] peptide with a kinase-dead version of Npr1 yielded no phosphorylation at all (Fig. 16D).

Since the Rpl24a[16-50] peptide contains five possible phosphorylation sites it was interesting to see if the same residue was phosphorylated as in the full length protein. Therefore, the mass of the

peptide after *in vitro* phosphorylation was determined. The peptide was observed as a mixture of unphosphorylated and singly phosphorylated peptide as highly charged ions (charge states ranging from +6 to +9) (Fig. 17A). Fragmentation of the phosphopeptide (+8 charge state) resulted in intense loss of phosphoric acid and in characteristic fragment ions (Fig. 17B). The y_{23} ion was not phosphorylated, indicating that no phosphorylation resides in the C-terminal portion of the peptide. The intense y_{30} ion at *m/z* of 611.16 was higher by 10 Da (*m/z*) than predicted, showing that the phosphate must reside at position 11 of the peptide (corresponds to Ser26 in the full-length protein).

Figure 17: Rpl24a[16-50] peptide phosphorylation

A: LC/MS/MS analysis of phosphorylated Rpl24a[16-50] peptide. The spectrum shows a mixture of unphosphorylated and singly phosphorylated peptide. The signals at 452.70, 509.17, 581.76, and 678.55 Da correspond to the unphosphorylated peptide, while the 461.59, 519.16, 593.19, and 691.88 Da correspond to the singly phosphorylated peptide. The charge states are indicated above the signals. **B:** MS/MS fragment spectrum of the 8+ charged phosphopeptide (boxed in panel A). The intense 506.91 ion corresponds to the precursor ion that underwent neutral loss (NL) of phosphoric acid. Phosphorylated fragment ions are indicated with a "P". The phosphorylated serine in the sequence is marked with an asterisk.

Next, a second peptide, encompassing residues 16-40 of Rpl24a (Table 4) was synthesized to investigate the effect of the very basic C-terminal residues of Rpl24a 16-50. Deletion of the C-terminal 10 amino acids had no effect on the V_{max} but reduced the K_m 8-fold. Further deletion of the N- and C-terminal residues to remove potentially interfering phosphorylation sites (corresponding to residues 21-33 of Rpl24a) left the V_{max} unchanged while the K_m dropped about 3-fold when compared to Rpl24a 16-40 (Table 4). Furthermore, Npr1 specifically phosphorylates

serine. Substituting the Ser by a Thr or Tyr in Rpl24a 21-33 completely abolished peptide phosphorylation (Table 4).

Peptide	**Sequence**	**V_{max} (pmol/min)**	**K_m (mM)**	**V_{max}/K_m**
[16-50]	GRGTLFVRGD**S**$_{26}$KIFRFQNSKSASLFKQRNKPRRIA	3.61	0.005	722.0
[16-50] A26	GRGTLFVRGD**A**$_{26}$KIFRFQNSKSASLFKQRNKPRRIA	n.d.	n.d.	-
[16-40]	GRGTLFVRGD**S**$_{26}$KIFRFQNSKSASLF----------	3.61	0.040	90.2
[21-33]	-----FVRGD**S**$_{26}$KIFRFQN----------	3.72	0.122	30.4
[21-33] K23	-----FV**K**GD**S**$_{26}$KIFRFQN----------	1.24	0.126	9.8
[21-33] A23	-----FV**A**GD**S**$_{26}$KIFRFQN----------	n.d.	n.d.	-
[21-33] R27	-----FVRGD**S**$_{26}$**R**IFRFQN----------	3.81	0.093	40.9
[21-33] A27	-----FVRGD**S**$_{26}$**A**IFRFQN----------	0.85	0.143	5.9
[21-33] P27	-----FVRGD**S**$_{26}$**P**IFRFQN----------	n.d.	n.d.	-
[21-33] T26	-----FVRGD**T**$_{26}$KIFRFQN----------	n.d.	n.d.	-
[21-33] Y26	-----FVRGD**Y**$_{26}$KIFRFQN----------	n.d.	n.d.	-

Table 4: Kinetic parameters of phosphorylation of Rpl24a-derived peptides

Peptides encompassing the phosphorylation site of Rpl24a were tested as substrates for GST-Npr1 to determine the kinetic parameters K_m and V_{max}. The phosphorylated Ser (position 26 of the full length Rpl24a protein) is marked in red and mutated residues in blue.

Changing the (P-3) position from Arg to Lys had only a slight effect on V_{max}, whereas replacement by Ala abolished peptide phosphorylation altogether. Substitution of the (P+1) Lys for Arg improved the kinetic parameters somewhat (Table 4). Interestingly, Ala at the (P+1) position was tolerated, although with a reduced efficiency in peptide phosphorylation, whereas Pro next to the site of phosphorylation was not tolerated at all (Table 4).

By increasing the concentration of the FVRGDSKIFR Rpl24a[21-30] decamer tenfold substrate phosphorylation could be achieved (Fig. 18). Replacement of the basic P+1 lysine by glutamate caused a five-fold drop in peptide phosphorylation, while replacement of both, P-3 and P+1 position by glutamates abolished peptide phosphorylation altogether (Fig. 18 B/C). It appears that the basic residues at position P-3 and P+1 were crucial determinants of the consensus sequence of Npr1.

Figure 18: Rpl24a[21-30] peptide phosphorylation

Base peak chromatograms of the decapeptides FVRGDSKIFR (A), FVRGDSEIFR (B), and FVEGDSEIFR (C) that were phosphorylated by GST-Npr1. The phosphorylation site is marked in red, residues that were mutated in blue. The *m/z* values originate from the triply charged peptides. The phosphorylated peptides are marked with an asterisk.

3.5 *In vivo* Phosphorylation of Rpl24a

In a global analysis of protein phosphorylation in yeast, Rpl24a was found to be phosphorylated *in vivo* at three different sites (Chi *et al*., 2007). Among them was Ser26, the same site that becomes phosphorylated *in vitro* by GST-Npr1.

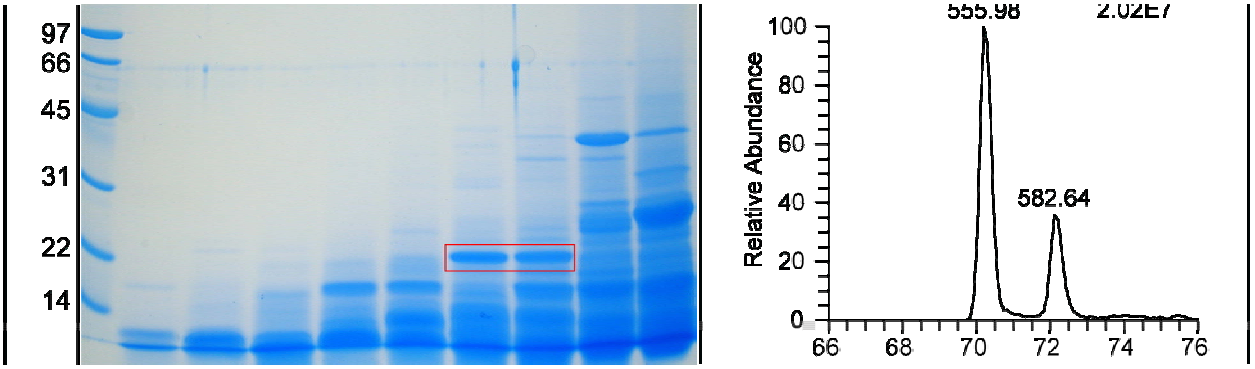

Figure 19: *in vitro* phosphorylation of Rpl24a by GST-Npr1

A: SDS PAGE of a CNBr-digested yeast lysate that was separated by C4 reverse-phase chromatography. Rpl24a (boxed) elutes in fraction 36 and 37. **B:** Base peak chromatogram of unphosphorylated (*m/z* 555.98) and phosphorylated (*m/z* 582.64) Rpl24a peptide IYPGRGTLFVRGDSK (residues 13-27). **C:** MS/MS fragmentation spectrum of the triply charged unphosphorylated peptide (*m/z* 555.98). **D:** MS/MS fragmentation spectrum of the triply charged phosphorylated peptide (*m/z* 582.64). NL: neutral loss of H_3PO_4 from the triply charged precursor ion (32.66 Da).

The fraction containing ribosomal protein Rpl24a (Fig. 19A) was digested with endoproteinase LysC and the resulting digest was analyzed by LC/MS/MS. Due to the complexity of the digest, neither the predicted peptide encompassing Ser26 (IYPGRGTLFVRGDSK, residues 13-27), nor its phosphorylated counterpart was found (results not shown). To reduce the complexity of the sample, LysC digested fraction was fractionated off-line on a C18 reverse-phase column. To calibrate the elution position of the Ser26-containing peptide, the fraction containing Rpl24a was phosphorylated with GST-Npr1 and, after removal of unbound [γ^{32}P]-ATP, digested with endoproteinase LysC and separated by C18 reverse-phase HPLC. Phosphorylated IYPGRGTLFVRGDSK peptide from Rpl24a was located by liquid scintillation counting. To show that the radioactively labeled fraction contained the IYPGRGTLFVRGDSK Rpl24a peptide, LC/MS/MS analysis was carried out (Fig. 19B-D). The LC/MS analysis proved the presence of both, unphosphorylated and singly phosphorylated IYPGRGTLFVRGDSK peptide (Fig. 19B). Also, the MS/MS spectrum was in agreement with Ser14 (Ser26 of Rpl24a) as the phosphorylated residue. Next, Rpl24a was partially purified from either untreated or rapamycin-treated YPA1 cells, digested individually with endoproteinase LysC and chromatographed in successive runs on a C18 reverse-phase column. The corresponding fractions containing the presumed IYPGRGTLFVRGDSK peptide (from untreated or rapamycin-treated cells) was analyzed by LC/MS/MS. Even though the nonphosphorylated IYPGRGTLFVRGDSK peptide was recovered with good yields in both runs, the presence of phosphorylated peptide could not be unambiguously detected (results not shown), presumably due to low stoichiometry of phosphorylation. To avoid that the phosphorylated peptides would go undetected due to ion suppression effects, the LysC digests containing the IYPGRGTLFVRGDSK peptide were passed individually over a TiO_2 column to enrich for possible phosphopeptides. After desalting, LC/MS/MS analysis could indeed detect the phosphopeptide (*m/z* 582.63, Fig. 20) although at very low levels. In addition, unphosphorylated peptide was also detected with comparable intensity (*m/z* 555.97, Fig. 20). This underlines the low stoichiometry of Rpl24a phosphorylation *in vivo* since the phosphopeptide was selected against a considerable excess of unphosphorylated peptide. When comparing the ion intensities of the phosphorylated IYPGRGTLFVRGDSK peptide isolated from untreated- and rapamycin-treated cells, no significant increase was seen in the phosphopeptide from rapamycin-treated cells. Therefore, it is questionable whether Rpl24a is an *in vivo* substrate for Npr1.

Figure 20: Comparison of *in vivo* phosphorylation of Rpl24a from untreated and rapamycin treated cells

Mass spectrometric analysis of the peptide IYPGRGTLFVRGDSK of Rpl24a that was isolated from cells grown in nitrogen-rich media (A) and nitrogen-rich media and treated with rapamycin (B). The graphs show the base peak chromatogram (black) and the ion tracings for the unphosphorylated (red) and the phosphorylated form (green) of the peptide.

3.6 Snf1 and Rsp5 Interact with Npr1

The search for Npr1 substrates and upstream kinases was extended to pull-down assays followed by mass spectrometric identification and western blotting (Fig. 21). GST-Npr1 was isolated from cells that had been grown in nitrogen-rich medium. One part was loaded on a 10% Tris-tricine gel and the proteins were stained (Fig. 21A). The other part was loaded on a 10% mini-gel and after blotting onto nitrocellulose GST-Npr1 was probed with an anti-GST antibody (Fig. 21B). As a control, GST alone was used. GST-Npr1 migrated at about 120 kDa on polyacrylamide gels. The three most intense bands at the lower part of the gel at a molecular weight between about 25 and 40 kDa (Fig. 21A) were identified as C-terminal degradation products of GST-Npr1 by mass spectrometry. In the lowest band only GST fragments were found whereas for the other two bands also N-terminal

peptides of Npr1 were identified (results not shown). The same three bands also reacted with an anti-GST antibody (Fig. 21B). The diffuse bands at a molecular weight of about 43 kDa and 66 kDa (Fig. 21B) were also GST-Npr1 degradation products since they also reacted with the anti-GST antibody. The doublet at a molecular weight of about 67 kDa (Fig. 15A, marked with an asterisk) was identified as Hsp70 (Table 5).

Figure 21: GST-Npr1 pull-down

A: Colloidal-blue stained gel of a GST-Npr1 pull-down from cells grown in nitrogen-rich media. **B:** Western blot of a GST-Npr1 pull-down (GST-NPR1) and a pull-down where GST alone was used (GST). Both pull-downs were done with cells grown on nitrogen-rich media. The blot was probed with an anti-GST antibody. Bands marked with circles correspond to C-terminal degradation products of GST-NPR1 and the doublet marked with an asterisk is Hsp70. GST is marked with a triangle.

GST-Npr1 from either untreated or rapamycin-treated cells was analyzed by mass spectrometry. GST-Npr1 from both conditions was loaded separately on a polyacrylamide gel, the gel was cut in slices and the proteins were in-gel digested with trypsin and identified by MALDI-TOF-TOF mass spectrometry. The top 20 matches are listed in Table 5. The largest group of protein identified was comprised of heat shock proteins of the Hsp70 family. In addition, a number of ribosomal proteins were identified.

Name	Description	Molecular Weight	# peptides +rap	# peptides - rap
SSA1	Heat shock protein of the Hsp70 family	70 kDa	17	17
SSA2	Heat shock protein of the Hsp70 family	69 kDa	16	17
SSB1	Heat shock protein of the Hsp70 family	67 kDa	14	13
SSB2	Heat shock protein of the Hsp70 family	67 kDa	14	13
NPR1	Protein kinase that stabilizes several plasma membrane amino acid transporters	112 kDa	9	14
SNF1	AMP-activated Ser/Thr protein kinase, required for transcription of glucose-repressed genes	72 kDa	9	6
SSE1	Heat shock protein of the Hsp70 family	77 kDa	7	7
SSC1	Heat shock protein of the Hsp70 family	71 kDa	6	1
SSA4	Heat shock protein of the Hsp70 family	70 kDa	6	0
RSP5	Ubiquitin-protein ligase involved in ubiquitin-mediated protein degradation	92 kDa	8	17
SNF4	Activating gamma subunit of the AMP-activated Snf1p kinase complex	36 kDa	6	4
RL4A	60S ribosomal protein	39 kDa	7	5
GRP78	Heat shock protein of the Hsp70 family	74 kDa	6	3
RL3	60S ribosomal protein	44 kDa	5	6
RL8	60S ribosomal protein	28 kDa	6	3
RL20	60S ribosomal protein	20 kDa	4	7
RS3	40S ribosomal protein	27 kDa	5	3
RL27	60S ribosomal protein	16 kDa	4	1
RLA0	60S ribosomal protein	34 kDa	4	5
GAL83	One of three possible beta-subunits of the Snf1 kinase complex	47 kDa	5	2

Table 5: GST-Npr1 pull-down analysis

Top 20 matches of proteins that were identified from GST-Npr1 pull-downs from cells grown in a nitrogen-rich medium. +/-rap indicates rapamycin-treated and untreated cells. #peptides: number of peptides that were identified of each protein.

An interesting Npr1 interactor, the Snf1 kinase, together with its regulatory subunits Gal83 and Snf4 was identified in the pull-down. Snf1 is the yeast homolog of the mammalian AMP-activated protein kinase (AMPK) an enzyme involved in carbon dependent regulation of specific transcription factors (Carlson, 1999). Snf1 also phosphorylates Gln3, a transcription factor involved in nitrogen catabolite repression (Bertram *et al*., 2002). Further, Snf1 was shown to be involved in pseudohyphal differentiation of diploid cells in response to nitrogen limitation (Kuchin *et al*., 2002). Also present in the pull-down, although not among the top twenty candidates, was the glutamine synthetase Gln1 that catalyzes the formation of glutamine from glutamate and ammonia (Mitchell and Magasanik, 1983). Interestingly, the E3 ubiquitin ligase Rsp5 was also found in the pull-down. Rsp5 was shown to ubiquitinate the general amino acid permease Gap1 which in turn leads to endocytosis and degradation in the vacuole (Hein *et al*., 1995). Since Npr1 prevents Gap1 from degradation in nitrogen-poor media (De Craene *et al*., 2001) it was decided to investigate the interaction between Npr1 and Rsp5 in more detail (see 3.7). With the exception of Gln1, the same repertoire of candidate interactors were found in a GST-Npr1 pull-down from cells treated with rapamycin. Gln1 was only found in the rapamycin-treated pull-down.

3.7 Npr1 Interacts via a Short C-terminal Sequence Stretch with Rsp5

The E3 ubiquitin ligase Rsp5 that was found in the pull-down of GST-Npr1 contains three WW-domains that were shown to bind a Pro-Pro-X-Tyr (PPXY) motif in client proteins (Ingham *et al*., 2004). Npr1 contains a PPSY sequence between residues 673-676 in the catalytic domain that is a likely candidate to interact with Rsp5. To analyze Rsp5-Npr1 interaction in more detail, the tyrosine of the PPSY sequence was mutated to a glycine. From yeast cells expressing wild-type GST-Npr1 or the GST-Npr1 (Y-G676) mutant Npr1 was isolated with glutathione beads and the presence of Rsp5 in the pull-down was probed with an anti-Rsp5 antibody. Mock pull-downs were done from cells producing GST alone. Rsp5 was clearly detected in the pull downs, confirming the proteomics data with GST-Npr1 as bait. Rsp5 remained stably bound to Npr1 regardless whether the cells were grown in nitrogen-rich or nitrogen-poor medium (Fig. 22B). However, the interaction is considerably weakened when using the PPSG mutant (Fig. 22B). Residual interaction probably still occurs via the two remaining prolines with the WW-domains in Rsp5. No binding was observed with GST alone. Therefore, Rsp5 binds specifically to Npr1 via its PPSY sequence, although in a nitrogen-independent fashion.

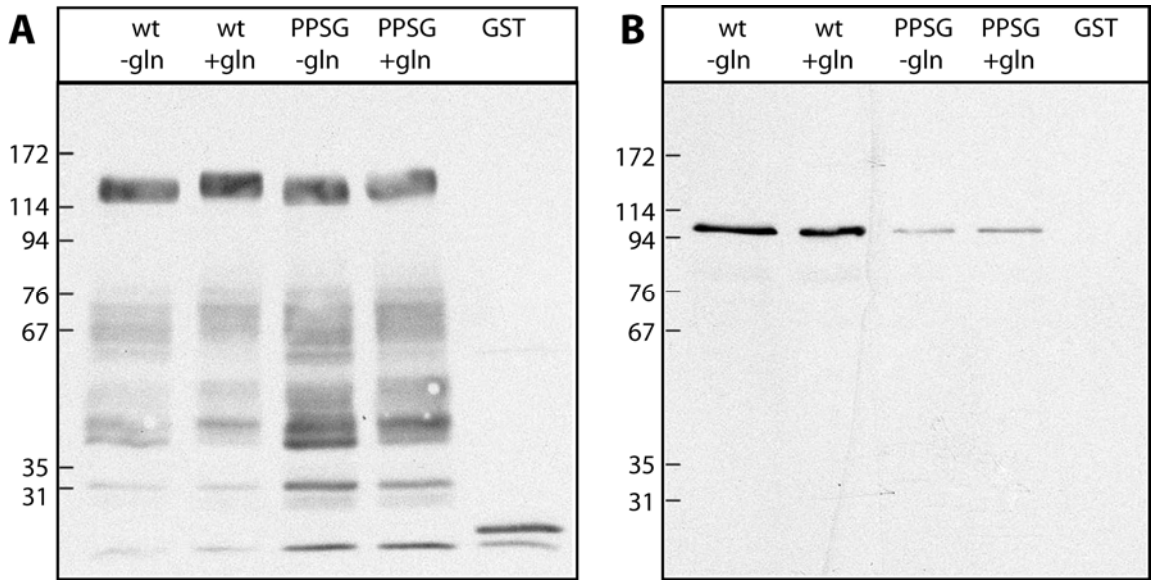

Figure 22: Npr1-Rsp5 interaction

GST-Npr1 wild-type (wt) and GST-Npr1(Y-G676) was isolated from cells grown in proline medium either treated with (+gln) or without glutamine (-gln). As a control GST alone was used as bait from cells grown in a nitrogen-rich medium (GST). Western blots were probed with anti-GST antibodies (A) or with anti-Rsp5 antibodies (B).

One explanation for this interaction is that the activity of Rsp5 is controlled by Npr1 phosphorylation. In nitrogen-poor medium, active Npr1 phosphorylates and inactivates Rsp5 to prevent ubiquitination of the Gap1 permease. Therefore, GST-tagged Rsp5 was isolated from yeast cells and phosphorylated *in vitro* with GST-Npr1 (Fig. 23). Since both proteins have similar molecular weights when fused to GST, the tag from Rsp5 was cleaved off with PreScission protease to reduce its molecular weight. Incubating the protease-cleaved Rsp5 with GST-Npr1 unfortunately yielded no detectable phosphorylation other than Npr1 autophosphorylation (Fig. 23B).

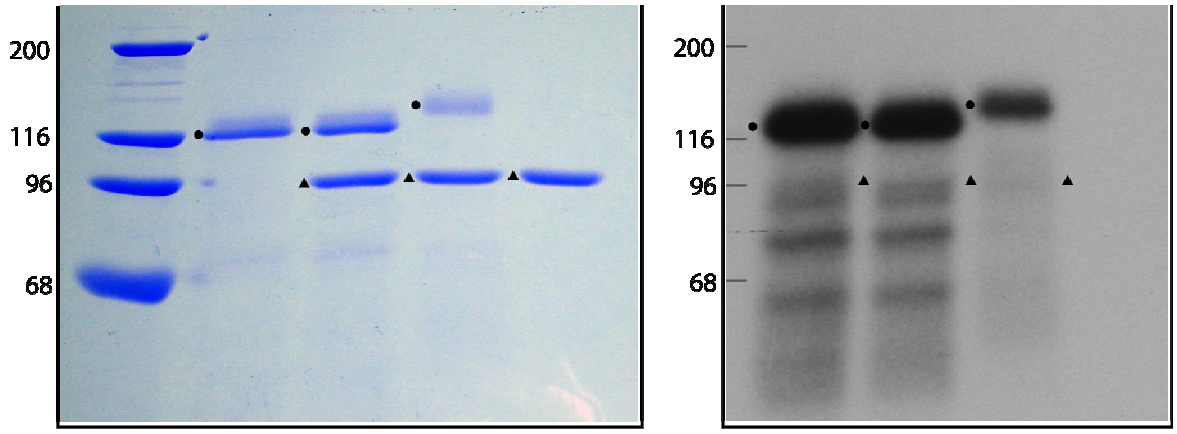

Figure 23: *In vitro* phosphorylation of Rsp5

Phosphorylation of Rsp5 by rapamycin-treated (+rapa) or untreated (-rapa) GST-Npr1. **A:** Coomassie-blue stained gel of the kinase assays. GST-Npr1 is marked with filled circles and Rsp5 with a filled triangle.
B: Autoradiograph of the kinase assays.

Alternatively, Npr1 could be a substrate for ubiquitination by Rsp5. Short-lived proteins generally contain regions enriched with Pro, Glu, Ser, and Thr (Rogers *et al*., 1986). These so-called PEST sequences are signals for protein instability. Phosphorylation within PEST sequences often specify their recognition and processing by the ubiquitination pathway (Lanker *et al*., 1996). Sequence analysis of Npr1 revealed three PEST sequences. Two of them are located at the N-terminal hyperphosphorylated domain of Npr1. Interestingly, the PPSY motif is located in a predicted PEST sequence encompassing residues 667-681 of Npr1 and the PEST sequence is followed by a highly basic stretch of three lysines that could act as ubiquitin acceptors. To test if Npr1 becomes ubiquitinated, GST-Npr1 was isolated from cells that had been grown in proline medium or from proline-grown cells that had been treated with glutamine to inactivate Npr1. To prevent inadvertent deubiquitination, N-ethylmaleimide was added to the lysis buffer and ubiquitination was probed with an anti-ubiquitin antibody (Fig. 24).

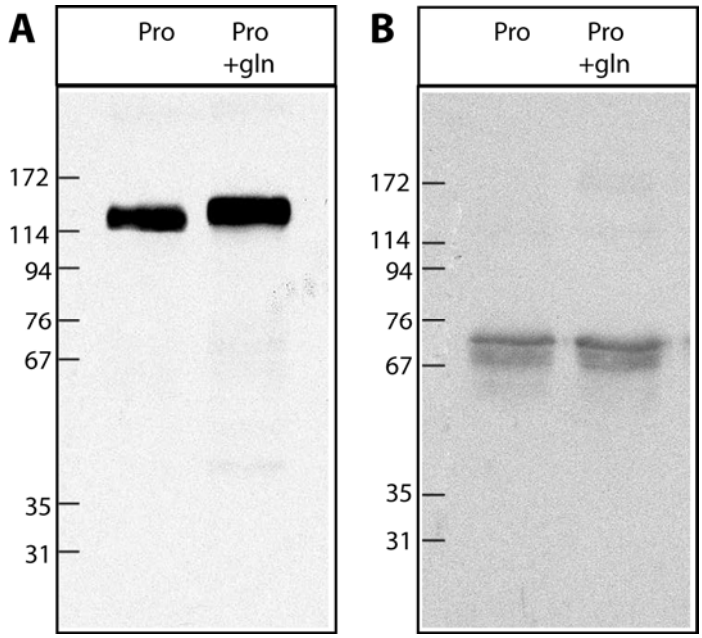

Figure 24: Npr1 ubiquitination

GST-Npr1 was isolated from cells grown in proline medium (Pro) and from glutamine treated cells (Pro +gln) and probed with anti-GST antibodies (A) or with anti-ubiquitin antibodies (B).

By using an anti-GST antibody, the transition from active, hypophosphorylated to inactive hyperphosphorylated Npr1 was evident. However, probing the two Npr1 pull-downs with an anti-ubiquitin antibody yielded no signal at the molecular weight of GST-Npr1. Instead of, proteins between 67 and 75 kDa molecular weight were decorated with the antibody. If this were ubiquitinated Npr1 degradation products, they must have arisen from C-terminal proteolysis following ubiquitination as the corresponding region could not be decorated with the anti-GST antibody. On the other hand, the immunoreactive signals with the anti-ubiquitin antibody could have well been generated by crossreactivity with keratins that are particularly abundant in the 67 to 75 kDa region in SDS gels (results not shown). Therefore, the biological significance of the interaction between Npr1 and Rsp5 clearly needs further investigation.

3.8 The role of the N-terminal Domain of Npr1

As mentioned in the introduction, three N-terminal mutations of GST-Npr1 were constructed to delete the first (GST-Npr1Δ1-143) and the second (GST-Npr1Δ252-413) phosphorylation cluster individually or in combination (GST-Npr1Δ1-431). The mutants grew equally well as the cells with full length GST-Npr1. The strain carrying kinase-dead GST-Npr1 was unable to grow in nitrogen-poor medium, emphasizing the importance of the kinase activity of Npr1. To see if the mutations had any effect on the kinase activity of Npr1, full-length GST-Npr1, GST-Npr1Δ1-143, GST-Npr1Δ252-413 and GST-Npr1Δ1-431 was isolated from rapamycin-treated cells and tested with MBP, Rpl24a and the 35-mer Rpl24a[16-50] peptide as substrates (Fig. 25).

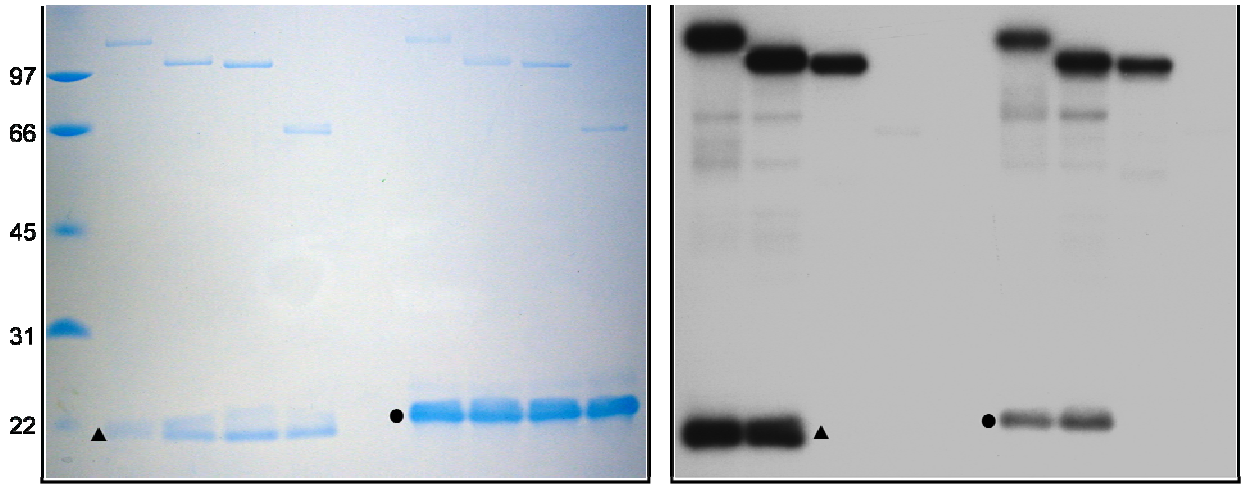

Figure 25: Phosphorylation with Npr1 mutants

Phosphorylation of Rpl24a, myelin basic protein and the Rpl24a[16-50] peptide with full-length GST-Npr1 (wt) and the N-terminal GST-Npr1deletion constructs where residues 1-143 (Δ1), 252-413 (Δ2) and 1-431 (Δr) of Npr1 are deleted. All constructs were isolated from rapamycin-treated cells. **A:** Coomassie-blue stained gel and autoradiograph of a kinase assay with Rpl24a (marked with a triangle) and MBP (marked with a circle) as substrates. **B:** Reverse-phase HPLC of the Rpl24a[16-50] peptide phosphorylated with full-length (wt), or GST-Npr1 Δ1, Δ2, and Δr mutants. The phosphorylated peptide is marked with an asterisk.

Full-length GST-Npr1 phosphorylated both, Rpl24a and MBP in a robust manner, although Rpl24a proved to be a much better substrate than MBP (Fig. 25A). In addition to substrate phosphorylation, intense autophosphorylation of GST-Npr1 occurred. GST-Npr1Δ1-143 was able to phosphorylate the substrates to about the same extent than wild-type GST-Npr1, whereas GST-Npr1Δ252-413 and GST-Npr1Δ1-431 lost their ability to phosphorylate MBP and Rpl24a (Fig. 25A). Identical results were obtained using the Rpl24a[16-50] peptide as a substrate (Fig 25B). No peptide phosphorylation was observable in a kinase assay with GST-Npr1Δ252-413 and GST-Npr1Δ1-431. Therefore, the second cluster of phosphorylation presumably contains a substrate interacting domain that is required for locking the substrate for subsequent phosphorylation. Identical results were obtained when the cells were isolated from proline-grown cells (results not shown). These results are in sharp contrast to the findings that deletions of neither phosphorylation cluster nor the entire regulatory domain showed any phenotype during growth of yeast cells in nitrogen-poor media.

4 Discussion

The uptake and processing of nutrients is a tightly regulated process. To optimally use the available nutrients, the yeast *Saccharomyces cerevisiae* responds to the quality of the carbon and nitrogen source present in the environment. Depending on the availability of nutrients, the cells execute the appropriate developmental program and adapt their metabolic and transcriptional programs to provide the proper set of proteins responsible for uptake, transport, and processing of nutrients. The Ser/Thr protein kinase Npr1 plays a major role in the adaptational process of amino acid transporters. Npr1 is required for optimal activity of several transport systems for nitrogenous compounds like the general amino acid permease Gap1 and the proline permease Put4 under nitrogen-poor conditions (Magasanik and Kaiser, 2002). In contrast, it was suggested that Npr1 promotes the down-regulation of the high affinity/low capacity permease Tat2, which is responsible for the uptake of tryptophan (Schmidt *et al*., 1998). Although it is known that Npr1 is involved in these processes, a direct target of Npr1 has not been found so far. Permeases like Gap1 could be direct targets of Npr1. Phosphorylation by Npr1 under poor nitrogen conditions would prevent their ubiquitination and subsequent degradation in the vacuole. It was shown that Gap1 is indeed phosphorylated in proline-grown cells and that its degree of phosphorylation is reduced in an *npr1Δ* mutant. However, in an *npr1/npi1* double mutant Gap1 remains extensively phosphorylated indicating that Gap1 phosphorylation is not strictly dependent on Npr1 (De Craene *et al*., 2001). Another possibility is that Npr1 inhibits the activity of the Rsp5/Bul1/Bul2 complex by phosphorylating one of its components to prevent Gap1 ubiquitination in a nitrogen-poor medium. Although Npr1 was shown to bind to Rsp5, attempts to phosphorylate Rsp5 *in vitro* failed (Fig. 23).

The Search for an Npr1 Substrate

To screen for Npr1 substrates in an unbiased way, whole cell lysates were used as substrates for *in vitro* kinase assays with purified GST-Npr1. In a KESTREL assay (Knebel *et al*., 2001) the cell lysate is usually separated on an anion exchange column to reduce the complexity of the sample before testing the fractions for the presence of substrates with exogenously added kinase. One major pitfall of the KESTREL method is that cell extracts contain both, the target protein as well as protein kinases capable of phosphorylating endogenous substrates. In this way, hundreds of proteins become phosphorylated upon incubation with MgATP and this high background masks potential target proteins. Therefore, one needs to be able to distinguish between endogenous and exogenous substrate phosphorylation by the kinase of interest. In the assays described in this work, however,

the major problem was not the presence of endogenous protein kinases, but the pronounced proteolysis of GST-Npr1. Analysis of radioactively labeled bands revealed only degradation products of Npr1. Therefore, phosphorylated degradation products of GST-Npr1 masked potential substrate proteins. The high background caused by phosphorylation of Npr1 degradation products can of course be overcome by using very low amounts of exogenously added Npr1 kinase. This proved to be unsuitable as the reaction is considerably slowed down. Naturally, preventing proteolysis by refining the mixture of added protease inhibitors could also cure the problem. Unfortunately, none of these simple tricks alleviated the high phosphorylation background caused by degradation products of GST-Npr1.

The Npr1 autophosphorylation products were particularly disturbing in the range between 40 to 120 kDa. To separate potential Npr1 substrates from Npr1 autophosphorylation products, the lysate was digested with CNBr. It was hoped that upon CNBr cleavage the molecular weight of potential substrates is reduced to below the phosphorylation products caused by proteolysis. By using the same amount of a cell lysate, distinct bands well below the Npr1 proteolysis products were efficiently phosphorylated by GST-Npr1. Surprisingly, all radioactive bands analyzed by mass spectrometry were ribosomal proteins. Although non-ribosomal protein fragments were also present in the fractions of the reverse-phase column, only ribosomal proteins were substrates for Npr1. The harsh conditions (70% formic acid) in the CNBr assay caused ribosomes in the cell lysate to dissociate into its components. Due to their high abundance, they can outcompete low abundance *bona fide* substrates. In contrast, in the KESTREL assay ribosomes remained intact and were not recovered during the separation process. Nevertheless, a persistent problem of KESTREL screens is the detection of low abundance Npr1 substrates.

The ribosomal protein that was most efficiently phosphorylated by Npr1 was Rpl24a. Rpl24 is a component of the large ribosomal subunit in yeast. It is encoded by two functional genes (*RPL24A* and *RPL24B*) which differ in only 5 of 155 amino acids. Both of them are not essential proteins but disruption of both genes causes a slightly longer doubling time for the cells compared to wild-type cells. In addition polysome profiles suggested that the absence of Rpl24 leads to stalled translation initiation complexes (Baronas-Lowell and Warner, 1990). Rpl24 was suggested to influence the kinetics of translation (Dresios *et al*., 2000). Growth of yeast cells in nitrogen poor media slows down the translation rate (Smirnova *et al*., 2005). Since Npr1 is active under these conditions it would be plausible if it phosphorylated Rpl24a directly for slowing down translation. In addition, in a global analysis of protein phosphorylation in yeast, Rpl24a was found to be phosphorylated *in vivo* at three different sites (Chi *et al*., 2007). Among them was Ser26, the same site that becomes

phosphorylated *in vitro* by GST-Npr1. This was evidence enough to test if Npr1 phosphorylates Rpl24a *in vivo*. Investigating Rpl24a *in vivo* phosphorylation turned out to be difficult because of the low stoichiometry of phosphorylation. The results suggest that Rpl24a becomes phosphorylated in an Npr1 independent way (see 3.5).

Future experiments will aim at designing more sensitive substrate screens than the KESTREL method. This could be achieved by reducing the complexity of the sample with multiple chromatographic steps to find low abundance substrates. Since Npr1 facilitates sorting of proteins en route to the plasma membrane, membrane enriched fractions could be a good starting point for searching substrates. Alternatively, yeast protein chips containing the ensemble of the yeast proteome (Ptacek *et al*., 2005) could be tested in kinase assays with purified Npr1 alleviating the problem of detecting low abundance substrates.

Is Npr1 a Basophilic Protein Kinase?

The specificity of protein kinases is determined to a large extent by the amino acids that surround the site of phosphorylation. The minimal substrates for protein kinases are peptides that can be exploited to probe kinase-substrate recognition. The results obtained in this study suggest a preference of Npr1 for basic substrates. The peptide FVRGDSKIFRFQN modeled around the phosphorylation site of Rpl24a has basic residues at position P-3 and P+1. Replacement of this position with Ala abolished phosphorylation by Npr1 altogether underlining the strong preference for basic P-3 sites. Basic residues at P-3 and P-2 are common determinants of basophilic protein kinases (Zhu *et al*., 2005). Mutational and structural analysis of bovine protein kinase A (PKA) revealed that the strong preference of PKA for Arg at position P-3 is mediated by a single acidic residue (Glu127) in the kinase domain of PKA (Fig. 26) (Fujii *et al*., 2004; Yaffe *et al*., 2001). Sequence alignment of the catalytic domain of PKA and Npr1 (Fig. 27) shows that an acidic residue is also present at a homologous position in the kinase domain (residues 438-742) of Npr1 (Asp523). The strong preference of PKA for arginine at the P-2 position is mediated by two glutamates at position 170 and 230 (Fig. 26). Interestingly, the alignment of PKA and the catalytic domain of Npr1 does not reveal significant homology in this region of the protein. Therefore, it is unlikely that Npr1 requires a basic residue at P-2 position. This will have to be tested to see if another basic residue at the P-2 position increases the affinity of the peptide for Npr1. Also, the AGC family kinases often accommodate Arg at the P-5 position via the same pocket as the P-3/P-2 position (Kreegipuu *et al*., 1998). The P-5 position in the Rpl24a peptide is a bulky Phe making it unlikely that Npr1 recognizes P-3/P-2 or P-5 substrates.

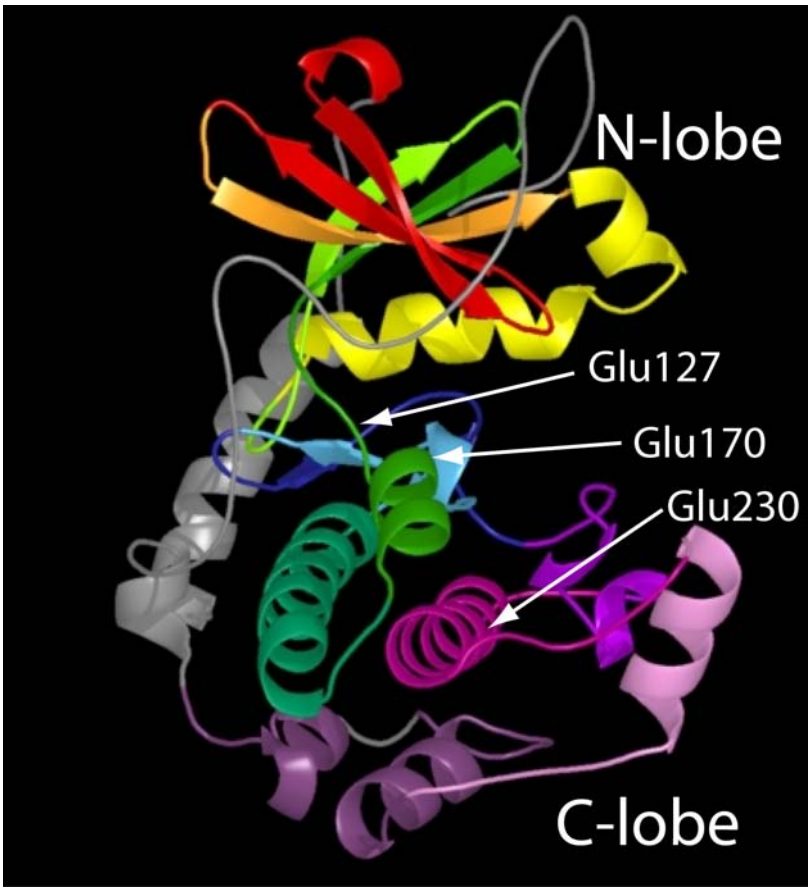

Figure 26: Ribbon diagram of bovine protein kinase A

(from http://alpha.kinasenet.org/pkr/flash.do?id=1ATP). Glu127 forms a negatively charged surface for interaction with the positively charged arginine of the P-3 position, while both, Glu170 and Glu230, interact with the Arg of the P-2 position.

In common with the typical basophilic protein kinases is the disfavor of Npr1 for Pro at the P+1 position (Zhu *et al*., 2005). Replacement of the P+1 Lys by Pro reduces the phosphorylation of the Rpl24a peptides to nearly undetectable levels (Table 4). The kinase domain that is most important for the recognition of the P+1 position in PKA is the activation loop. The carbonyl group of Gly200 facilitates binding by the formation of a hydrogen bond with the backbone amide of the P+1 residue (Knighton *et al*., 1991; Lowe *et al*., 1997). Whether Npr1 possesses a similar activation loop is questionable since the sequence homology between PKA and Npr1 in this region is low. In addition, up to date, no phosphorylation has been observed in the catalytic domain of Npr1. However, mutating the P+1 position in the Rpl24a peptide from a Lys to an Ala had only a slight effect on the K_m (Table 4), indicating that Npr1 might be flexible in accommodating P+1 a variety of amino acids. Naturally, mutational and structural analysis need to clarify what residues in Npr1 are involved in recognizing substrates with basic P-3 sites. In conclusion, we propose the consensus sequence of Npr1 to be (R/K)XXS(R/K).

Fig. 27: Alignment of Npr1 and PKA

Sequence alignment of the catalytic subunit of bovine protein kinase A and the catalytic domain of yeast Npr1 (residues 438-742).

The consensus sequence can be used to search for potential substrates of Npr1. 2,518 of the 6,163 yeast proteins present in the Swiss-Prot database (http://www.expasy.org) contain the (R/K)XXS(R/K) consensus sequence. To reduce the high number of candidates, proteins that are involved in the sorting of amino acid permeases or the nitrogen-regulated transcription should be considered first. Several candidate proteins were found to belong to this group of proteins. Among them the motif occurs six times in the transcription factor Gln3 and twice in Bul1 and Bul2. These proteins could be tested *in vitro* with Npr1. On the other hand, neither Gap1 nor Rsp5 contain the consensus sequence which would explain why they were not phosphorylated by Npr1.

Npr1 Phosphorylation Regulates Substrate Accessibility

Npr1 is highly phosphorylated in cells grown in nitrogen-rich media. Mapping of Npr1 phosphorylation revealed 24 sites clustered in two regions in the N-terminal serine-rich domain of Npr1. No phosphorylation was found in the C-terminal catalytic domain. All of the ten phosphopeptides of Npr1, except the first two, showed a reduced extent of phosphorylation when isolated from rapamycin treated cells (Bonenfant, 2003). Npr1 isolated from cells grown in a nitrogen-poor medium and Npr1 isolated from rapamycin-treated cells become activated to the same extent by dephosphorylation when measured with MBP as a substrate (Fig. 8). Glutamine treatment of proline cells re-established the phosphorylation state of Npr1 to the same level as cells grown in nitrogen-rich medium. Concomitantly, MBP phosphorylation was abolished altogether, whereas autophosphorylation was not, indicating that glutamine treatment does not switch off the kinase activity. The fact that substrate phosphorylation paralleled dephosphorylation of Npr1 and *vice versa* suggests that the N-terminal part of Npr1 has a regulatory effect on substrate

phosphorylation rather than on kinase activity *per se* (Fig. 28). Interestingly, complete dephosphorylation of Npr1 by alkaline phosphatase led to a decrease in substrate phosphorylation indicating that a delicate balance between phosphorylation and dephosphorylation governs the activity of Npr1. Further, autophosphorylation did not affect substrate phosphorylation because autophosphorylation of GST-Npr1 prior to the addition of a substrate did not lead to a decrease in MBP phosphorylation and no difference in electrophoretic mobility was observed after autophosphorylation. Since the extent to which Npr1 phosphorylates itself is minimal when compared to phosphorylation caused by nitrogen inactivation, the majority of Npr1 phosphorylation must be caused by upstream protein kinases.

Some of the phosphorylation sites of Npr1 closely resemble the phosphorylation sites present in two targets of the mammalian TOR kinase, namely the ribosomal S6 kinase (S6k) and the translational regulator 4E-BP1. S6k is phosphorylated on three rapamycin-sensitive sites contained in a hydrophobic motive of Ser/Thr flanked by aromatic amino acids (Pearson *et al*., 1995) and 4EBP1 is phosphorylated on seven rapamycin-sensitive sites contained in a Ser/Thr-Pro motif (Fadden *et al*., 1997; Gingras *et al*., 2001; Heesom *et al*., 1998; Wang *et al*., 2003b). However, attempts to phosphorylate kinase-dead Npr1 *in vitro* with purified TORC1 complexes failed (Bonenfant, 2003). Two other phosphorylation sites at Ser125 and Ser317 show the basic mammalian PKB/Akt consensus motif RXRXXS (Obata *et al*., 2000). The yeast orthologue of PKB/Akt is SCH9 (Fabrizio *et al*., 2001) which was shown to be involved in nutrient-dependent control of cell growth (Jorgensen *et al*., 2004). In a recent study Sch9 was found to be a direct target of TORC1 (Urban *et al*., 2007). Further, the phosphorylation site at Ser85 lies in a sequence stretch that conforms to a casein kinase motif with an acidic residue three residues N-terminal of the phosphorylation site (Flotow and Roach, 1991). Yeast casein kinase 1 is encoded by the YCK1 and YCK2 genes. The other phosphorylation sites of Npr1 do not conform to known phosphorylation motifs (Bonenfant, 2003).

A possible model that describes the mechanism of Npr1 regulation is shown in Figure 28. In a nitrogen-rich medium the N-terminal serine-rich domain of Npr1 is maintained in a highly phosphorylated state by yet unknown protein kinases. Phosphorylation of a substrate is inhibited by the N-terminal domain which masks the constitutively active catalytic domain. Autophosphorylation of Npr1 is still possible. If the cells are treated with rapamycin or shifted to a nitrogen-poor medium, Npr1 becomes dephosphorylated by the Sit4 phosphatase. Dephosphorylation causes a conformational change that allows the substrate to access the catalytic site where it gets phosphorylated.

Figure: 28: Model of Npr1 regulation

The model assumes two conformations of Npr1: an open, substrate-accessible conformation (bottom) and a closed, substrate-inaccessible conformation (top). Both conformations undergo autophosphorylation due to constitutively active Npr1. The two phosphorylation clusters on the N-terminal domain of Npr1 are numbered with 1 and 2. Autophosphorylation is marked with a red "P".

N-terminal Substrate Binding Site

According to the model described above, deletion of one or both of the N-terminal phosphorylation clusters allows substrate phosphorylation. To test this, the first and second cluster of phosphorylation sites were deleted individually or in combination yielding the GST-Npr1Δ1-143, GST-Npr1Δ252-413 and GST-Npr1Δ1-431 mutations. Growth behavior and citrulline uptake by Gap1 on nitrogen-poor medium was not affected at all in the mutant cells whereas expression of kinase-dead Npr1 caused a severe growth defect and abolished citrulline uptake (Altermatt 2005). In agreement with the model described above, the kinase domain alone is sufficient for kinase activity. However, conflicting results were obtained when the N-terminal deletion mutants were tested for their ability to phosphorylate MBP, Rpl24a and the Rpl24a[16-50] peptide (Fig. 25). Npr1Δ1-143 had still wild-type activity, whereas Npr1Δ252-413 and Npr1Δ1-431 failed to phosphorylate protein as well as peptide substrates. Interestingly, autophosphorylation was unaffected in the Npr1Δ252-413 mutant. If Npr1Δ1-431 is still active cannot be answered because all autophosphorylation sites are deleted. Therefore, the region harboring the second cluster of phosphorylation sites most likely contains a substrate interacting domain that is required for locking the substrate for subsequent phosphorylation. One explanation for the discrepancy between the *in*

vivo and *in vitro* findings could be that a *bona fide* Npr1 substrate does not require the assistance of the serine-rich domain to become phosphorylated. MBP and the ribosomal proteins are highly basic proteins and may need a negatively charged surface for interaction with Npr1. The *in vivo* substrate for Npr1 could be brought in close proximity to the catalytic center by additional factors or by its location in the same vesicle or membrane compartment.

According to the model described above, deletion of the N-terminal part of Npr1 (Npr1Δ1-431) would render Npr1 constitutively active. However, if S288C wild-type cells containing Npr1Δ1-431 were grown on glutamate, Gap1 activity remained low in spite of normal Gap1 transcription (Altermatt 2005). Since Npr1Δ1-431 was not able to phosphorylate MBP or Rpl24a *in vitro*, nitrogen source independent activity could not be assayed.

Therefore, to unravel the molecular details of Npr1 regulation, it is important to find an *in vivo* target of Npr1. One possibility would be to improve the sensitivity of the KESTREL method so that tracking of low-abundance targets becomes possible. This could be achieved by reducing the complexity via multiple rounds of protein fractionation. In a more biased approach, possible Npr1 substrates containing the Npr1 consensus sequence could be bacterially expressed and tested as substrates in kinase assays. Interesting candidates are the Bul1/Bul2 and Gln3 proteins. More up to date technologies like protein chips containing the yeast proteome will certainly yield a plethora of candidate Npr1 substrates (Ptacek *et al*., 2005). The hunt for upstream kinases that evoke such complex phosphorylation patterns could be done with suitably tagged yeast kinase collections to phosphorylate bacterially expressed domains of Npr1 encompassing the individual clusters of phosphorylation individually or in combination.

5 References

Aebersold, R., and Goodlett, D.R. (2001). Mass spectrometry in proteomics. Chem Rev *101*, 269-295.

Altermatt, P. (2005). Functional analysis of the yeast protein kinase Npr1p. In Biochemical Department (Basel, University of Basel).

Andre, B. (1995). An overview of membrane transport proteins in Saccharomyces cerevisiae. Yeast *11*, 1575-1611.

Andre, B., Hein, C., Grenson, M., and Jauniaux, J.C. (1993). Cloning and expression of the UGA4 gene coding for the inducible GABA-specific transport protein of Saccharomyces cerevisiae. Mol Gen Genet *237*, 17-25.

Andreasson, C., and Ljungdahl, P.O. (2002). Receptor-mediated endoproteolytic activation of two transcription factors in yeast. Genes Dev *16*, 3158-3172.

Babst, M., Katzmann, D.J., Snyder, W.B., Wendland, B., and Emr, S.D. (2002). Endosome-associated complex, ESCRT-II, recruits transport machinery for protein sorting at the multivesicular body. Dev Cell *3*, 283-289.

Barnes, D., Lai, W., Breslav, M., Naider, F., and Becker, J.M. (1998). PTR3, a novel gene mediating amino acid-inducible regulation of peptide transport in Saccharomyces cerevisiae. Mol Microbiol *29*, 297-310.

Baronas-Lowell, D.M., and Warner, J.R. (1990). Ribosomal protein L30 is dispensable in the yeast Saccharomyces cerevisiae. Mol Cell Biol *10*, 5235-5243.

Beck, T., and Hall, M.N. (1999). The TOR signalling pathway controls nuclear localization of nutrient-regulated transcription factors. Nature *402*, 689-692.

Beck, T., Schmidt, A., and Hall, M.N. (1999). Starvation induces vacuolar targeting and degradation of the tryptophan permease in yeast. J Cell Biol *146*, 1227-1238.

Bertram, P.G., Choi, J.H., Carvalho, J., Ai, W., Zeng, C., Chan, T.F., and Zheng, X.F. (2000). Tripartite regulation of Gln3p by TOR, Ure2p, and phosphatases. J Biol Chem *275*, 35727-35733.

Bertram, P.G., Choi, J.H., Carvalho, J., Chan, T.F., Ai, W., and Zheng, X.F. (2002). Convergence of TOR-nitrogen and Snf1-glucose signaling pathways onto Gln3. Mol Cell Biol *22*, 1246-1252.

Biondi, R.M., and Nebreda, A.R. (2003). Signalling specificity of Ser/Thr protein kinases through docking-site-mediated interactions. Biochem J *372*, 1-13.

Blinder, D., Coschigano, P.W., and Magasanik, B. (1996). Interaction of the GATA factor Gln3p with the nitrogen regulator Ure2p in Saccharomyces cerevisiae. J Bacteriol *178*, 4734-4736.

Boeckstaens, M., Andre, B., and Marini, A.M. (2007). The yeast ammonium transport protein Mep2 and its positive regulator, the Npr1 kinase, play an important role in normal and pseudohyphal growth on various nitrogen media through retrieval of excreted ammonium. Mol Microbiol *64*, 534-546.

Bonenfant, D. (2003). Mass spectrometric analysis of the rapamycin-sensitive phosphorylation sites of the yeast protein kinase NPR1. In Biochemical Department, Biozentrum (Basel, University of Basel).

Bonenfant, D., Schmelzle, T., Jacinto, E., Crespo, J.L., Mini, T., Hall, M.N., and Jenoe, P. (2003). Quantitation of changes in protein phosphorylation: a simple method based on stable isotope labeling and mass spectrometry. Proc Natl Acad Sci U S A *100*, 880-885.

Cafferkey, R., Young, P.R., McLaughlin, M.M., Bergsma, D.J., Koltin, Y., Sathe, G.M., Faucette, L., Eng, W.K., Johnson, R.K., and Livi, G.P. (1993). Dominant missense mutations in a novel yeast protein related to mammalian phosphatidylinositol 3-kinase and VPS34 abrogate rapamycin cytotoxicity. Mol Cell Biol *13*, 6012-6023.

Cardenas, M.E., Cutler, N.S., Lorenz, M.C., Di Como, C.J., and Heitman, J. (1999). The TOR signaling cascade regulates gene expression in response to nutrients. Genes Dev *13*, 3271-3279.

Carlson, M. (1999). Glucose repression in yeast. Curr Opin Microbiol *2*, 202-207.

Chen, E.J., and Kaiser, C.A. (2003). LST8 negatively regulates amino acid biosynthesis as a component of the TOR pathway. J Cell Biol *161*, 333-347.

Chi, A., Huttenhower, C., Geer, L.Y., Coon, J.J., Syka, J.E., Bai, D.L., Shabanowitz, J., Burke, D.J., Troyanskaya, O.G., and Hunt, D.F. (2007). Analysis of phosphorylation sites on proteins from Saccharomyces cerevisiae by electron transfer dissociation (ETD) mass spectrometry. Proc Natl Acad Sci U S A *104*, 2193-2198.

Coffman, J.A., Rai, R., Loprete, D.M., Cunningham, T., Svetlov, V., and Cooper, T.G. (1997). Cross regulation of four GATA factors that control nitrogen catabolic gene expression in Saccharomyces cerevisiae. J Bacteriol *179*, 3416-3429.

Cooper, T.G. (1982). Nitrogen metabolism in *Saccharomyces cerevisiae* (Cold Spring Harbour, NY, Cold Spring Harbour Laboratory Press).

Cooper, T.G. (2002). Transmitting the signal of excess nitrogen in Saccharomyces cerevisiae from the Tor proteins to the GATA factors: connecting the dots. FEMS Microbiol Rev *26*, 223-238.

Courchesne, W.E., and Magasanik, B. (1983). Ammonia regulation of amino acid permeases in Saccharomyces cerevisiae. Mol Cell Biol *3*, 672-683.

Courchesne, W.E., and Magasanik, B. (1988). Regulation of nitrogen assimilation in Saccharomyces cerevisiae: roles of the URE2 and GLN3 genes. J Bacteriol *170*, 708-713.

Cox, K.H., Kulkarni, A., Tate, J.J., and Cooper, T.G. (2004). Gln3 phosphorylation and intracellular localization in nutrient limitation and starvation differ from those generated by rapamycin inhibition of Tor1/2 in Saccharomyces cerevisiae. J Biol Chem *279*, 10270-10278.

Crespo, J.L., Helliwell, S.B., Wiederkehr, C., Demougin, P., Fowler, B., Primig, M., and Hall, M.N. (2004). NPR1 kinase and RSP5-BUL1/2 ubiquitin ligase control GLN3-dependent transcription in Saccharomyces cerevisiae. J Biol Chem *279*, 37512-37517.

Cutler, N.S., Pan, X., Heitman, J., and Cardenas, M.E. (2001). The TOR signal transduction cascade controls cellular differentiation in response to nutrients. Mol Biol Cell *12*, 4103-4113.

de Boer, M., Nielsen, P.S., Bebelman, J.P., Heerikhuizen, H., Andersen, H.A., and Planta, R.J. (2000). Stp1p, Stp2p and Abf1p are involved in regulation of expression of the amino acid transporter gene BAP3 of Saccharomyces cerevisiae. Nucleic Acids Res *28*, 974-981.

De Craene, J.O., Soetens, O., and Andre, B. (2001). The Npr1 kinase controls biosynthetic and endocytic sorting of the yeast Gap1 permease. J Biol Chem *276*, 43939-43948.

De Virgilio, C., and Loewith, R. (2006). Cell growth control: little eukaryotes make big contributions. Oncogene *25*, 6392-6415.

De Vit, M.J., Waddle, J.A., and Johnston, M. (1997). Regulated nuclear translocation of the Mig1 glucose repressor. Mol Biol Cell *8*, 1603-1618.

Deshaies, R.J., and Ferrell, J.E., Jr. (2001). Multisite phosphorylation and the countdown to S phase. Cell *107*, 819-822.

Di Como, C.J., and Arndt, K.T. (1996). Nutrients, via the Tor proteins, stimulate the association of Tap42 with type 2A phosphatases. Genes Dev *10*, 1904-1916.

Didion, T., Regenberg, B., Jorgensen, M.U., Kielland-Brandt, M.C., and Andersen, H.A. (1998). The permease homologue Ssy1p controls the expression of amino acid and peptide transporter genes in Saccharomyces cerevisiae. Mol Microbiol *27*, 643-650.

Dresios, J., Derkatch, I.L., Liebman, S.W., and Synetos, D. (2000). Yeast ribosomal protein L24 affects the kinetics of protein synthesis and ribosomal protein L39 improves translational accuracy, while mutants lacking both remain viable. Biochemistry *39*, 7236-7244.

Dubois, E., and Grenson, M. (1979). Methylamine/ammonia uptake systems in saocharomyces cerevisiae: multiplicity and regulation. Mol Gen Genet *175*, 67-76.

Duvel, K., Santhanam, A., Garrett, S., Schneper, L., and Broach, J.R. (2003). Multiple roles of Tap42 in mediating rapamycin-induced transcriptional changes in yeast. Mol Cell *11*, 1467-1478.

Eng, J.K., Mccormack, A.L., and Yates, J.R. (1994). An Approach to Correlate Tandem Mass-Spectral Data of Peptides with Amino-Acid-Sequences in a Protein Database. Journal of the American Society for Mass Spectrometry *5*, 976-989.

Fabrizio, P., Pozza, F., Pletcher, S.D., Gendron, C.M., and Longo, V.D. (2001). Regulation of longevity and stress resistance by Sch9 in yeast. Science *292*, 288-290.

Fadden, P., Haystead, T.A., and Lawrence, J.C., Jr. (1997). Identification of phosphorylation sites in the translational regulator, PHAS-I, that are controlled by insulin and rapamycin in rat adipocytes. J Biol Chem *272*, 10240-10247.

Fadri, M., Daquinag, A., Wang, S., Xue, T., and Kunz, J. (2005). The pleckstrin homology domain proteins Slm1 and Slm2 are required for actin cytoskeleton organization in yeast and bind phosphatidylinositol-4,5-bisphosphate and TORC2. Mol Biol Cell *16*, 1883-1900.

Feller, A., Boeckstaens, M., Marini, A.M., and Dubois, E. (2006). Transduction of the nitrogen signal activating Gln3-mediated transcription is independent of Npr1 kinase and Rsp5-Bul1/2 ubiquitin ligase in Saccharomyces cerevisiae. J Biol Chem *281*, 28546-28554.

Ferrari, S., Marin, O., Pagano, M.A., Meggio, F., Hess, D., El-Shemerly, M., Krystyniak, A., and Pinna, L.A. (2005). Aurora-A site specificity: a study with synthetic peptide substrates. Biochem J *390*, 293-302.

Ficarro, S.B., McCleland, M.L., Stukenberg, P.T., Burke, D.J., Ross, M.M., Shabanowitz, J., Hunt, D.F., and White, F.M. (2002). Phosphoproteome analysis by mass spectrometry and its application to Saccharomyces cerevisiae. Nat Biotechnol *20*, 301-305.

Flotow, H., and Roach, P.J. (1991). Role of acidic residues as substrate determinants for casein kinase I. J Biol Chem *266*, 3724-3727.

Forsberg, H., and Ljungdahl, P.O. (2001). Sensors of extracellular nutrients in Saccharomyces cerevisiae. Curr Genet *40*, 91-109.

Fujii, K., Zhu, G., Liu, Y., Hallam, J., Chen, L., Herrero, J., and Shaw, S. (2004). Kinase peptide specificity: improved determination and relevance to protein phosphorylation. Proc Natl Acad Sci U S A *101*, 13744-13749.

Gerber, S.A., Rush, J., Stemman, O., Kirschner, M.W., and Gygi, S.P. (2003). Absolute quantification of proteins and phosphoproteins from cell lysates by tandem MS. Proc Natl Acad Sci U S A *100*, 6940-6945.

Gietz, R.D., Schiestl, R.H., Willems, A.R., and Woods, R.A. (1995). Studies on the transformation of intact yeast cells by the LiAc/SS-DNA/PEG procedure. Yeast *11*, 355-360.

Gimeno, C.J., Ljungdahl, P.O., Styles, C.A., and Fink, G.R. (1992). Unipolar cell divisions in the yeast S. cerevisiae lead to filamentous growth: regulation by starvation and RAS. Cell *68*, 1077-1090.

Gingras, A.C., Raught, B., Gygi, S.P., Niedzwiecka, A., Miron, M., Burley, S.K., Polakiewicz, R.D., Wyslouch-Cieszynska, A., Aebersold, R., and Sonenberg, N. (2001). Hierarchical phosphorylation of the translation inhibitor 4E-BP1. Genes Dev *15*, 2852-2864.

Goodlett, D.R., Keller, A., Watts, J.D., Newitt, R., Yi, E.C., Purvine, S., Eng, J.K., von Haller, P., Aebersold, R., and Kolker, E. (2001). Differential stable isotope labeling of peptides for quantitation and de novo sequence derivation. Rapid Commun Mass Spectrom *15*, 1214-1221.

Grenson, M. (1983a). Inactivation-reactivation process and repression of permease formation regulate several ammonia-sensitive permeases in the yeast Saccharomyces cerevisiae. Eur J Biochem *133*, 135-139.

Grenson, M. (1983b). Study of the positive control of the general amino-acid permease and other ammonia-sensitive uptake systems by the product of the NPR1 gene in the yeast Saccharomyces cerevisiae. Eur J Biochem *133*, 141-144.

Grenson, M., Dubois, E., Piotrowska, M., Drillien, R., and Aigle, M. (1974). Ammonia assimilation in Saccharomyces cerevisiae as mediated by the two glutamate dehydrogenases. Evidence for the gdhA locus being a structural gene for the NADP-dependent glutamate dehydrogenase. Mol Gen Genet *128*, 73-85.

Grenson, M., Hou, C., and Crabeel, M. (1970). Multiplicity of the amino acid permeases in Saccharomyces cerevisiae. IV. Evidence for a general amino acid permease. J Bacteriol *103*, 770-777.

Hanks, S.K., and Hunter, T. (1995). Protein kinases 6. The eukaryotic protein kinase superfamily: kinase (catalytic) domain structure and classification. FASEB J *9*, 576-596.

Hanks, S.K., Quinn, A.M., and Hunter, T. (1988). The protein kinase family: conserved features and deduced phylogeny of the catalytic domains. Science *241*, 42-52.

Hardwick, J.S., Kuruvilla, F.G., Tong, J.K., Shamji, A.F., and Schreiber, S.L. (1999). Rapamycin-modulated transcription defines the subset of nutrient-sensitive signaling pathways directly controlled by the Tor proteins. Proc Natl Acad Sci U S A *96*, 14866-14870.

Hedbacker, K., and Carlson, M. (2008). SNF1/AMPK pathways in yeast. Front Biosci *13*, 2408-2420.

Heesom, K.J., Avison, M.B., Diggle, T.A., and Denton, R.M. (1998). Insulin-stimulated kinase from rat fat cells that phosphorylates initiation factor 4E-binding protein 1 on the rapamycin-insensitive site (serine-111). Biochem J *336 (Pt 1)*, 39-48.

Hein, C., and Andre, B. (1997). A C-terminal di-leucine motif and nearby sequences are required for NH4(+)-induced inactivation and degradation of the general amino acid permease, Gap1p, of Saccharomyces cerevisiae. Mol Microbiol *24*, 607-616.

Hein, C., Springael, J.Y., Volland, C., Haguenauer-Tsapis, R., and Andre, B. (1995). NPl1, an essential yeast gene involved in induced degradation of Gap1 and Fur4 permeases, encodes the Rsp5 ubiquitin-protein ligase. Mol Microbiol *18*, 77-87.

Heitman, J., Movva, N.R., and Hall, M.N. (1991). Targets for cell cycle arrest by the immunosuppressant rapamycin in yeast. Science *253*, 905-909.

Helliwell, S.B., Howald, I., Barbet, N., and Hall, M.N. (1998). TOR2 is part of two related signaling pathways coordinating cell growth in Saccharomyces cerevisiae. Genetics *148*, 99-112.

Helliwell, S.B., Losko, S., and Kaiser, C.A. (2001). Components of a ubiquitin ligase complex specify polyubiquitination and intracellular trafficking of the general amino acid permease. J Cell Biol *153*, 649-662.

Helliwell, S.B., Wagner, P., Kunz, J., Deuter-Reinhard, M., Henriquez, R., and Hall, M.N. (1994). TOR1 and TOR2 are structurally and functionally similar but not identical phosphatidylinositol kinase homologues in yeast. Mol Biol Cell *5*, 105-118.

Henderson, L.E., Oroszlan, S., and Konigsberg, W. (1979). A micromethod for complete removal of dodecyl sulfate from proteins by ion-pair extraction. Anal Biochem *93*, 153-157.

Hicke, L. (1997). Ubiquitin-dependent internalization and down-regulation of plasma membrane proteins. Faseb J *11*, 1215-1226.

Hinnebusch, A.G. (1986). The general control of amino acid biosynthetic genes in the yeast Saccharomyces cerevisiae. CRC Crit Rev Biochem *21*, 277-317.

Hinnebusch, A.G., and Natarajan, K. (2002). Gcn4p, a master regulator of gene expression, is controlled at multiple levels by diverse signals of starvation and stress. Eukaryot Cell *1*, 22-32.

Hochstrasser, M. (1996). Ubiquitin-dependent protein degradation. Annu Rev Genet *30*, 405-439.

Hoffmann, W. (1985). Molecular characterization of the CAN1 locus in Saccharomyces cerevisiae. A transmembrane protein without N-terminal hydrophobic signal sequence. J Biol Chem *260*, 11831-11837.

Holland, P.M., and Cooper, J.A. (1999). Protein modification: docking sites for kinases. Curr Biol *9*, R329-331.

Hong, S.P., Leiper, F.C., Woods, A., Carling, D., and Carlson, M. (2003). Activation of yeast Snf1 and mammalian AMP-activated protein kinase by upstream kinases. Proc Natl Acad Sci U S A *100*, 8839-8843.

Huibregtse, J.M., Scheffner, M., Beaudenon, S., and Howley, P.M. (1995). A family of proteins structurally and functionally related to the E6-AP ubiquitin-protein ligase. Proc Natl Acad Sci U S A *92*, 2563-2567.

Hunter, T., and Plowman, G.D. (1997). The protein kinases of budding yeast: six score and more. Trends Biochem Sci *22*, 18-22.

Hutti, J.E., Jarrell, E.T., Chang, J.D., Abbott, D.W., Storz, P., Toker, A., Cantley, L.C., and Turk, B.E. (2004). A rapid method for determining protein kinase phosphorylation specificity. Nat Methods *1*, 27-29.

Ingham, R.J., Gish, G., and Pawson, T. (2004). The Nedd4 family of E3 ubiquitin ligases: functional diversity within a common modular architecture. Oncogene *23*, 1972-1984.

Iraqui, I., Vissers, S., Bernard, F., de Craene, J.O., Boles, E., Urrestarazu, A., and Andre, B. (1999). Amino acid signaling in Saccharomyces cerevisiae: a permease-like sensor of external amino acids and F-Box protein Grr1p are required for transcriptional induction of the AGP1 gene, which encodes a broad-specificity amino acid permease. Mol Cell Biol *19*, 989-1001.

Jacinto, E., Guo, B., Arndt, K.T., Schmelzle, T., and Hall, M.N. (2001). TIP41 interacts with TAP42 and negatively regulates the TOR signaling pathway. Mol Cell *8*, 1017-1026.

Jauniaux, J.C., and Grenson, M. (1990). GAP1, the general amino acid permease gene of Saccharomyces cerevisiae. Nucleotide sequence, protein similarity with the other bakers yeast amino acid permeases, and nitrogen catabolite repression. Eur J Biochem *190*, 39-44.

Jiang, R., and Carlson, M. (1997). The Snf1 protein kinase and its activating subunit, Snf4, interact with distinct domains of the Sip1/Sip2/Gal83 component in the kinase complex. Mol Cell Biol *17*, 2099-2106.

Jiang, Y., and Broach, J.R. (1999). Tor proteins and protein phosphatase 2A reciprocally regulate Tap42 in controlling cell growth in yeast. Embo J *18*, 2782-2792.

Jorgensen, P., Rupes, I., Sharom, J.R., Schneper, L., Broach, J.R., and Tyers, M. (2004). A dynamic transcriptional network communicates growth potential to ribosome synthesis and critical cell size. Genes Dev *18*, 2491-2505.

Kallunki, T., Su, B., Tsigelny, I., Sluss, H.K., Derijard, B., Moore, G., Davis, R., and Karin, M. (1994). JNK2 contains a specificity-determining region responsible for efficient c-Jun binding and phosphorylation. Genes Dev *8*, 2996-3007.

Kaouass, M., Audette, M., Ramotar, D., Verma, S., De Montigny, D., Gamache, I., Torossian, K., and Poulin, R. (1997). The STK2 gene, which encodes a putative Ser/Thr protein kinase, is required for high-affinity spermidine transport in Saccharomyces cerevisiae. Mol Cell Biol *17*, 2994-3004.

Katzmann, D.J., Babst, M., and Emr, S.D. (2001). Ubiquitin-dependent sorting into the multivesicular body pathway requires the function of a conserved endosomal protein sorting complex, ESCRT-I. Cell *106*, 145-155.

Kemp, B.E., Bylund, D.B., Huang, T.S., and Krebs, E.G. (1975). Substrate specificity of the cyclic AMP-dependent protein kinase. Proc Natl Acad Sci U S A *72*, 3448-3452.

Klasson, H., Fink, G.R., and Ljungdahl, P.O. (1999). Ssy1p and Ptr3p are plasma membrane components of a yeast system that senses extracellular amino acids. Mol Cell Biol *19*, 5405-5416.

Kleinschmidt, M., Grundmann, O., Bluthgen, N., Mosch, H.U., and Braus, G.H. (2005). Transcriptional profiling of Saccharomyces cerevisiae cells under adhesion-inducing conditions. Mol Genet Genomics *273*, 382-393.

Knebel, A., Morrice, N., and Cohen, P. (2001). A novel method to identify protein kinase substrates: eEF2 kinase is phosphorylated and inhibited by SAPK4/p38delta. Embo J *20*, 4360-4369.

Knighton, D.R., Zheng, J.H., Ten Eyck, L.F., Xuong, N.H., Taylor, S.S., and Sowadski, J.M. (1991). Structure of a peptide inhibitor bound to the catalytic subunit of cyclic adenosine monophosphate-dependent protein kinase. Science *253*, 414-420.

Kokubu, M., Ishihama, Y., Sato, T., Nagasu, T., and Oda, Y. (2005). Specificity of immobilized metal affinity-based IMAC/C18 tip enrichment of phosphopeptides for protein phosphorylation analysis. Anal Chem *77*, 5144-5154.

Kreegipuu, A., Blom, N., Brunak, S., and Jarv, J. (1998). Statistical analysis of protein kinase specificity determinants. FEBS Lett *430*, 45-50.

Kruckeberg, A.L. (1996). The hexose transporter family of Saccharomyces cerevisiae. Arch Microbiol *166*, 283-292.

Kuchin, S., Vyas, V.K., and Carlson, M. (2002). Snf1 protein kinase and the repressors Nrg1 and Nrg2 regulate FLO11, haploid invasive growth, and diploid pseudohyphal differentiation. Mol Cell Biol *22*, 3994-4000.

Kunz, J., Henriquez, R., Schneider, U., Deuter-Reinhard, M., Movva, N.R., and Hall, M.N. (1993). Target of rapamycin in yeast, TOR2, is an essential phosphatidylinositol kinase homolog required for G1 progression. Cell *73*, 585-596.

Lanker, S., Valdivieso, M.H., and Wittenberg, C. (1996). Rapid degradation of the G1 cyclin Cln2 induced by CDK-dependent phosphorylation. Science *271*, 1597-1601.

Larsen, M.R., Thingholm, T.E., Jensen, O.N., Roepstorff, P., and Jorgensen, T.J. (2005). Highly selective enrichment of phosphorylated peptides from peptide mixtures using titanium dioxide microcolumns. Mol Cell Proteomics *4*, 873-886.

Lasko, P.F., and Brandriss, M.C. (1981). Proline transport in Saccharomyces cerevisiae. J Bacteriol *148*, 241-247.

Lee, T., Hoofnagle, A.N., Kabuyama, Y., Stroud, J., Min, X., Goldsmith, E.J., Chen, L., Resing, K.A., and Ahn, N.G. (2004). Docking motif interactions in MAP kinases revealed by hydrogen exchange mass spectrometry. Mol Cell *14*, 43-55.

Loewith, R., Jacinto, E., Wullschleger, S., Lorberg, A., Crespo, J.L., Bonenfant, D., Oppliger, W., Jenoe, P., and Hall, M.N. (2002). Two TOR complexes, only one of which is rapamycin sensitive, have distinct roles in cell growth control. Mol Cell *10*, 457-468.

Lorenz, M.C., and Heitman, J. (1998). The MEP2 ammonium permease regulates pseudohyphal differentiation in Saccharomyces cerevisiae. Embo J *17*, 1236-1247.

Lowe, E.D., Noble, M.E., Skamnaki, V.T., Oikonomakos, N.G., Owen, D.J., and Johnson, L.N. (1997). The crystal structure of a phosphorylase kinase peptide substrate complex: kinase substrate recognition. EMBO J *16*, 6646-6658.

Magasanik, B. (1992). Regulation of nitrogen utilization (Cold Spring Harbour, NY, Cold Spring Harbour Laboratory Press).

Magasanik, B., and Kaiser, C.A. (2002). Nitrogen regulation in Saccharomyces cerevisiae. Gene *290*, 1-18.

Mann, M., Ong, S.E., Gronborg, M., Steen, H., Jensen, O.N., and Pandey, A. (2002). Analysis of protein phosphorylation using mass spectrometry: deciphering the phosphoproteome. Trends Biotechnol *20*, 261-268.

Manning, G., Plowman, G.D., Hunter, T., and Sudarsanam, S. (2002). Evolution of protein kinase signaling from yeast to man. Trends Biochem Sci *27*, 514-520.

Marini, A.M., and Andre, B. (2000). In vivo N-glycosylation of the mep2 high-affinity ammonium transporter of Saccharomyces cerevisiae reveals an extracytosolic N-terminus. Mol Microbiol *38*, 552-564.

Marini, A.M., Vissers, S., Urrestarazu, A., and Andre, B. (1994). Cloning and expression of the MEP1 gene encoding an ammonium transporter in Saccharomyces cerevisiae. Embo J *13*, 3456-3463.

McLachlin, D.T., and Chait, B.T. (2003). Improved beta-elimination-based affinity purification strategy for enrichment of phosphopeptides. Anal Chem *75*, 6826-6836.

Miller, S.M., and Magasanik, B. (1990). Role of NAD-linked glutamate dehydrogenase in nitrogen metabolism in Saccharomyces cerevisiae. J Bacteriol *172*, 4927-4935.

Mitchell, A.P. (1985). The GLN1 locus of Saccharomyces cerevisiae encodes glutamine synthetase. Genetics *111*, 243-258.

Mitchell, A.P., and Magasanik, B. (1983). Purification and properties of glutamine synthetase from Saccharomyces cerevisiae. J Biol Chem *258*, 119-124.

Mulet, J.M., Leube, M.P., Kron, S.J., Rios, G., Fink, G.R., and Serrano, R. (1999). A novel mechanism of ion homeostasis and salt tolerance in yeast: the Hal4 and Hal5 protein kinases modulate the Trk1-Trk2 potassium transporter. Mol Cell Biol *19*, 3328-3337.

Natarajan, K., Meyer, M.R., Jackson, B.M., Slade, D., Roberts, C., Hinnebusch, A.G., and Marton, M.J. (2001). Transcriptional profiling shows that Gcn4p is a master regulator of gene expression during amino acid starvation in yeast. Mol Cell Biol *21*, 4347-4368.

Nath, N., McCartney, R.R., and Schmidt, M.C. (2003). Yeast Pak1 kinase associates with and activates Snf1. Mol Cell Biol *23*, 3909-3917.

Nuhse, T.S., Stensballe, A., Jensen, O.N., and Peck, S.C. (2003). Large-scale analysis of in vivo phosphorylated membrane proteins by immobilized metal ion affinity chromatography and mass spectrometry. Mol Cell Proteomics *2*, 1234-1243.

Obata, T., Yaffe, M.B., Leparc, G.G., Piro, E.T., Maegawa, H., Kashiwagi, A., Kikkawa, R., and Cantley, L.C. (2000). Peptide and protein library screening defines optimal substrate motifs for AKT/PKB. J Biol Chem *275*, 36108-36115.

Omichinski, J.G., Clore, G.M., Schaad, O., Felsenfeld, G., Trainor, C., Appella, E., Stahl, S.J., and Gronenborn, A.M. (1993). NMR structure of a specific DNA complex of Zn-containing DNA binding domain of GATA-1. Science *261*, 438-446.

Ong, S.E., Blagoev, B., Kratchmarova, I., Kristensen, D.B., Steen, H., Pandey, A., and Mann, M. (2002). Stable isotope labeling by amino acids in cell culture, SILAC, as a simple and accurate approach to expression proteomics. Mol Cell Proteomics *1*, 376-386.

Ozcan, S., Dover, J., Rosenwald, A.G., Wolfl, S., and Johnston, M. (1996). Two glucose transporters in Saccharomyces cerevisiae are glucose sensors that generate a signal for induction of gene expression. Proc Natl Acad Sci U S A *93*, 12428-12432.

Ozcan, S., and Johnston, M. (1995). Three different regulatory mechanisms enable yeast hexose transporter (HXT) genes to be induced by different levels of glucose. Mol Cell Biol *15*, 1564-1572.

Papa, F.R., and Hochstrasser, M. (1993). The yeast DOA4 gene encodes a deubiquitinating enzyme related to a product of the human tre-2 oncogene. Nature *366*, 313-319.

Pearson, R.B., Dennis, P.B., Han, J.W., Williamson, N.A., Kozma, S.C., Wettenhall, R.E., and Thomas, G. (1995). The principal target of rapamycin-induced p70s6k inactivation is a novel phosphorylation site within a conserved hydrophobic domain. EMBO J *14*, 5279-5287.

Pearson, R.B., and Kemp, B.E. (1991). Protein kinase phosphorylation site sequences and consensus specificity motifs: tabulations. Methods Enzymol *200*, 62-81.

Perez-Valle, J., Jenkins, H., Merchan, S., Montiel, V., Ramos, J., Sharma, S., Serrano, R., and Yenush, L. (2007). Key role for intracellular K+ and protein kinases Sat4/Hal4 and Hal5 in the plasma membrane stabilization of yeast nutrient transporters. Mol Cell Biol *27*, 5725-5736.

Pinkse, M.W., Uitto, P.M., Hilhorst, M.J., Ooms, B., and Heck, A.J. (2004). Selective isolation at the femtomole level of phosphopeptides from proteolytic digests using 2D-NanoLC-ESI-MS/MS and titanium oxide precolumns. Anal Chem *76*, 3935-3943.

Posewitz, M.C., and Tempst, P. (1999). Immobilized gallium(III) affinity chromatography of phosphopeptides. Anal Chem *71*, 2883-2892.

Ptacek, J., Devgan, G., Michaud, G., Zhu, H., Zhu, X., Fasolo, J., Guo, H., Jona, G., Breitkreutz, A., Sopko, R., *et al.* (2005). Global analysis of protein phosphorylation in yeast. Nature *438*, 679-684.

Qian, W.J., Goshe, M.B., Camp, D.G., 2nd, Yu, L.R., Tang, K., and Smith, R.D. (2003). Phosphoprotein isotope-coded solid-phase tag approach for enrichment and quantitative analysis of phosphopeptides from complex mixtures. Anal Chem *75*, 5441-5450.

Regenberg, B., During-Olsen, L., Kielland-Brandt, M.C., and Holmberg, S. (1999). Substrate specificity and gene expression of the amino-acid permeases in Saccharomyces cerevisiae. Curr Genet *36*, 317-328.

Reinke, A., Anderson, S., McCaffery, J.M., Yates, J., 3rd, Aronova, S., Chu, S., Fairclough, S., Iverson, C., Wedaman, K.P., and Powers, T. (2004). TOR complex 1 includes a novel component, Tco89p (YPL180w), and cooperates with Ssd1p to maintain cellular integrity in Saccharomyces cerevisiae. J Biol Chem *279*, 14752-14762.

Roberg, K.J., Bickel, S., Rowley, N., and Kaiser, C.A. (1997a). Control of amino acid permease sorting in the late secretory pathway of Saccharomyces cerevisiae by SEC13, LST4, LST7 and LST8. Genetics *147*, 1569-1584.

Roberg, K.J., Rowley, N., and Kaiser, C.A. (1997b). Physiological regulation of membrane protein sorting late in the secretory pathway of Saccharomyces cerevisiae. J Cell Biol *137*, 1469-1482.

Rogers, S., Wells, R., and Rechsteiner, M. (1986). Amino acid sequences common to rapidly degraded proteins: the PEST hypothesis. Science *234*, 364-368.

Rolfes, R.J., and Hinnebusch, A.G. (1993). Translation of the yeast transcriptional activator GCN4 is stimulated by purine limitation: implications for activation of the protein kinase GCN2. Mol Cell Biol *13*, 5099-5111.

Rolland, F., Winderickx, J., and Thevelein, J.M. (2002). Glucose-sensing and -signalling mechanisms in yeast. FEMS Yeast Res *2*, 183-201.

Ross, P.L., Huang, Y.N., Marchese, J.N., Williamson, B., Parker, K., Hattan, S., Khainovski, N., Pillai, S., Dey, S., Daniels, S., *et al.* (2004). Multiplexed protein quantitation in Saccharomyces cerevisiae using amine-reactive isobaric tagging reagents. Mol Cell Proteomics *3*, 1154-1169.

Rubenstein, E.M., and Schmidt, M.C. (2007). Mechanisms regulating the protein kinases of Saccharomyces cerevisiae. Eukaryot Cell *6*, 571-583.

Santangelo, G.M. (2006). Glucose signaling in Saccharomyces cerevisiae. Microbiol Mol Biol Rev *70*, 253-282.

Schmidt, A., Beck, T., Koller, A., Kunz, J., and Hall, M.N. (1998). The TOR nutrient signalling pathway phosphorylates NPR1 and inhibits turnover of the tryptophan permease. Embo J *17*, 6924-6931.

Schmidt, A., Hall, M.N., and Koller, A. (1994). Two FK506 resistance-conferring genes in Saccharomyces cerevisiae, TAT1 and TAT2, encode amino acid permeases mediating tyrosine and tryptophan uptake. Mol Cell Biol *14*, 6597-6606.

Schneper, L., Duvel, K., and Broach, J.R. (2004). Sense and sensibility: nutritional response and signal integration in yeast. Curr Opin Microbiol *7*, 624-630.

Schnolzer, M., Jedrzejewski, P., and Lehmann, W.D. (1996). Protease-catalyzed incorporation of 18O into peptide fragments and its application for protein sequencing by electrospray and matrix-assisted laser desorption/ionization mass spectrometry. Electrophoresis *17*, 945-953.

Smirnova, J.B., Selley, J.N., Sanchez-Cabo, F., Carroll, K., Eddy, A.A., McCarthy, J.E., Hubbard, S.J., Pavitt, G.D., Grant, C.M., and Ashe, M.P. (2005). Global gene expression profiling reveals widespread yet distinctive translational responses to different eukaryotic translation initiation factor 2B-targeting stress pathways. Mol Cell Biol *25*, 9340-9349.

Smith, A., Ward, M.P., and Garrett, S. (1998). Yeast PKA represses Msn2p/Msn4p-dependent gene expression to regulate growth, stress response and glycogen accumulation. Embo J *17*, 3556-3564.

Soetens, O., De Craene, J.O., and Andre, B. (2001). Ubiquitin is required for sorting to the vacuole of the yeast general amino acid permease, Gap1. J Biol Chem *276*, 43949-43957.

Songyang, Z., Blechner, S., Hoagland, N., Hoekstra, M.F., Piwnica-Worms, H., and Cantley, L.C. (1994). Use of an oriented peptide library to determine the optimal substrates of protein kinases. Curr Biol *4*, 973-982.

Springael, J.Y., and Andre, B. (1998). Nitrogen-regulated ubiquitination of the Gap1 permease of Saccharomyces cerevisiae. Mol Biol Cell *9*, 1253-1263.

Springael, J.Y., Galan, J.M., Haguenauer-Tsapis, R., and Andre, B. (1999). NH4+-induced down-regulation of the Saccharomyces cerevisiae Gap1p permease involves its ubiquitination with lysine-63-linked chains. J Cell Sci *112 (Pt 9)*, 1375-1383.

Stanbrough, M., and Magasanik, B. (1995). Transcriptional and posttranslational regulation of the general amino acid permease of Saccharomyces cerevisiae. J Bacteriol *177*, 94-102.

Sudol, M., and Hunter, T. (2000). NeW wrinkles for an old domain. Cell *103*, 1001-1004.

Sugiyama, N., Masuda, T., Shinoda, K., Nakamura, A., Tomita, M., and Ishihama, Y. (2007). Phosphopeptide enrichment by aliphatic hydroxy acid-modified metal oxide chromatography for nano-LC-MS/MS in proteomics applications. Mol Cell Proteomics *6*, 1103-1109.

Sutherland, C.M., Hawley, S.A., McCartney, R.R., Leech, A., Stark, M.J., Schmidt, M.C., and Hardie, D.G. (2003). Elm1p is one of three upstream kinases for the Saccharomyces cerevisiae SNF1 complex. Curr Biol *13*, 1299-1305.

Tanaka, J., and Fink, G.R. (1985). The histidine permease gene (HIP1) of Saccharomyces cerevisiae. Gene *38*, 205-214.

Tanoue, T., Adachi, M., Moriguchi, T., and Nishida, E. (2000). A conserved docking motif in MAP kinases common to substrates, activators and regulators. Nat Cell Biol *2*, 110-116.

Tao, W.A., Wollscheid, B., O'Brien, R., Eng, J.K., Li, X.J., Bodenmiller, B., Watts, J.D., Hood, L., and Aebersold, R. (2005). Quantitative phosphoproteome analysis using a dendrimer conjugation chemistry and tandem mass spectrometry. Nat Methods *2*, 591-598.

Tashiro, K., Konishi, H., Sano, E., Nabeshi, H., Yamauchi, E., and Taniguchi, H. (2006). Suppression of the ligand-mediated down-regulation of epidermal growth factor receptor by Ymer, a novel tyrosine-phosphorylated and ubiquitinated protein. J Biol Chem *281*, 24612-24622.

Tate, J.J., Rai, R., and Cooper, T.G. (2005). Methionine sulfoximine treatment and carbon starvation elicit Snf1-independent phosphorylation of the transcription activator Gln3 in Saccharomyces cerevisiae. J Biol Chem *280*, 27195-27204.

Tate, J.J., Rai, R., and Cooper, T.G. (2006). Ammonia-specific regulation of Gln3 localization in Saccharomyces cerevisiae by protein kinase Npr1. J Biol Chem *281*, 28460-28469.

Taylor, S.S., Kim, C., Vigil, D., Haste, N.M., Yang, J., Wu, J., and Anand, G.S. (2005). Dynamics of signaling by PKA. Biochim Biophys Acta *1754*, 25-37.

Thaler, F., Valsasina, B., Baldi, R., Xie, J., Stewart, A., Isacchi, A., Kalisz, H.M., and Rusconi, L. (2003). A new approach to phosphoserine and phosphothreonine analysis in peptides and proteins: chemical modification, enrichment via solid-phase reversible binding, and analysis by mass spectrometry. Anal Bioanal Chem *376*, 366-373.

Thompson, A.J., Hart, S.R., Franz, C., Barnouin, K., Ridley, A., and Cramer, R. (2003). Characterization of protein phosphorylation by mass spectrometry using immobilized metal ion affinity chromatography with on-resin beta-elimination and Michael addition. Anal Chem *75*, 3232-3243.

Ubersax, J.A., and Ferrell, J.E., Jr. (2007). Mechanisms of specificity in protein phosphorylation. Nat Rev Mol Cell Biol *8*, 530-541.

Ubersax, J.A., Woodbury, E.L., Quang, P.N., Paraz, M., Blethrow, J.D., Shah, K., Shokat, K.M., and Morgan, D.O. (2003). Targets of the cyclin-dependent kinase Cdk1. Nature *425*, 859-864.

Urban, J., Soulard, A., Huber, A., Lippman, S., Mukhopadhyay, D., Deloche, O., Wanke, V., Anrather, D., Ammerer, G., Riezman, H., *et al.* (2007). Sch9 is a major target of TORC1 in Saccharomyces cerevisiae. Mol Cell *26*, 663-674.

Valenzuela, L., Aranda, C., and Gonzalez, A. (2001). TOR modulates GCN4-dependent expression of genes turned on by nitrogen limitation. J Bacteriol *183*, 2331-2334.

Van Belle, D., and Andre, B. (2001). A genomic view of yeast membrane transporters. Curr Opin Cell Biol *13*, 389-398.

Vandenbol, M., Jauniaux, J.C., and Grenson, M. (1989). Nucleotide sequence of the Saccharomyces cerevisiae PUT4 proline-permease-encoding gene: similarities between CAN1, HIP1 and PUT4 permeases. Gene *83*, 153-159.

Vandenbol, M., Jauniaux, J.C., and Grenson, M. (1990). The Saccharomyces cerevisiae NPR1 gene required for the activity of ammonia-sensitive amino acid permeases encodes a protein kinase homologue. Mol Gen Genet *222*, 393-399.

Vandenbol, M., Jauniaux, J.C., Vissers, S., and Grenson, M. (1987). Isolation of the NPR1 gene responsible for the reactivation of ammonia-sensitive amino-acid permeases in Saccharomyces cerevisiae. RNA analysis and gene dosage effects. Eur J Biochem *164*, 607-612.

Wang, H., Wang, X., and Jiang, Y. (2003a). Interaction with Tap42 is required for the essential function of Sit4 and type 2A phosphatases. Mol Biol Cell *14*, 4342-4351.

Wang, X., Li, W., Parra, J.L., Beugnet, A., and Proud, C.G. (2003b). The C terminus of initiation factor 4E-binding protein 1 contains multiple regulatory features that influence its function and phosphorylation. Mol Cell Biol *23*, 1546-1557.

Wang, Y., Pierce, M., Schneper, L., Guldal, C.G., Zhang, X., Tavazoie, S., and Broach, J.R. (2004). Ras and Gpa2 mediate one branch of a redundant glucose signaling pathway in yeast. PLoS Biol *2*, E128.

Wek, S.A., Zhu, S., and Wek, R.C. (1995). The histidyl-tRNA synthetase-related sequence in the eIF-2 alpha protein kinase GCN2 interacts with tRNA and is required for activation in response to starvation for different amino acids. Mol Cell Biol *15*, 4497-4506.

Wiame, J.M., Grenson, M., and Arst, H.N., Jr. (1985). Nitrogen catabolite repression in yeasts and filamentous fungi. Adv Microb Physiol *26*, 1-88.

Wilson, W.A., Hawley, S.A., and Hardie, D.G. (1996). Glucose repression/derepression in budding yeast: SNF1 protein kinase is activated by phosphorylation under derepressing conditions, and this correlates with a high AMP:ATP ratio. Curr Biol *6*, 1426-1434.

Woods, A., Munday, M.R., Scott, J., Yang, X., Carlson, M., and Carling, D. (1994). Yeast SNF1 is functionally related to mammalian AMP-activated protein kinase and regulates acetyl-CoA carboxylase in vivo. J Biol Chem *269*, 19509-19515.

Wullschleger, S., Loewith, R., and Hall, M.N. (2006). TOR signaling in growth and metabolism. Cell *124*, 471-484.

Yaffe, M.B., Leparc, G.G., Lai, J., Obata, T., Volinia, S., and Cantley, L.C. (2001). A motif-based profile scanning approach for genome-wide prediction of signaling pathways. Nat Biotechnol *19*, 348-353.

Yang, R., Wek, S.A., and Wek, R.C. (2000). Glucose limitation induces GCN4 translation by activation of Gcn2 protein kinase. Mol Cell Biol *20*, 2706-2717.

Yashiroda, H., Kaida, D., Toh-e, A., and Kikuchi, Y. (1998). The PY-motif of Bul1 protein is essential for growth of Saccharomyces cerevisiae under various stress conditions. Gene *225*, 39-46.

Zheng, J., Trafny, E.A., Knighton, D.R., Xuong, N.H., Taylor, S.S., Ten Eyck, L.F., and Sowadski, J.M. (1993). 2.2 A refined crystal structure of the catalytic subunit of cAMP-dependent protein kinase complexed with MnATP and a peptide inhibitor. Acta Crystallogr D Biol Crystallogr *49*, 362-365.

Zheng, X.F., Florentino, D., Chen, J., Crabtree, G.R., and Schreiber, S.L. (1995). TOR kinase domains are required for two distinct functions, only one of which is inhibited by rapamycin. Cell *82*, 121-130.

Zhu, G., Fujii, K., Liu, Y., Codrea, V., Herrero, J., and Shaw, S. (2005). A single pair of acidic residues in the kinase major groove mediates strong substrate preference for P-2 or P-5 arginine in the AGC, CAMK, and STE kinase families. J Biol Chem *280*, 36372-36379.

Zolnierowicz, S., and Bollen, M. (2000). Protein phosphorylation and protein phosphatases. De Panne, Belgium, September 19-24, 1999. EMBO J *19*, 483-488.

Acknowledgements

Ein besonders grosses Dankeschön möchte ich an Paul Jenö richten, dass ich in seinem Labor meine Doktorarbeit machen durfte und er mir jederzeit geduldig mit Rat und Tat zur Seite stand. Im speziellen möchte ich mich bei ihm für das kritische Durchlesen meiner Doktorarbeit bedanken.

Ebenfalls bedanken möchte ich mich bei meinen ehemaligen Laborkollegen, die mich bei meiner Arbeit unterstützt und zu einem guten Arbeitsklima beigetragen haben: Suzette Moes, für ihre fröhliche und hilfsbereite Art, sowie Patrick Altermatt, Alessio Cremonesi, Simon Hauri und bei allen die für kurze Zeit im Labor gearbeitet haben.

Nicht vergessen möchte ich meine Freundin und meine Familie, die mir geholfen haben mich in den freien Stunden zu erholen um neue Kreativität zu tanken.

I also like to thank all the members of the 5th floor of the Biozentrum that helped me during my studies and Jan Hofsteenge for being in my thesis committee.

Curriculum vitae

Personalien:

Name:	Stefan Gander
Geburtsdatum:	03.07.1980
Geburtsort:	Glarus
Bürgerort:	Zürich
Familienstand:	ledig
Staatsangehörigkeit:	Schweizer
Adresse:	Laupenring 9, 4054 Basel

Ausbildung:

1987-1993	Primarschule in Giswil (OW)
1993-2000	Kantonsschule Obwalden in Sarnen (OW) Matura am 14.04.2000
2000-2004	Biologiestudium an der Universität Basel
2004	Diplomarbeit „Topogenesis of membrane proteins“ bei Prof. Dr. Martin Spiess Diplom in Biologie (Studienrichtung Molekularbiologie) am 19.10.2004
2004-2007	Doktorat am Biozentrum in Basel (Abteilung Biochemie)
2007	Doktorarbeit „Functional analysis of the *Saccharomyces cerevisiae* Npr1 protein kinase“ bei Dr. Paul Jenö, Prof. Dr. Mike Hall Doktorexamen in Biochemie am 17.12.2007